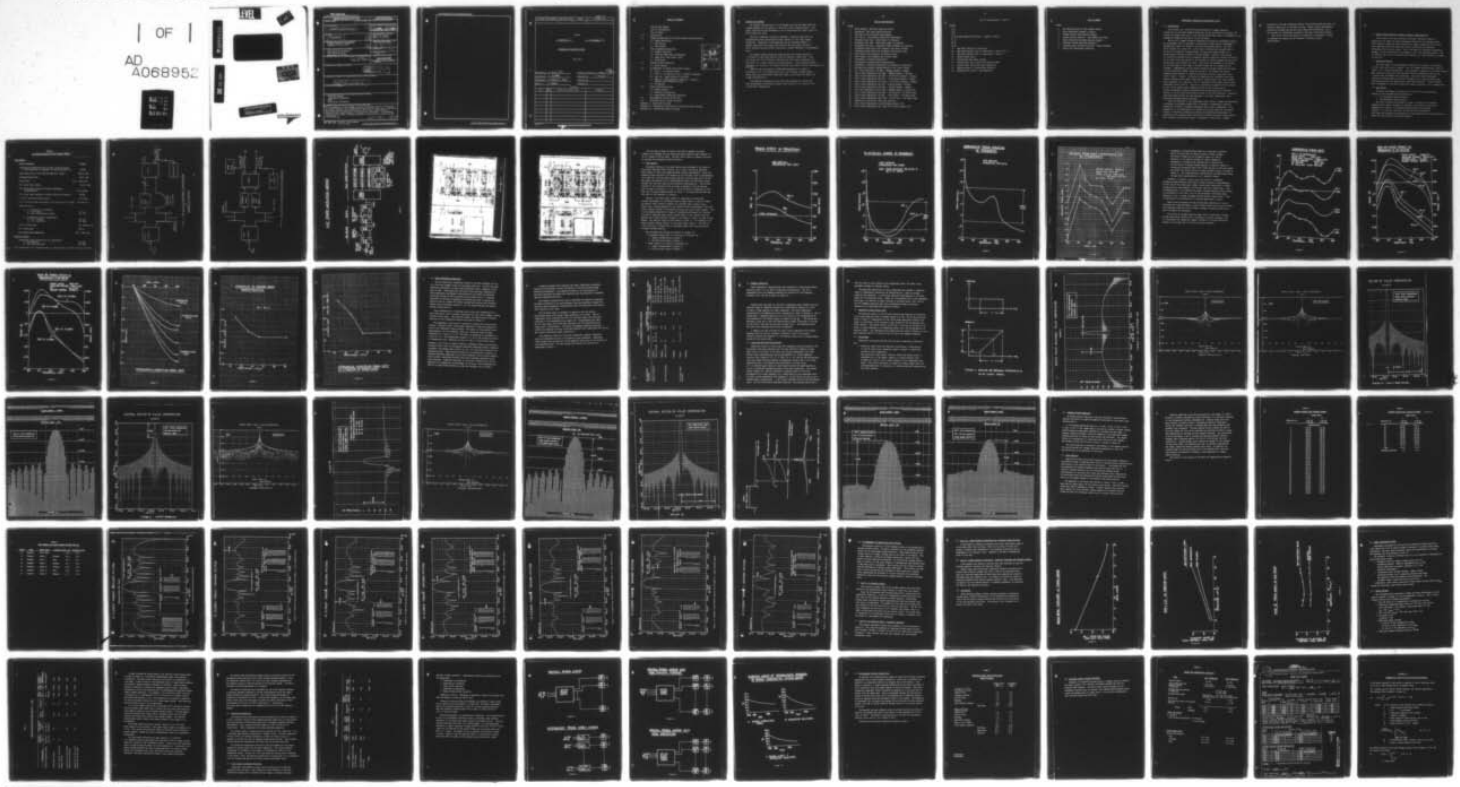
AD-A068 952 GRUMMAN AEROSPACE CORP BETHPAGE N Y F/G 17/9
LIGHTWEIGHT TRANSMITTER STUDY.(U)
NOV 78 R MCGILL N00173-78-C-0205
UNCLASSIFIED PDR-699D-1 NL

| OF |
AD A068952



END
DATE FILMED
7-79
DDC

UNCLASSIFIED

SECURITY CLASSIFICATION OF THIS PAGE (When Data Entered)

REPORT DOCUMENTATION PAGE	READ INSTRUCTIONS BEFORE COMPLETING FORM
1. REPORT NUMBER	2. GOVT ACCESSION NO. 3. RECIPIENT'S CATALOG NUMBER
4. TITLE (and Subtitle) (6) LIGHTWEIGHT TRANSMITTER STUDY.	(9) 5. TYPE OF REPORT & PERIOD COVERED Rept. for 31 Aug [illegible] - 30 Nov [illegible]78, 6. PERFORMING ORG. REPORT NUMBER
7. AUTHOR(s) (10) Robert McGill	8. CONTRACT OR GRANT NUMBER(s) (15) N00173-78-C-0205
9. PERFORMING ORGANIZATION NAME AND ADDRESS Grumman Aerospace Corporation Bethpage, New York 11714	10. PROGRAM ELEMENT, PROJECT, TASK AREA & WORK UNIT NUMBERS (11) 30 Nov 78
11. CONTROLLING OFFICE NAME AND ADDRESS Naval Research Laboratory 4555 Overlook Ave SW Washington, DC 20375	12. REPORT DATE 13. NUMBER OF PAGES 81
14. MONITORING AGENCY NAME & ADDRESS (if different from Controlling Office) (12) 84p.	15. SECURITY CLASS. (of this report) UNCLASSIFIED 15a. DECLASSIFICATION/DOWNGRADING SCHEDULE

16. DISTRIBUTION STATEMENT (of this Report)

This document has been approved for public release and sale; its distribution is unlimited.

17. DISTRIBUTION STATEMENT (of the abstract entered in Block 20, if different from Report)

(14) PDR-699D-1

18. SUPPLEMENTARY NOTES

19. KEY WORDS (Continue on reverse side if necessary and identify by block number)

Conformal Antenna
Lightweight Transmitter
Radar
Solid State Transmitter

20. ABSTRACT (Continue on reverse side if necessary and identify by block number)

The RF dependency of the Grumman procured UHF Transmit Modules is discussed in terms of various input parameters RF amplitude and phase, pulse compression and antenna pattern quality are related via dc input characteristics. Tentative power supply designs are comparatively evaluated. The preferred configuration is used to develop estimates of watts/lb for current and 1985 technologies.

388 847

DD FORM 1 JAN 73 1473 EDITION OF 1 NOV 65 IS OBSOLETE
S/N 0102-014-6601

SECURITY CLASSIFICATION OF THIS PAGE (When Data Entered)

CONTRACT REQUIREMENTS	CONTRACT ITEM	MODEL	CONTRACT NO.

REPORT

NO. PDR-699D-1 DATE: 30 November 1978

LIGHTWEIGHT TRANSMITTER STUDY

CODE 26512

PREPARED BY: R. McGill RM.

CHECKED BY: F. Ganz FG

DEPARTMENT: V. Albanese/C. Draghi

SECTION: C. Schmidt

TECHNICAL APPROVAL: R. Steele RS

APPROVED BY: M. Ciminera

APPROVED BY:

APPROVED BY:

REVISIONS

DATE	REV BY	REVISIONS & ADDED PAGES	REMARKS

TABLE OF CONTENTS

Overview and Summary

List of Illustrations

List of Tables

1.0 Introduction

2.0 Energy Storage Effects on Module Transfer Characteristics

- 2.1 Module Description
- 2.2 Test Set-up
- 2.3 Test Results

3.0 Pulse Compression Simulation

- 3.1 Nominal Conditions
- 3.2 Phase and Amplitude Perturbations
- 3.3 Sensitivity Time Control (STC)
- 3.4 Conclusions

4.0 Antenna Pattern Prediction

- 4.1 Error Analysis

5.0 RF Dependency of Steady State Pulse Voltage

- 5.1 Case I - No Capacitor Match
- 5.2 Case II - No Capacitor Match - Frequency Dependent
- 5.3 Case III - Phase Matched at Mid-Pulse
- 5.4 Case IV - Phase Matched at Mid-Pulse - Capacitor Tolerance and Frequency Effects
- 5.5 Conclusions

6.0 Power Distribution System

- 6.1 Design Concepts
- 6.2 Preferred Configuration
- 6.3 Power Supply Technology Prediction

7.0 Environmental Control System (ECS)

8.0 Projected Power to Weight Estimates

Appendix I - Acceptance Test Data

Appendix II - Mathematical Verification of Mid-Pulse Phase Matching

Appendix III - Series-Pass Regulator Design

ACCESSION for
NTIS White Section
DDC Buff Section
UNANNOUNCED
JUSTIFICATION
BY
DISTRIBUTION/AVAILABILITY CODES
Dist. Avail. and/or SPECIAL

OVERVIEW AND SUMMARY

RF transfer characteristics of the Grumman procured UHF power amplifier transmit modules are evaluated as a function of input characteristics. The output sensitivities are determined to be 6° phase shift/volt input, and 0.25 dB RF output/volt input.

The pulse compression operation underwent a computer simulation with representative phase and amplitude errors caused by 1 volt input supply variations. Variations of this magnitude had no noticeable effects. A several times worst case input error function was then used, with only minor sidelobe variations noted, along with a slight widening of the compressed pulse.

An antenna pattern simulation using several error models produced a 0.4 dB shift of mean peak sidelobe level per degree of phase shift. This data along with the RF transfer characteristics were used to determine the sensitivity to a simple capacitor voltage regulator. This scheme was deemed promising, but because of the dynamic waveforms anticipated, further investigation is required.

Several power distribution systems were evaluated on the basis of providing a 33 $\pm$ 1 volt supply with a $\pm$0.1 volt tracking between modules. A series pass type distributed system was chosen as providing best weight and volume characteristics.

The complete transmission system was then estimated for current and 1985 technologies as providing specific power densities of 25 watts/lb and 35 watts/lbs, respectively.

LIST OF ILLUSTRATIONS

FIGURE

1 Block Diagram - UHF Power Amplifier Module
2 Photograph - UHF Power Amplifier Module
3 Test Set-up Phase Deviation Measurements
4 Test Set-up - Inter-Module Phase Shift Measurements
5 Acceptance Test Data - Power Output vs Frequency
6 Acceptance Test Data - Electrical Length vs Frequency
7 Acceptance Test Data - Intermodule Phase Deviation vs Frequency
8 Intermodule Phase Shift with Frequency and Supply Voltage
9 Intermodule Phase Shift with Frequency and RF Drive Level
10 Power Output with Frequency and Supply Voltage
11 Power Output with Frequency and RF Drive Level
12 Intermodule, Intrapulse Phase Shift
13 Intrapulse DC Voltage Droop Characteristics
14 Intermodule, Intrapulse Phase Shift as Function of Capacitance
15 Envelope and Frequency Characteristics of FM "Chirp" Signal
16 64:1 Pulse Compression ($\pm$3 NMi) - Hamming Weights - Nominal
17 1024:1 Pulse Compression ($\pm$15 NMi) - Hamming Weights - Nominal
18 1024:1 Pulse Compression ($\pm$15 NMi) - 30 dB Taylor Weights - Nominal
19 1024:1 Pulse Compression ($\pm$1 NMi) - 30 dB Taylor Weights - Nominal
20 1024:1 Pulse Compression ($\pm$0.2 NMi) - 30 dB Taylor Weights - Nominal
21 1024:1 Pulse Compression ($\pm$1 NMi) - Uniform Weights - Nominal
22 1024:1 Pulse Compression ($\pm$15 NMi) - Uniform Weights - Nominal
23 64:1 Pulse Compression ($\pm$0.75 NMi) - Hamming Weights - Phase Error
24 1024:1 Pulse Compression ($\pm$15 NMi) - 30 dB Taylor - 90° Phase Slope
25 1024:1 Pulse Compression ($\pm$1 NMi) - 30 dB Taylor - 90° Phase Slope
26 1024:1 Pulse Compression ($\pm$0.2 NMi) - 30 dB Taylor - 90° Phase Slope
27 Sensitivity Time Control (STC) Gain Function
28 1024:1 Pulse Compression ($\pm$2 NMi) Hamming Weight, STC
29 1024:1 Pulse Compression ($\pm$0.2 NMi) 30 dB Taylor Weights, STC

List of Illustrations - (cont'd)

FIGURE	
30	Antenna Radiation Patterns - Indexed in Table 4
31	
32	
33	
34	
35	
36	
37	Mean Peak Sidelobe vs Phase Error
38	Mean Peak Sidelobe Level vs Capacitance - Cases I and II
39	Mean Peak Sidelobe Level vs Capacitance - Cases IV
40	Central Power Source
41	Distributed Power Supply System
42	Central Power Source with Local Energy Storage
43	Central Power Source with Local Regulation
44	Expected Impact of Technological Advances
45	Representative Series - Pass Regulator

LIST OF TABLES

TABLE

1 GAC Specifications for UHF Transmit Module
2 Pulse Compression Summary of Results
3 Antenna Pattern Peak Sidelobe Summary
4 Antenna Pattern Analysis - Data Summary and Index
5 Power Distribution Systems Analysis Summary
6 Preferred System Operating Parameters
7 Conformal Radar Cooling Provisions - Weight Estimate
8 Weight and Power/Weight Tabulation

LIGHTWEIGHT TRANSMITTER REQUIREMENTS STUDY

1.0 INTRODUCTION

This contract, No. N00173-78-C-0205, performed by Grumman Aerospace Corporation for the Naval Research Laboratory during the period of 31 August 1978 through 30 November 1978 was to study and define the power supply requirements of the transmitter system for the Navy's future AEW radar.

Late in 1972 Grumman Aerospace Corporation initiated an independent research and development study to determine if significant steps could be undertaken to substantially reduce the weight of tactical surveillance radars. From this effort evolved the concept for a solid state, electronically scanned radar to provide 360° azimuthal coverage without the associated weight burden of a conventionally externally mounted rotating antenna. Central to the concept are a series of antenna arrays, integrally mounted within the aircraft structure. Two of these arrays are mounted on the fuselage for abeam coverage and are of the conventional cavity-backed slot type. Four arrays are embedded in the leading and trailing edges of the wings to provide forward and aft quadrant sector coverage. Complementing the low weight innovative antenna system and providing a second substantial weight saving is the use of low voltage solid state transmit/receive modules to replace conventional, heavier, high power transmission chains. Because, solid-state transmitters are inherently peak power limited, adequate radar power levels must be established by very long transmit pulse operation (i.e. high duty cycle) in conjunction with large receiver pulse compression ratios (1024:1). The use of individual RF transmit/receive modules at each of the antenna array elements provides an additional benefit, two-way transmission losses are minimized and system sensitivity increased. Typically, the all solid-state module contains an RF power amplifier, a digitally controlled phase shifter for beam steering, a low noise preamplifier, and appropriate transmit/receive switches.

Since the inception of the lightweight radar concept, Grumman has undertaken a systematic development program that is designed to demonstrate technical feasibility in terms of hardware performance and aircraft integration. This program led to the development of a limited scale model radar for the express purpose of evaluating integration problems and establishing performance for operation of the scanning array concept with available low power L-band modules and a remotely located power supply. Subsequent to this effort, Grumman

procured two 1 KW UHF transmitter modules from Microwave Power Devices, and subjected these units to extensive testing. Energy storage measurements, coupled with antenna pattern and pulse compression predictions, led to new concepts for lightweight transmitter and power distribution designs.

This study contract developed the transmitter requirements in terms of coherence and regulation and estimated achievable weight effectiveness.

2.0 ENERGY STORAGE EFFECTS ON MODULE TRANSFER CHARACTERISTICS

Solid state is the only promising technology considered capable of meeting the low weight and high performance required by the Conformal Radar. Until recently, high peak power, medium pulse length, medium duty-cycle solid state amplifiers were not available from any source and the predicted performance data was very scarce. Due to the paucity of available information, Grumman, in 1976, sponsored the development of two 1 KW amplifier modules. The two modules were built by Microwave Power Devices, Inc. and delivered to Grumman in June 1977.

2.1 Module Description

The first stage in the development consisted of building a two transistor 300 Watt peak power output submodule with the Grumman specifications, shown in Table 1, as a ultimate design goal. Upon successful completion of the first development stage and verification that the specification requirements could be met, a second stage development was undertaken. The second stage development consisted of paralleling four 300 watt submodules for 1 KW peak power output, then packaging them with appropriate drivers and predrivers. A block diagram and a photograph of the subject module are shown in Figures 1 and 2, respectively.

2.2 Test Set-Up

Two basic performance criteria had to be met by the Power Amplifier modules for the Conformal Radar application:

1. Low intermodule phase deviation
2. Low intrapulse phase deviation.

The first criterion is necessary in order to achieve a low sidelobe antenna pattern while the second is necessary to provide both good pulse compression on receive, and minimum antenna pattern jitter during transmit. To this end, two basic test set-ups were instrumented, both using the bridge nulling technique for high sensitivity and the substitution method for high accuracy in the measurements.

TABLE 1

GAC SPECIFICATIONS FOR UHF TRANSMIT MODULE

Each Module	
Center Frequency	425 MHz
Instantaneous Bandwidth (for ±5° max. phase deviation from linearity, as measured in test setup diag. 1)	50 MHz
Peak Output Power (with 10mW max peak R.F. input)	1000 W. min.
Average Output Power	150 W. min.
Pulse Width	10 & 500 μ sec.
R.F. Input Power (peak)	10 m W. max.
R.F. Input Power variation (without degradation in performance)	±0.5 dB min.
R.F. Input Power overdrive (without failure of Modules)	+10 dB
V.S.W.R. (input and output ports)	1.3:1 max.
Gain and Output Power Variation (any 6 MHz portion of Band)	±0.2 dB max.
Phase Deviation	
a. vs. Frequency (at midpulse)	
1. Entire Band	±5° max.
2. Any 6 MHz portion of Band	±3° max.
b. Intrapulse (for all frequencies)	
1. 0.5 - 10 μsec	±6° max.
2. 10 - 500 μ sec	±3° max.
Turn on Time-Jitter	±5 nanosec max.
D.C. Power Input	430 W.
Cold Plate Face Temperature	22° - 50°C max.
Module to Module	
Intermodule Phase deviation at all frequencies	
1. for midpulse	±3° max.
2. all other positions	±6° max.

Test Frequencies (for acceptance testing) shall be 400, 415, 425, 435, and 450 MHz.

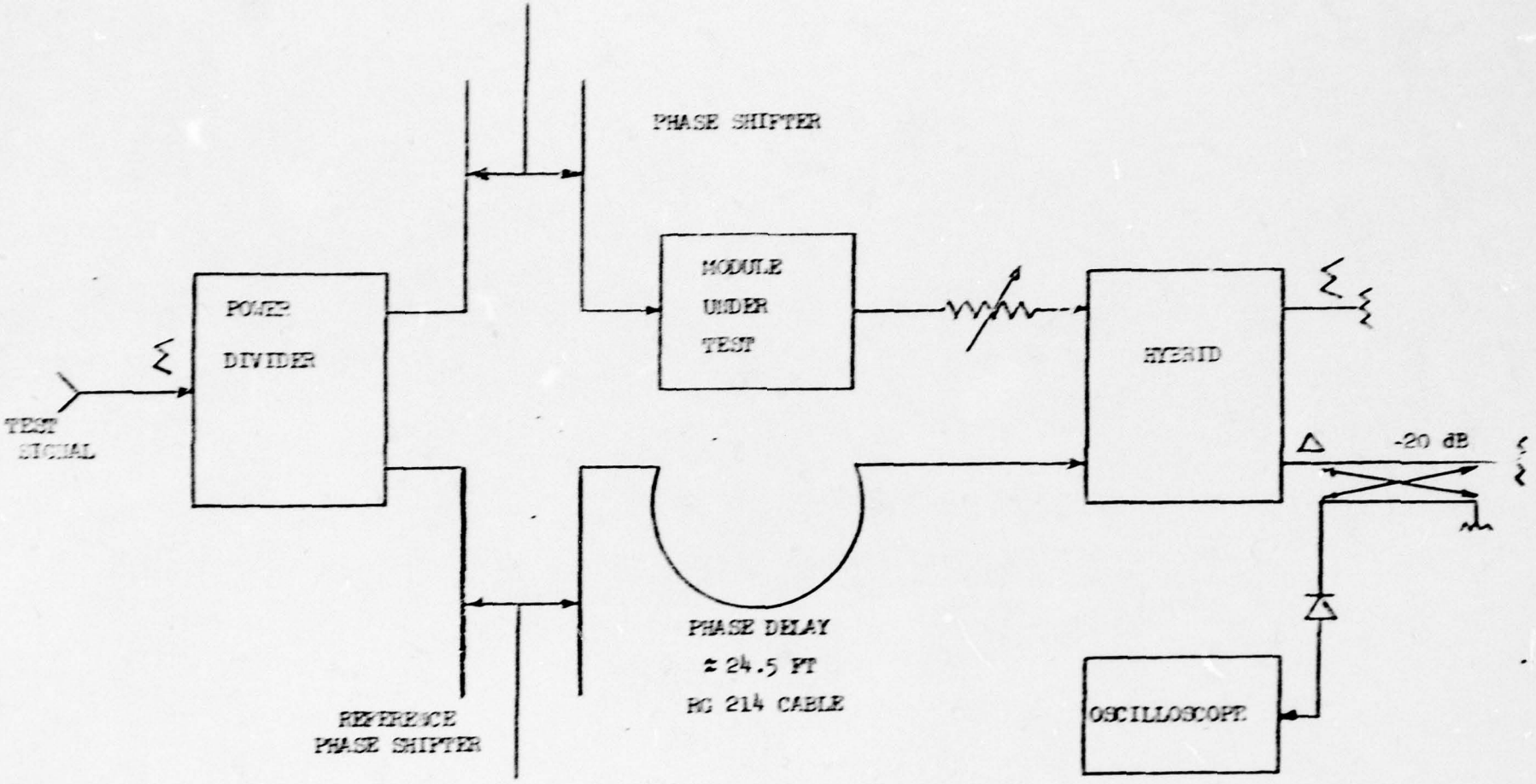


FIGURE 3 - TEST SET-UP FOR MEASUREMENT OF PHASE DEVIATION VS FREQUENCY AND INTRA-PULSE

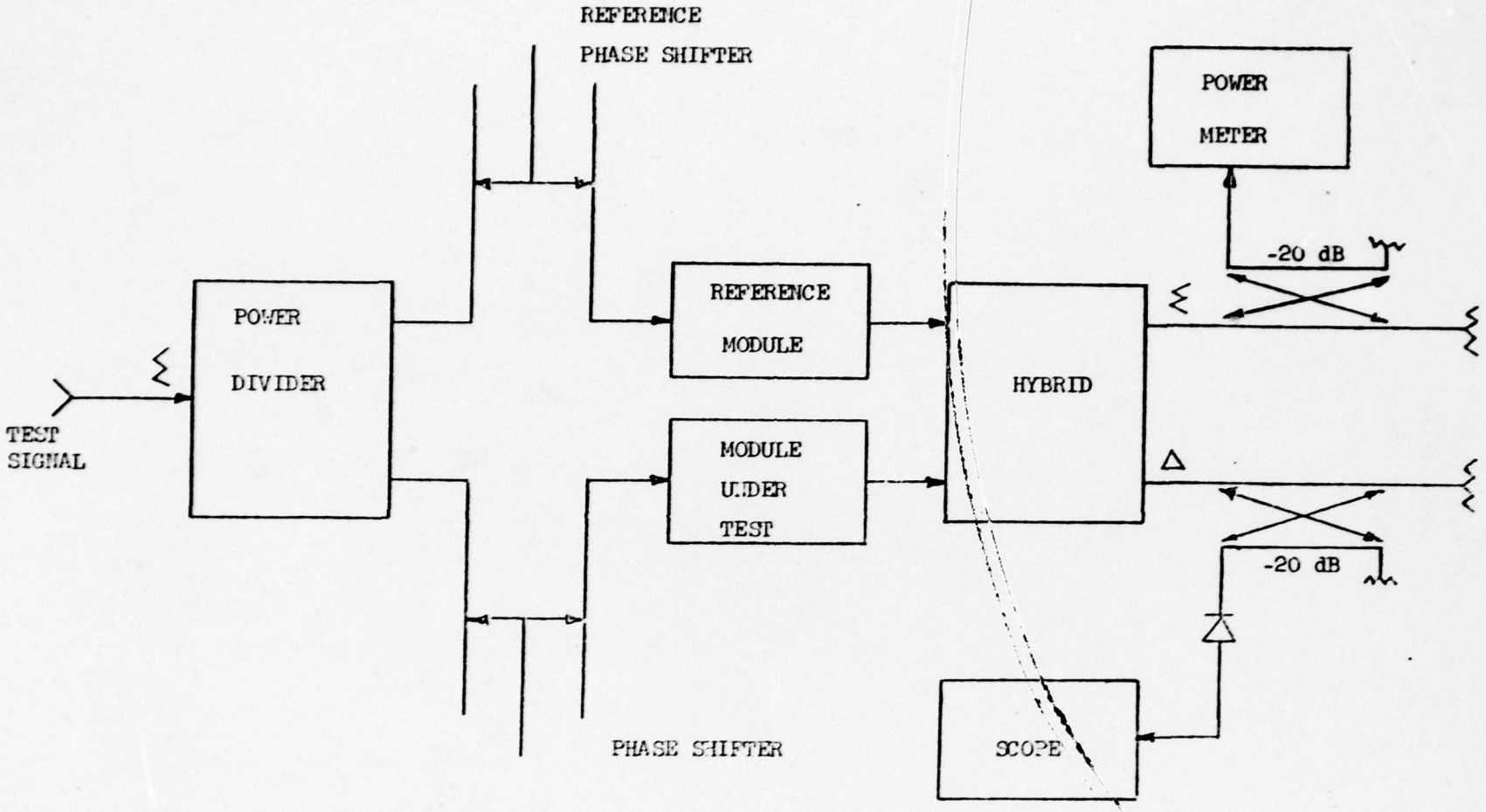


FIGURE 4 - TEST SET-UP FOR INTERMODULE PHASE SHIFT MEASUREMENTS

UHF POWER AMPLIFIER MODULE

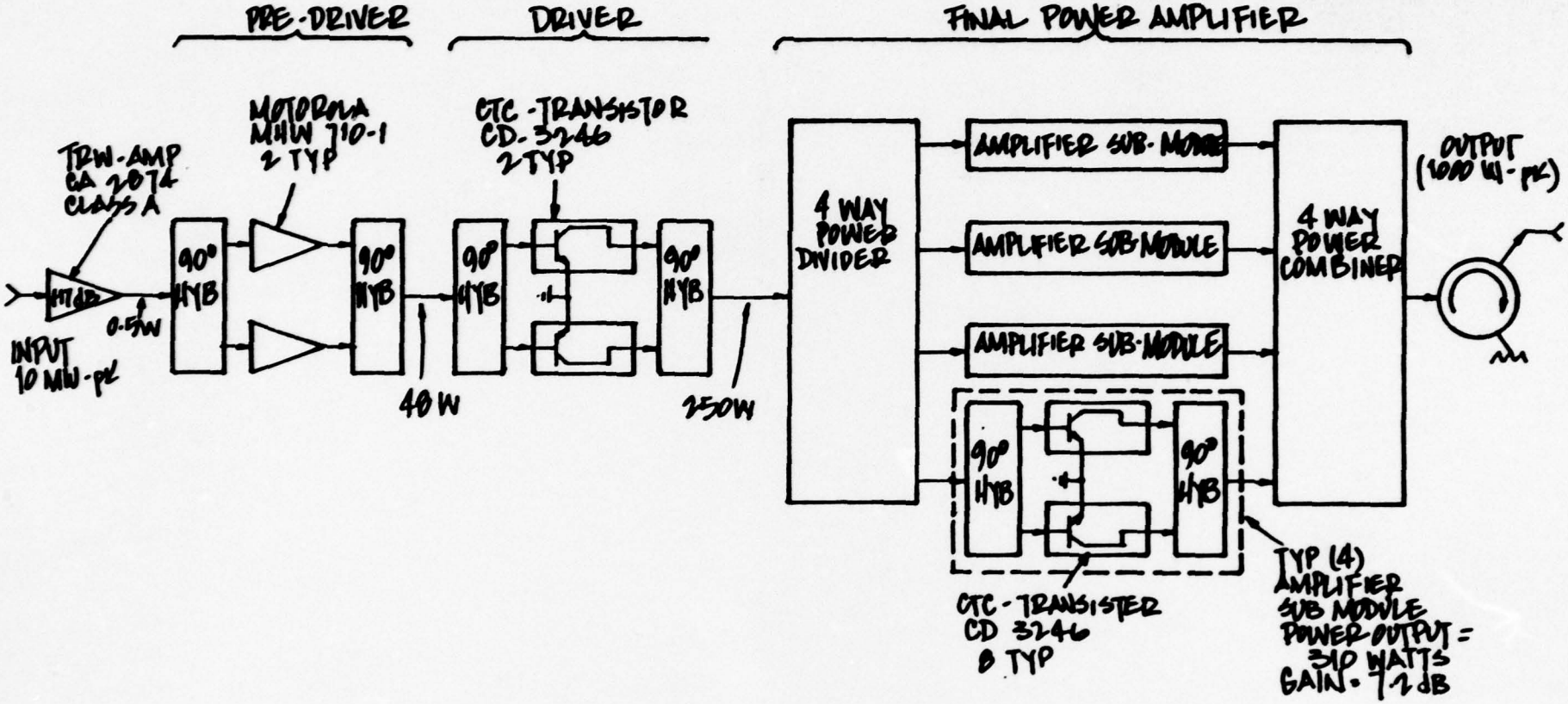
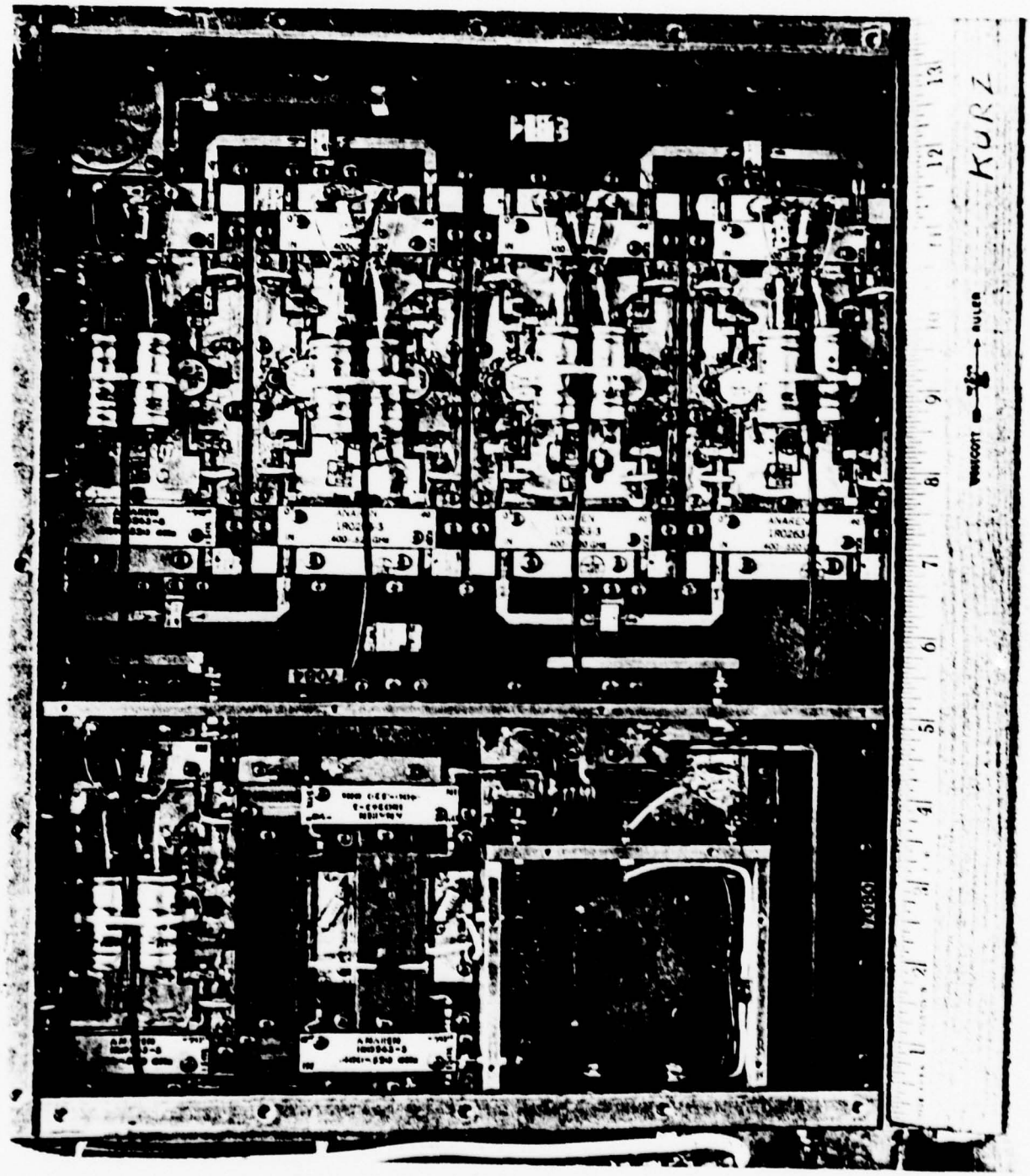


FIGURE 1

KURZ
VERICOTT
RULER



FIGURE

The test set-up shown in Figure 3 was used to measure the phase linearity vs frequency and the intrapulse phase deviation when compared to a 24.5 ft length of RG-214 cable. The test set-up shown in Figure 4 was used to evaluate the intermodule phase deviation.

2.3 Test Results

Acceptance testing of the power modules was performed at the vendor's facilities (Microwave Power Devices, Inc.) using a 200 amp DC regulated power supply for both the average and peak current requirements. Since the average current required by the modules at the 15% duty cycle is approximately 12-15 amps each, and the peak current required is 80-100 amps each, the 200 amp supply was adequate for the measurements without any additional energy storage even when both modules were energized simultaneously. The raw data obtained in the acceptance tests is shown in Appendix 1 and the reduced data is shown in Figures 5, 6 and 7. As can be seen by comparing the test data with the module specifications of Table 1, all specifications were met over most of the bandwidth of interest.

However, a DC power supply capable of supplying the entire peak current requirements of the modules would be many times (at least 5) larger and heavier (when conductor weights are included) than a smaller power supply with a rating adequate for the average current requirements, with some form of energy storage at the modules providing the peak current demands. This is the technique employed by Grumman in energizing the modules for testing; a 30 amp DC regulated power supply located about 20 feet distant from the modules and a large capacitor located at the module to supply the peak current demand. The capacity used with each module is 34000 μF, but because of the large internal storage capacity in the power supply itself ($\approx$ 100,000 μF) it was difficult to obtain data of intrapulse phase shift and pulse droop vs energy storage capacity.

Data obtained from testing the modules at Grumman are:

- Intermodule phase shift as a function of frequency and
  1. supply voltage shown in Figure 8
  2. RF drive level shown in Figure 9
- Power output as a function of frequency and
  1. supply voltage shown in Figure 10
  2. RF drive level shown in Figure 11

POWER OUTPUT VS FREQUENCY

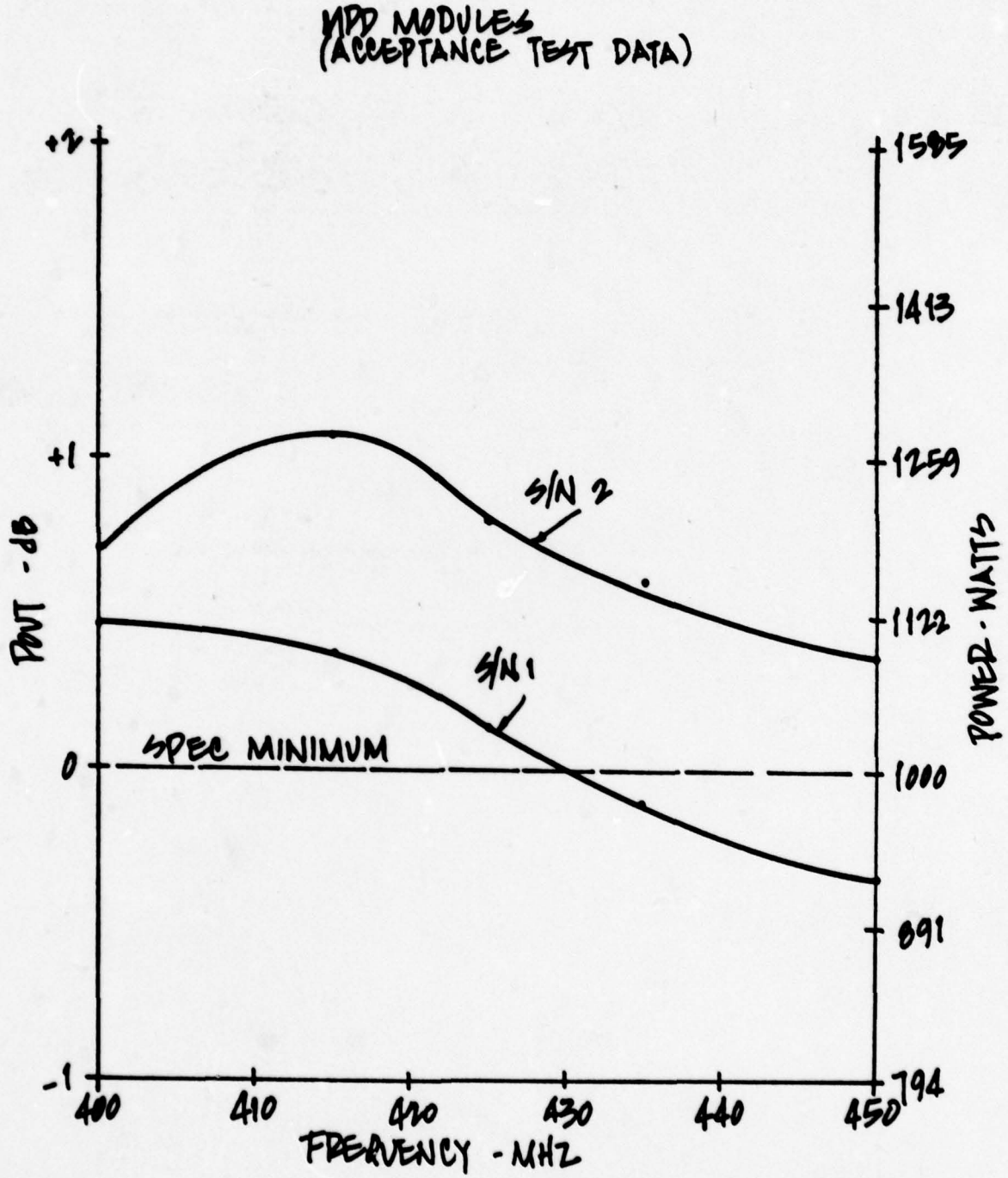


FIGURE 5

ELECTRICAL LENGTH VS FREQUENCY

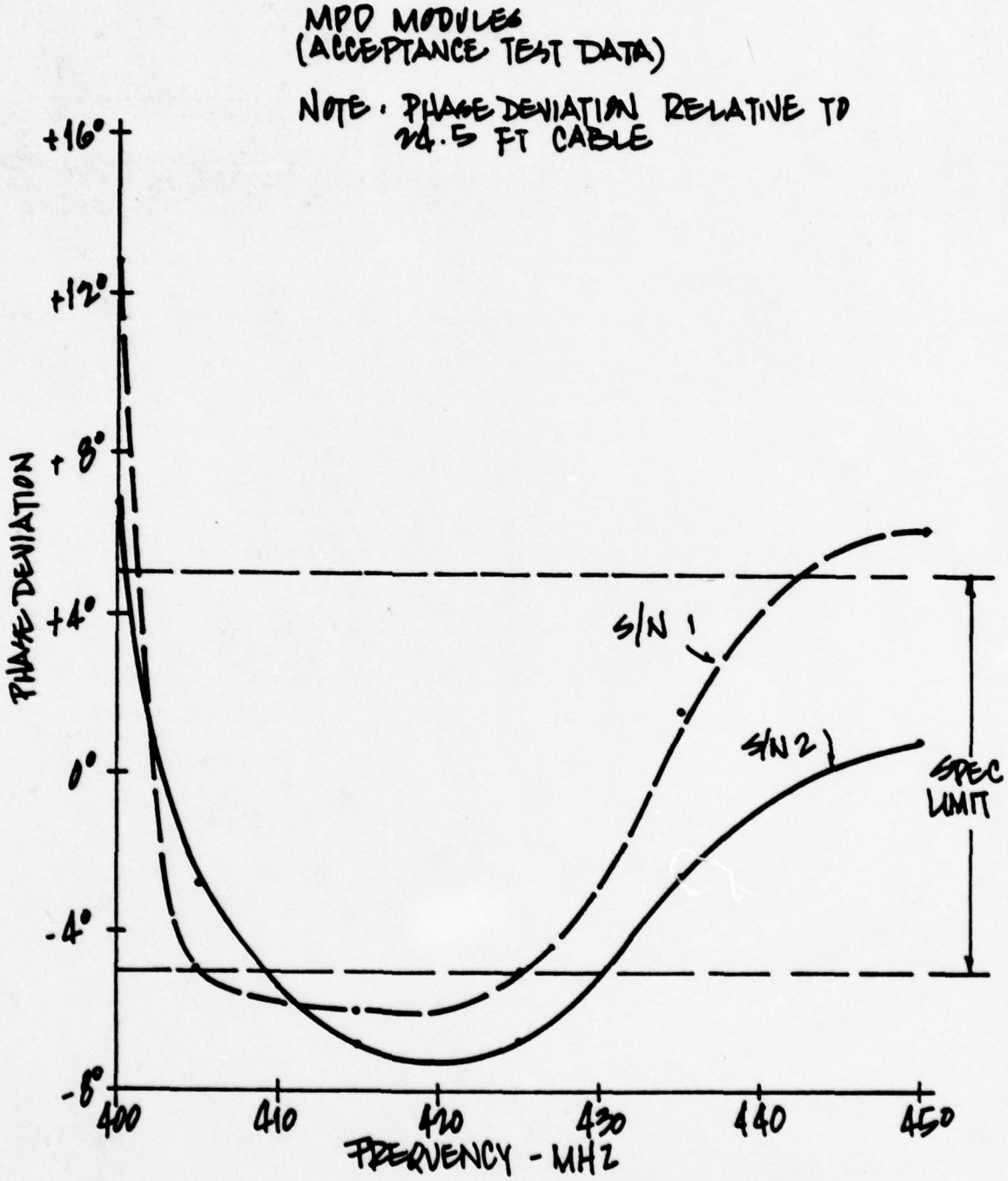


FIGURE 6

INTERMODULE PHASE DEVIATION VS FREQUENCY

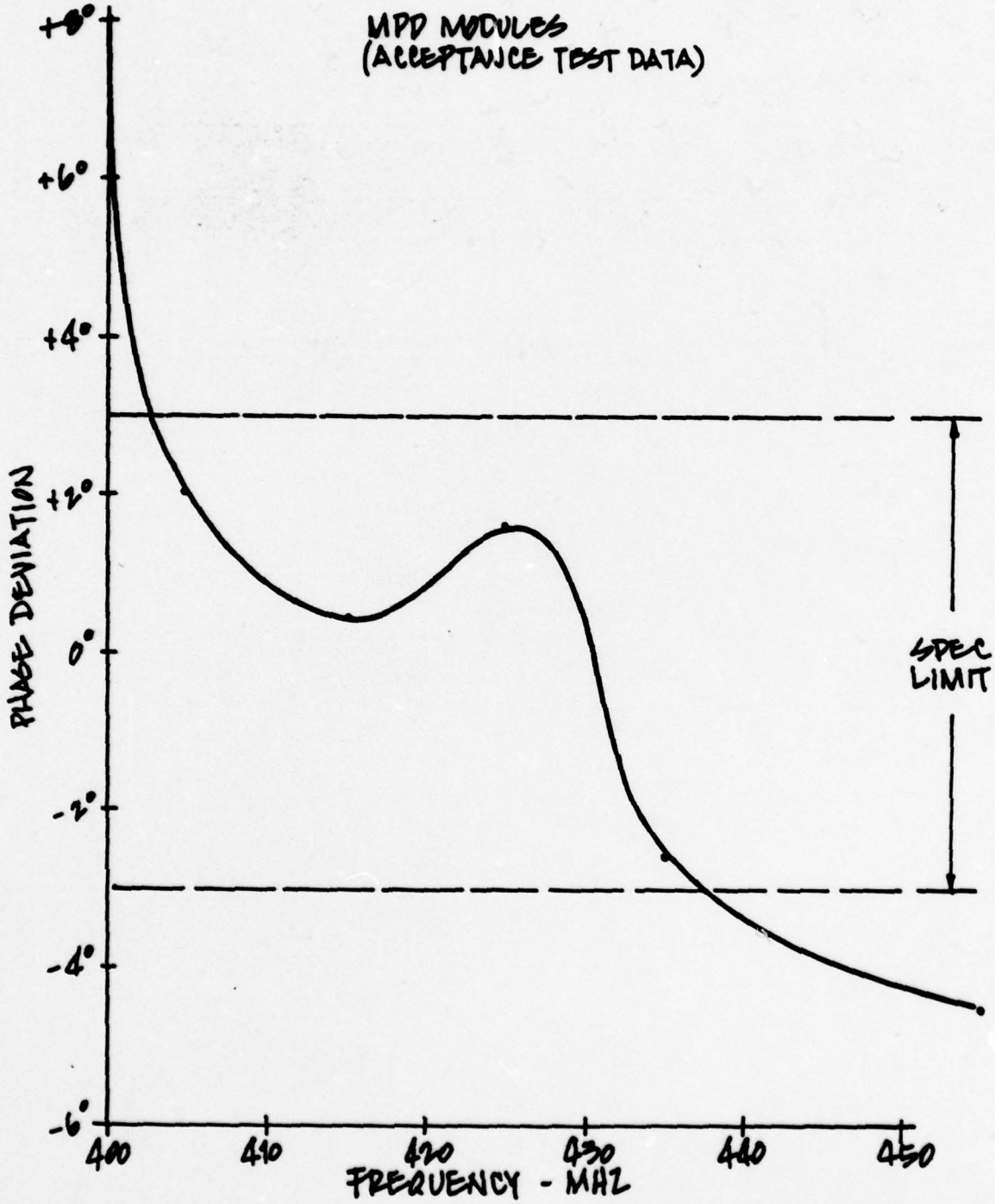


FIGURE 7

RELATED PHASE SHIFT (INTERMODULE) VS B+ & FREQUENCY

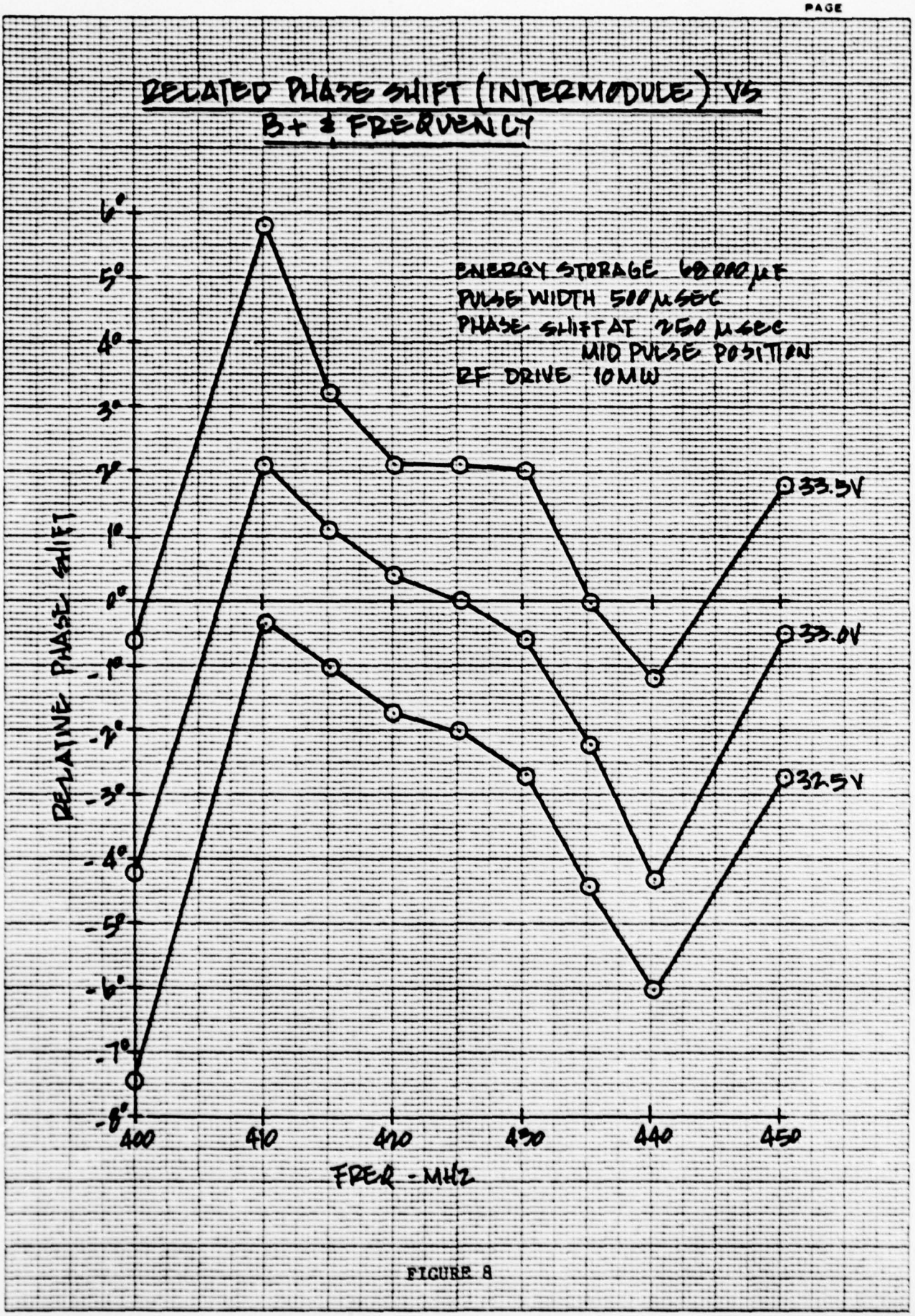


FIGURE 8

- o Intermodule, intrapulse phase shift as a function of position within the pulse and for various levels of energy storage. This data is shown for the 425 MHz in Figure 12, and is identical to the results obtained at other frequencies.
- o Intrapulse dc voltage droop characteristics, obtained for various levels of energy storage capacity is shown in Figure 13.
- o Intermodule intrapulse phase shift (from 100 μsec to 500 μsec within the pulse) for various levels of energy storage capacity is shown in Figure 14. This representing an extrapolation of phase match versus voltage droop characteristics (i.e. capacitor values).

Reference to Figures 8 and 10 will show that the intermodule intrapulse phase deviation with supply voltage variation is approximately 6°/volt and the RF pulsed power output (pulse droop) sensitivity to supply voltage droop is approximately 0.25 dB/volt (5%/volt) respectively. From the measured data it is deduced that supply voltage variation (droop) should be constrained to less than 1 volt if the intermodule intrapulse phase deviation is not to exceed tolerable antenna pattern jitter values. This is particularly true because of the limited sample base (2 units).

Based on data obtained from the two UHF power amplifiers it can be concluded that high performance, tight tolerance units can be built provided that operating conditions such as supply voltage tolerances and RF drive level tolerances are optimized.

The studies of voltage droop and phase shift as functions of energy storage capacitance indicate that a relatively low value capacitor, with its concomitant low weight and volume, followed by a precise regulating element at the module may be the most favorable approach.

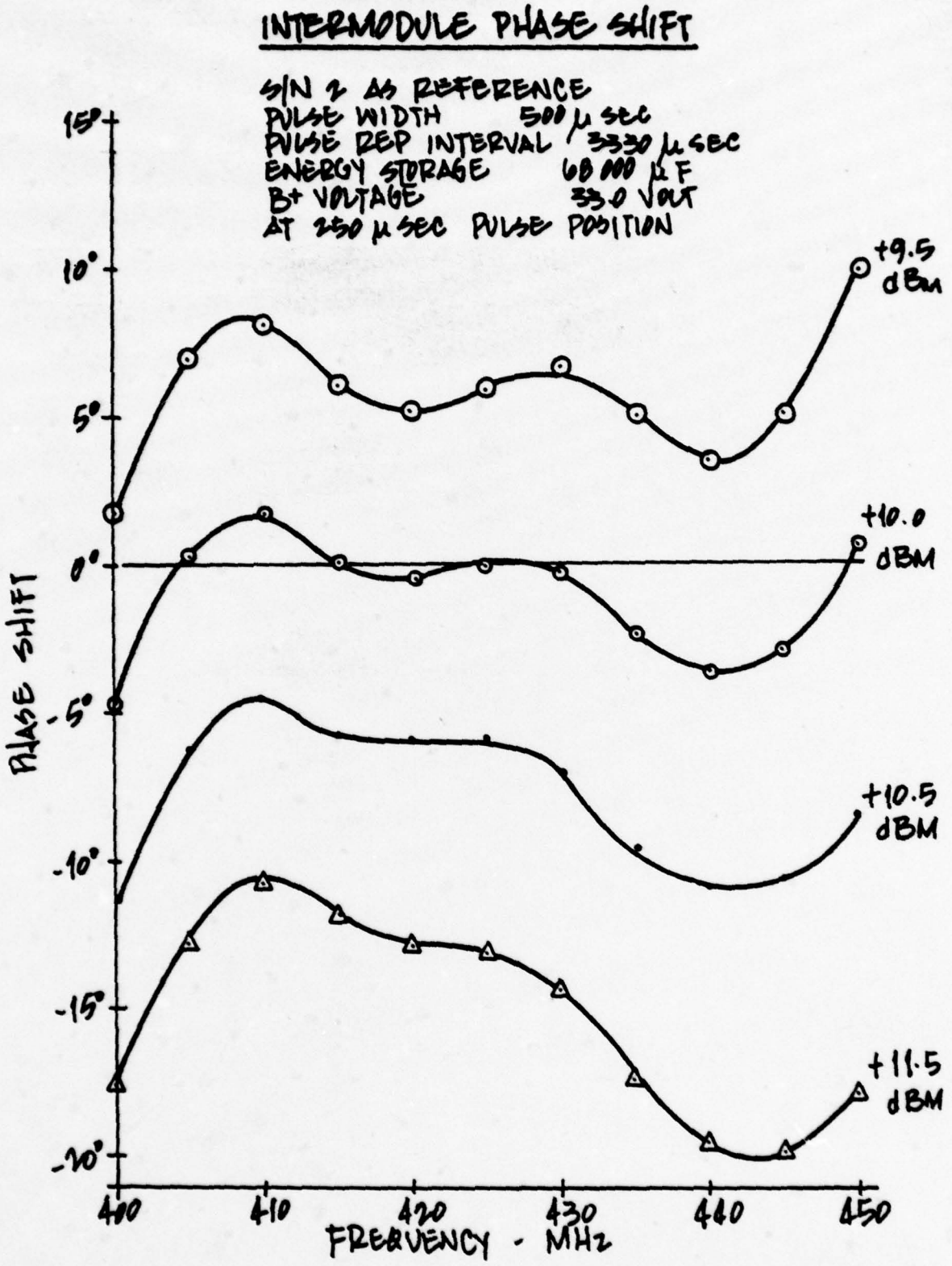

INTERMODULE PHASE SHIFT
S/N 2 AS REFERENCE
PULSE WIDTH 500 μ sec
PULSE REP INTERVAL 3330 μ sec
ENERGY STORAGE 68 000 μ F
B+ VOLTAGE 330 VOLT
AT 250 μ sec PULSE POSITION
15°
10°
5°
0°
-5°
-10°
-15°
-20°
PHASE SHIFT
+9.5 dBm
+10.0 dBM
+10.5 dBM
+11.5 dBM
400
410
420
430
440
450
FREQUENCY - MHz

FIGURE 9

PEAK RF OUTPUT POWER VS. FREQUENCY & DC VOLTAGE

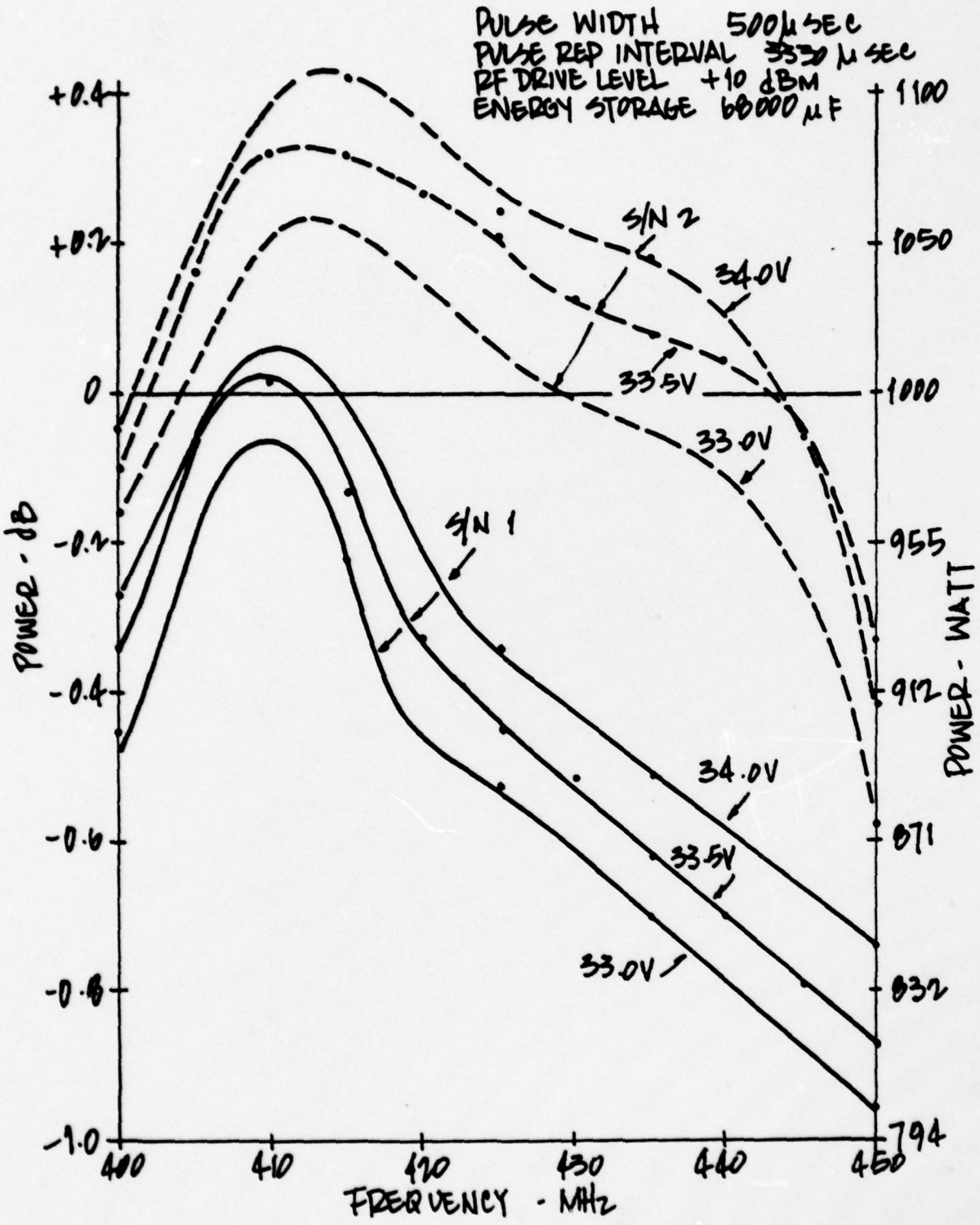


FIGURE 10

PEAK RF POWER OUTPUT Vs FREQUENCY & RF DRIVE

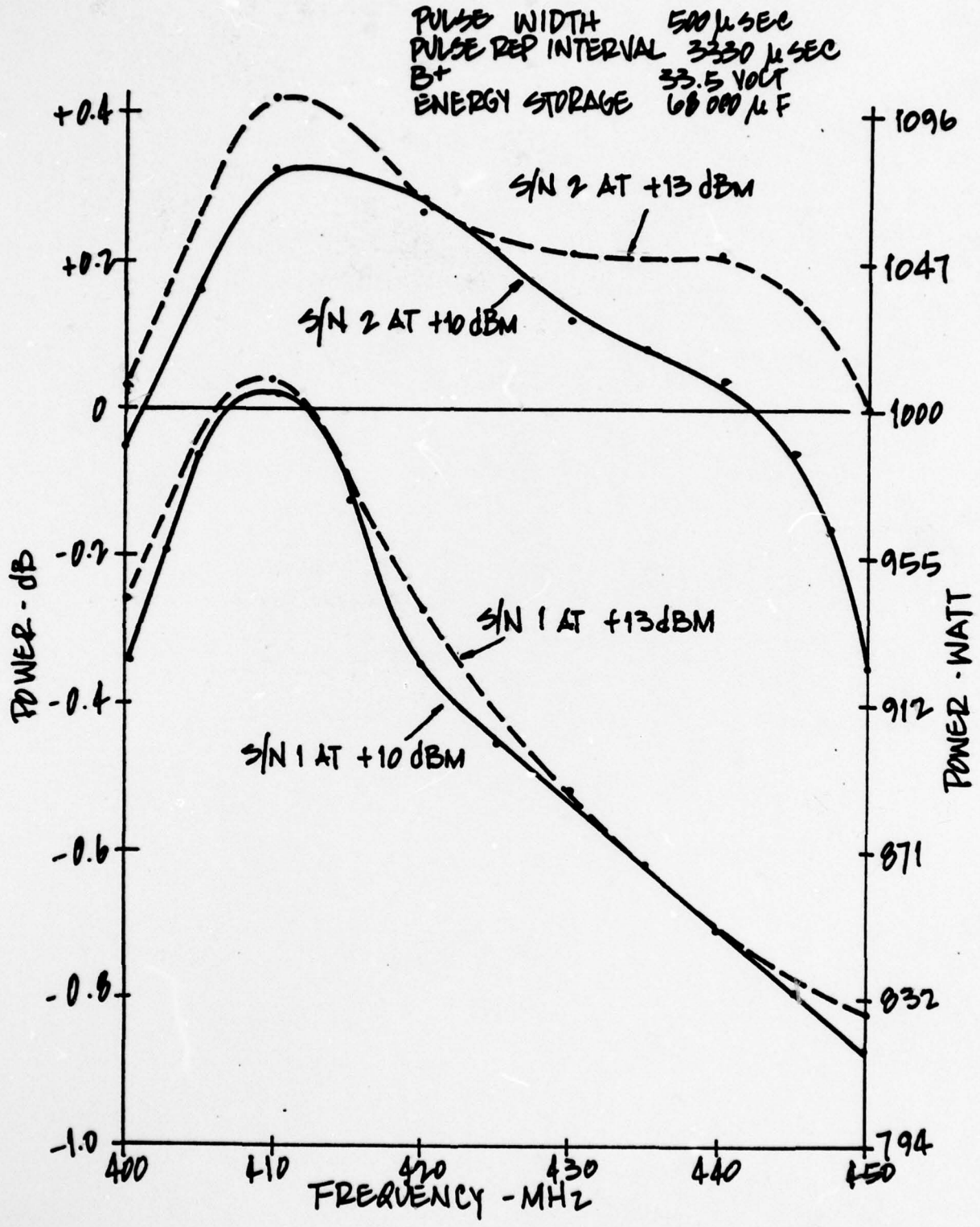


FIGURE 11

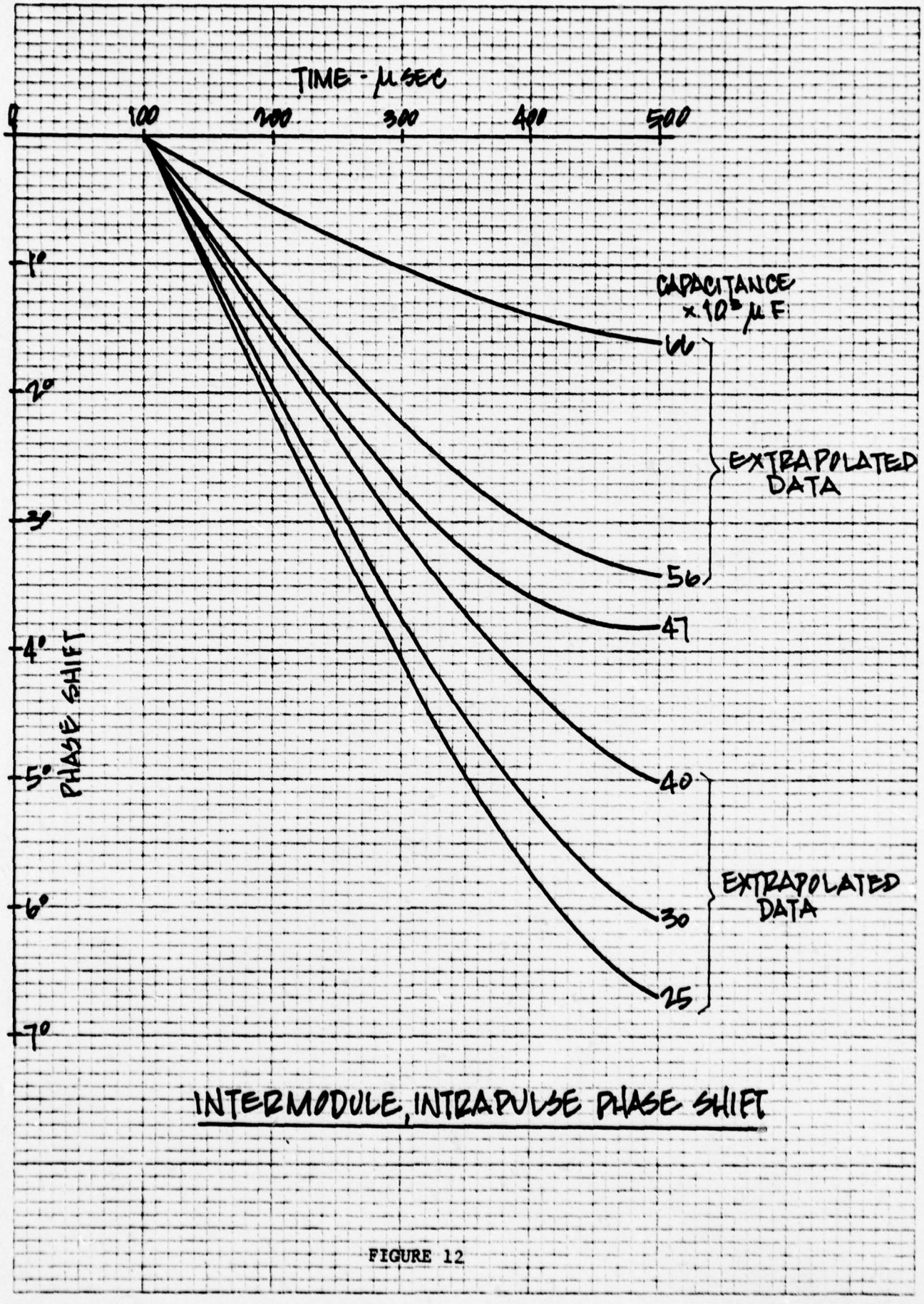

TIME - μSEC
0
100
200
300
400
500
1°
2°
3°
4°
5°
6°
7°
PHASE SHIFT
CAPACITANCE
×10⁻⁵ μF
100
56
47
40
30
25
EXTRAPOLATED DATA
EXTRAPOLATED DATA
INTERMODULE, INTRAPULSE PHASE SHIFT

FIGURE 12

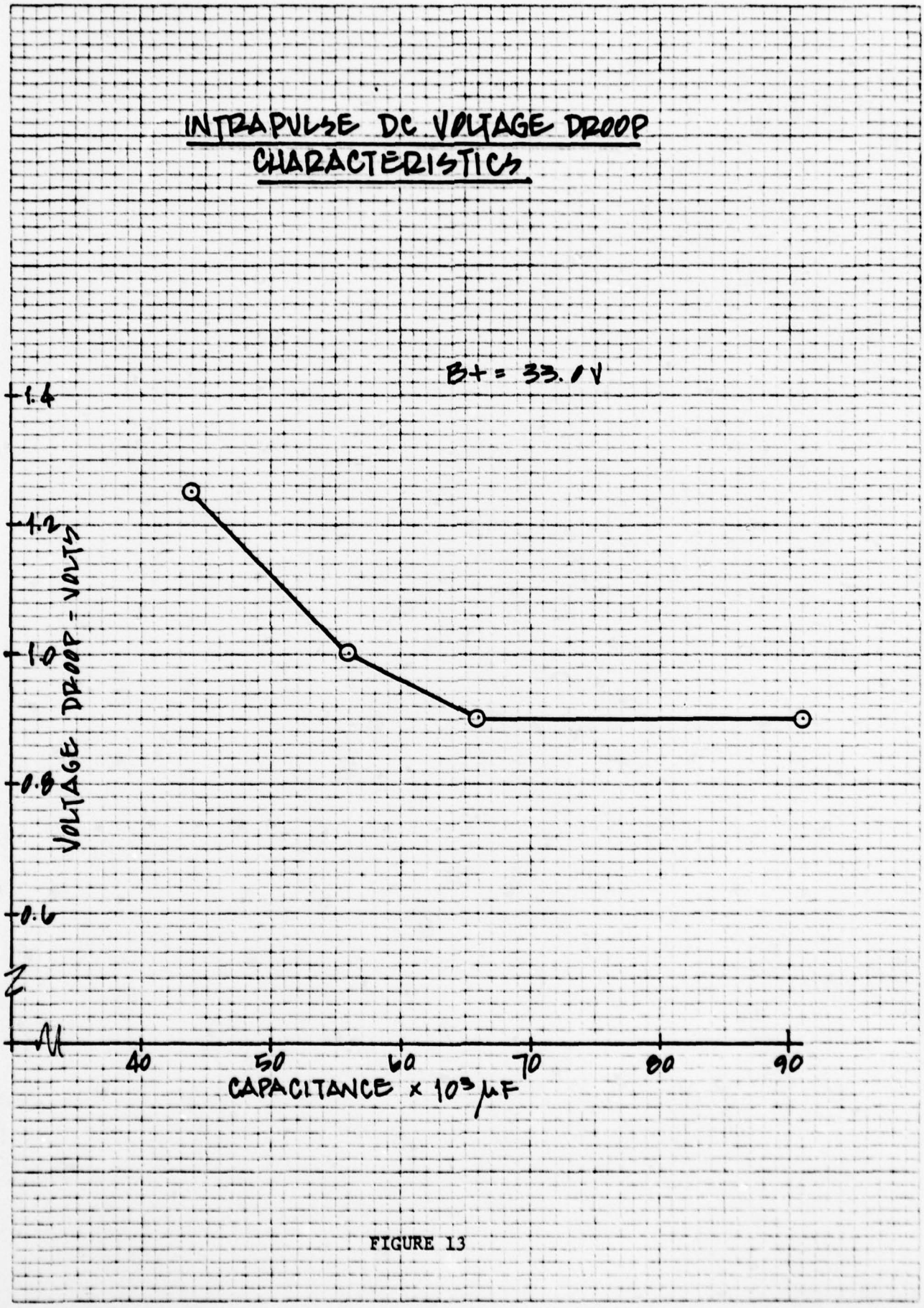
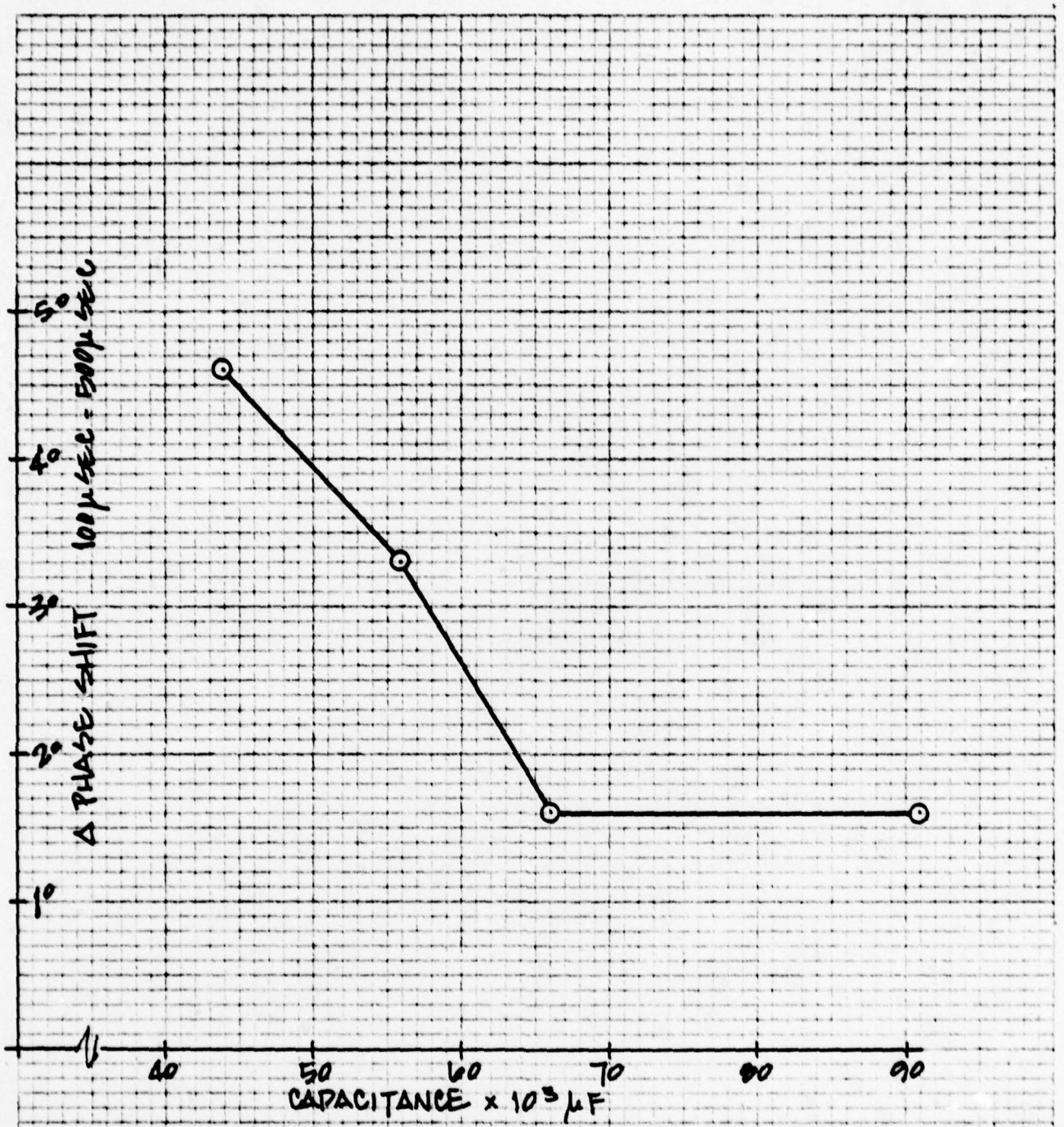

INTRAPULSE D.C. VOLTAGE DROOP CHARACTERISTICS
B+ = 33.0 V
1.4
1.2
1.0
0.8
0.6
VOLTAGE DROOP - VOLTS
40
50
60
70
80
90
CAPACITANCE x 10³ µF

FIGURE 13



INTERMODULE, INTRAPULSE PHASE SHIFT AS A FUNCTION OF CAPACITANCE

FIGURE 14

3.0 PULSE COMPRESSION SIMULATION

The all solid-state transmitter design of the radar mandates the use of a very wide transmit pulse for long range detection. To meet the range resolution requirement, a high pulse compression ratio, nominally 1024:1 must be used. These operating conditions raise questions regarding the pulse compression performance characteristics with phase and amplitude variations during the 395 microsecond pre-processor pulse. A computer simulation of the pulse compression processing was used to analyze the specific case of a linear FM "chirp" transmitted waveform (the preferred system choice principally because of its low range sidelobes and doppler tolerant charactertics).

Pulse compression is a technique which allows the transmission of a long coded pulse, and by suitably processing the radar return signal, obtains a narrow output pulse. The linear FM signal, the amplitude and frequency functions of the transmitted waveform are shown in Figure 15.

The compressed narrow pulse is obtained by passing the received echo through a "matched filter" whose phase dispersion is equal and opposite to that of the transmitted pulse waveform. The output of this matched filter approximates a sin x/x waveshape, where the 4 dB pulse width has been compressed by a factor of $1/\Delta$ fT and where the amplitude is increased by a factor of Δ fT. The dimensionless number $D = \Delta$ fT is the dispersion factor, or compression ratio, defining the ratio of input to output pulse width.

Generally, the filter's transfer response is modified because the perfectly "matched filter" with its rectangular amplitude weighting produces undesired sidelobes, the maximum peak of which is only 13.2 dB below the peak of the compressed pulse. These sidelobe levels can be substantially reduced by a suitable amplitude weighting of the filter response, such as Taylor weights which provide a specified sidelobe level with a minimum compressed pulse width widening. Weighting (tapering) of the filter response will also de-emphasize the leading and trailing edges of the pulse, thus minimizing the effects of large phase deviations during the transient turn on region.

A computer program which simulates the pulse compression processing algorithm was developed to study the effects of various pre-processing waveform perturbations. The program provides for the introduction of arbitrary amplitude and phase error functions and the selection of standard amplitude weighting functions.

The computer simulation was used to determine the effects of amplitude and phase variations in the pre-processed long pulse waveform arising from the solid state transmitter characteristics and the sensitivity time control (STC) function of the radar.

The Conformal Radar is designed to operate in air and surface surveillance modes with nominal range resolution of 190 feet. The two compression ratios selected were 64:1 for the short range (8-40 NM) mode, requiring a 2 NM transmitted pulse length (24.7 microseconds), and 1024:1 for the long range (40-250 NM) mode requiring a 32 NM transmitted pulse length (395.1 microseconds). The Taylor and Hamming weighting functions provide the required 30 dB and 40 dB peak sidelobe level suppression for the air and surface surveillance modes respectively.

The analytical results of the pulse compression computer simulation study are presented for each of the special cases considered. Compressed output pulses were plotted and include expanded range plots in the vicinity of the compressed pulse. The most significant results are tabulated and summarized in Table 2.

TABLE 2

PULSE COMPRESSION SUMMARY OF RESULTS

PRE-COMPRESSED WAVEFORM	WEIGHTING	FIGURES	COMPRESSED PULSE GAIN-LOSS dB	COMPRESSED PULSE 3 DB PLS WIDTH feet	SIDELOBE LEVEL, REMARKS (below mainbeam)
Nominal Condition	uniform	21, 22	0.0	165	>13.2 dB
	Taylor (30 dB)	18, 19, 20	0.0	216	>30.7 dB, >40 dB at >±.4 NM, >50 dB at >±1.1 NM
	Hamming	17	0.0	246	>43.5 dB, >60 dB >±1.7 NM
STC (40 NM Target)	Taylor (30 dB)	29	-8.1	250	>27.8 dB, >40 dB at> ±.5 NM, >78 dB at + 32 NM, >97 dB at -32 NM
	Hamming	28	-8.3	266	>40 dB, >78 dB at +32 NM >106 dB at -32NM
90° Linear Phase Function	Taylor	24, 25, 26	0.0	217	>30.4 dB, 3 dB center shifted 109 feet
	Hamming				

3.1 Nominal Conditions

Pulse compression characteristics were obtained for ideal pre-processed received pulses (i.e. no phase or amplitude perturbations). The 64:1 compression ratio with Hamming weighting was computed for 1024 sampling intervals (16 x 64) and is shown in Figure 16.

Similar runs were made for the 1024:1 compression ratio, except that the relative number of sampling intervals was substantially reduced (5 x 1024) in order to keep computer run times reasonable. The pulse compression characteristics for Hamming and Taylor weighting are shown in Figures 17 and 18 respectively. Expanded range plots in the vicinity of the compressed pulse are presented for the Taylor weights in Figures 19 and 20. The latter plot includes a print out of both the range interval number (equivalent to 38 feet for the 1024:1 case) and the relative dB power level. The sidelobe levels and pulse width widening effects were as expected.

A computer run was also made for 1024:1 pulse compression with uniform weighting and the results, included in Figures 21 and 22 for general interest, produced the expected 13.2 dB sidelobe levels with a correspondingly narrow 164 foot pulse width.

3.2 Phase and Amplitude Perturbations

Laboratory tests of a solid state UHF transmitter module producing a 500 microsecond wide pulse indicate that the power amplifier exhibits a large phase shift at the start of the pulse that decays exponentially with time. Typical phase characteristics can be approximated by a linear segmented function, with values of 15°, 9°, 6° and 2° at 1, 10, 100 and 500 microseconds. Since this phase function produced no significant effects upon a 64:1 pulse compression ratio, the function was multiplied by a safety factor of 3 to simulate upper limits of phase characteristics and again applied to the 24.7 microsecond transmitted pulse of the short range mode. The primary effects (Figure 23) were an increase in sidelobe levels to -38.3 dB, accompanied by a slight asymmetry (i.e. range shift) in the compressed pulse. The 1024:1 pulse compression case (Figures 24, 25 and 26) was run with a more extreme phase characteristic, a 90° linear variation over the 395 microsecond pulse. For the 30 dB Taylor weighting condition, the principal effect was a

109 foot shift in the location of the compressed pulse 3 dB center, with negligible changes in sidelobe levels.

The amplitude sensitivity of pulse compression was studied to establish limits of permissible transmitter AM characteristics. Again an extreme condition was simulated, a 4 dB linear amplitude taper applied to the short range (24.7 microsecond) pulse. Except for the expected loss in the compressed pulse gain (-1.6 dB) and a slight increase in sidelobe levels (-38.1 dB for the 64:1 Hamming weighting case) pulse compression appears relatively insensitive to large amplitude modulation effects.

3.3 Sensitivity Time Control (STC)

The amplitude effect of the STC gain function was analyzed for operation in the long range mode with an assumed target at 40 NM. The STC gain function shown in Figure 27 compensates for the fourth power amplitude variation with range, by providing a 28 dB increase in gain during the 395 microsecond echo pulse interval. The primary effects of STC are a 8 dB loss in the peak of the pulse, a sligth widening of the compressed pulse, and a few dB degradation in sidelobe levels. The compressed pulse characteristics shown in Figures 28 and 29 have sidelobes below -27.9 dB and 40 dB for Taylor and Hamming weighting.

3.4 Conclusions

Significant conclusions derived from the pulse compression simulations are:

- Relatively small phase and amplitude disturbances, characteristic of the UHF solid state transmitter module, present no significant problem to pulse compression
- The sensitivity time control function, whose most severe effect is exhibited for a 40 NM target, results in a range sidelobe level increase of a few dB, and a slight widening in the compressed pulse width. This effect decreases for targets at longer ranges since the pre-compressed pulse is subjected to a smaller amplitude change during the pulse interval.

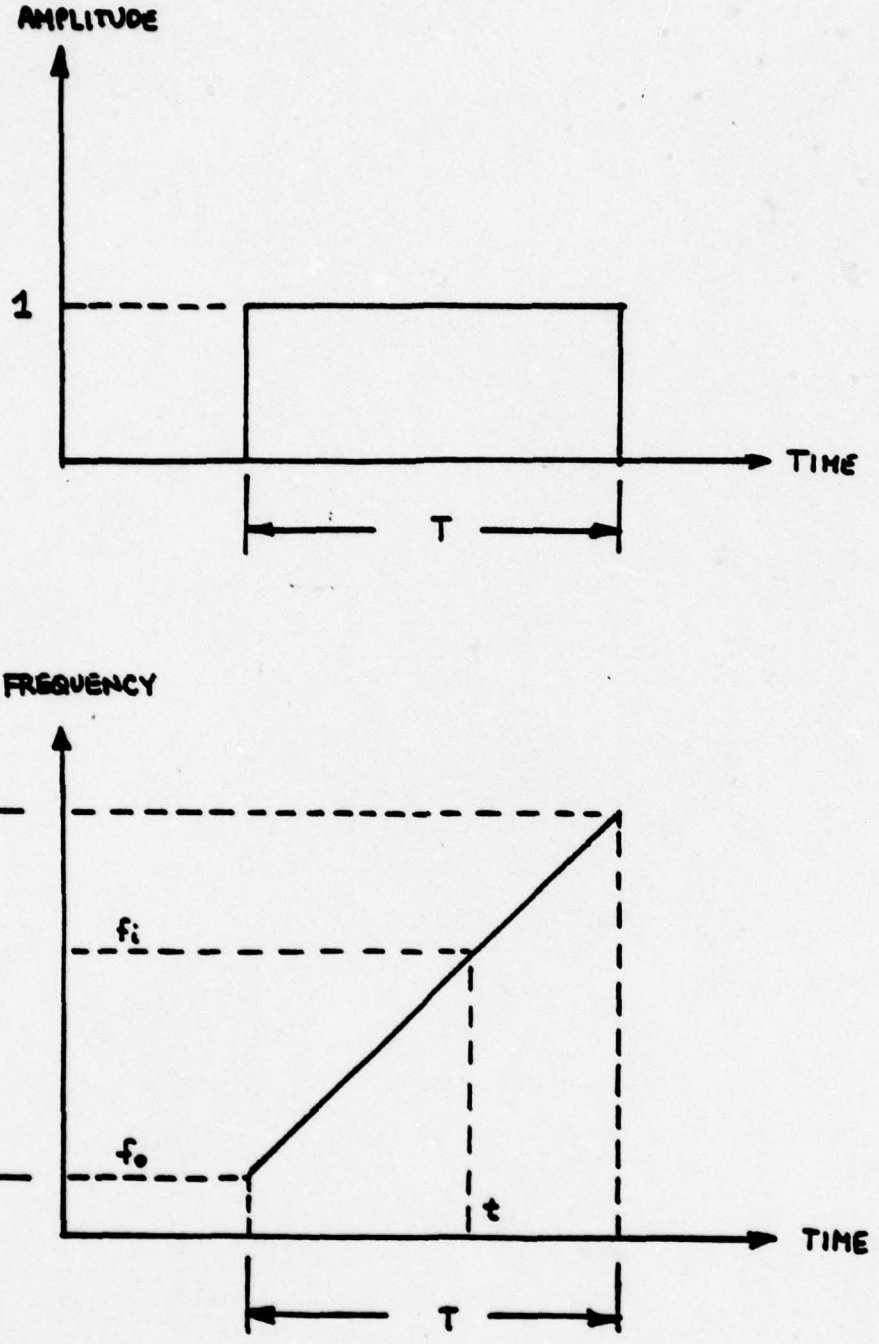


FIGURE 15 ENVELOPE AND FREQUENCY CHARACTERISTICS OF FM "CHIRP" SIGNAL

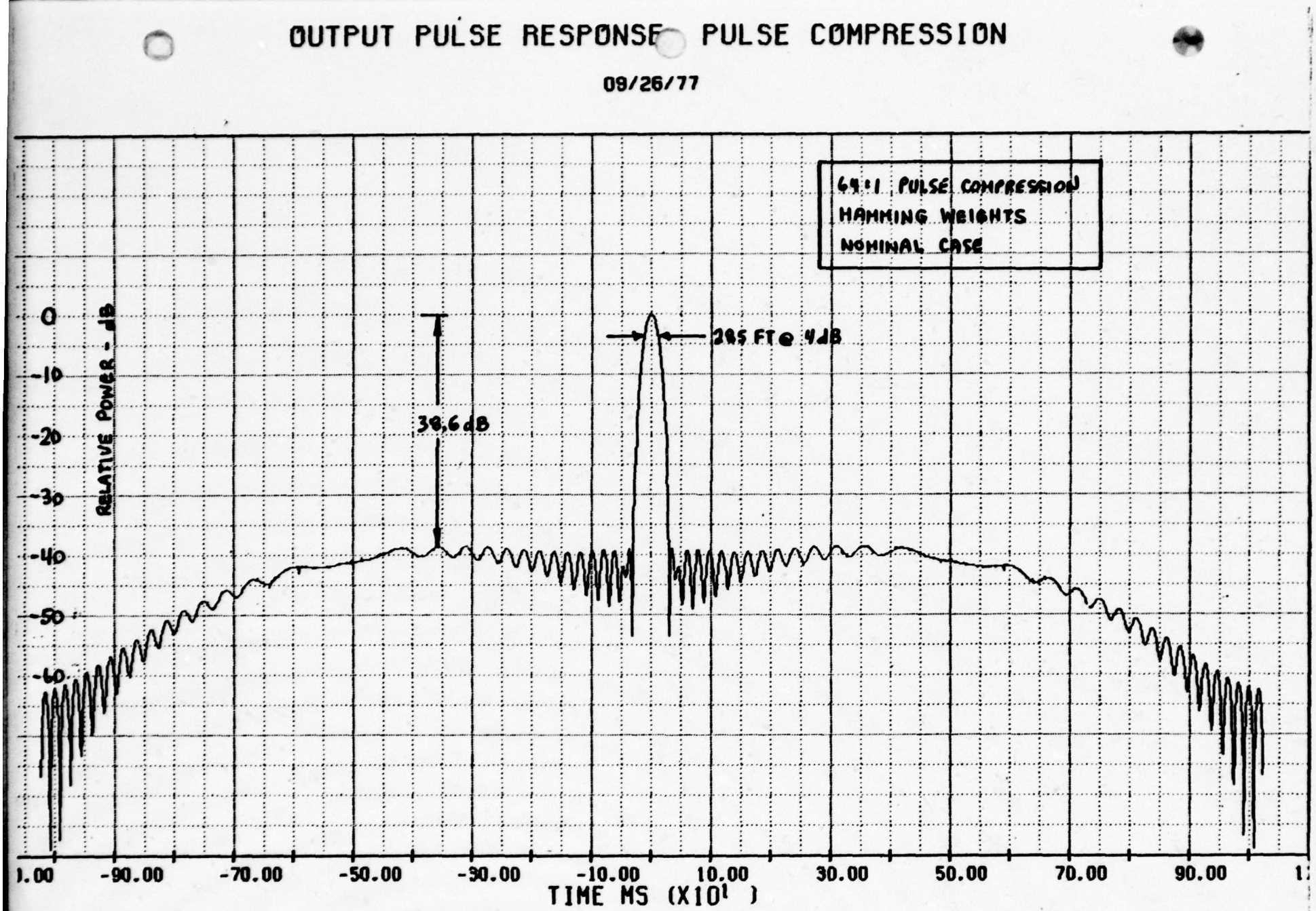


FIGURE 16 - (64:1) NOMINAL CASE

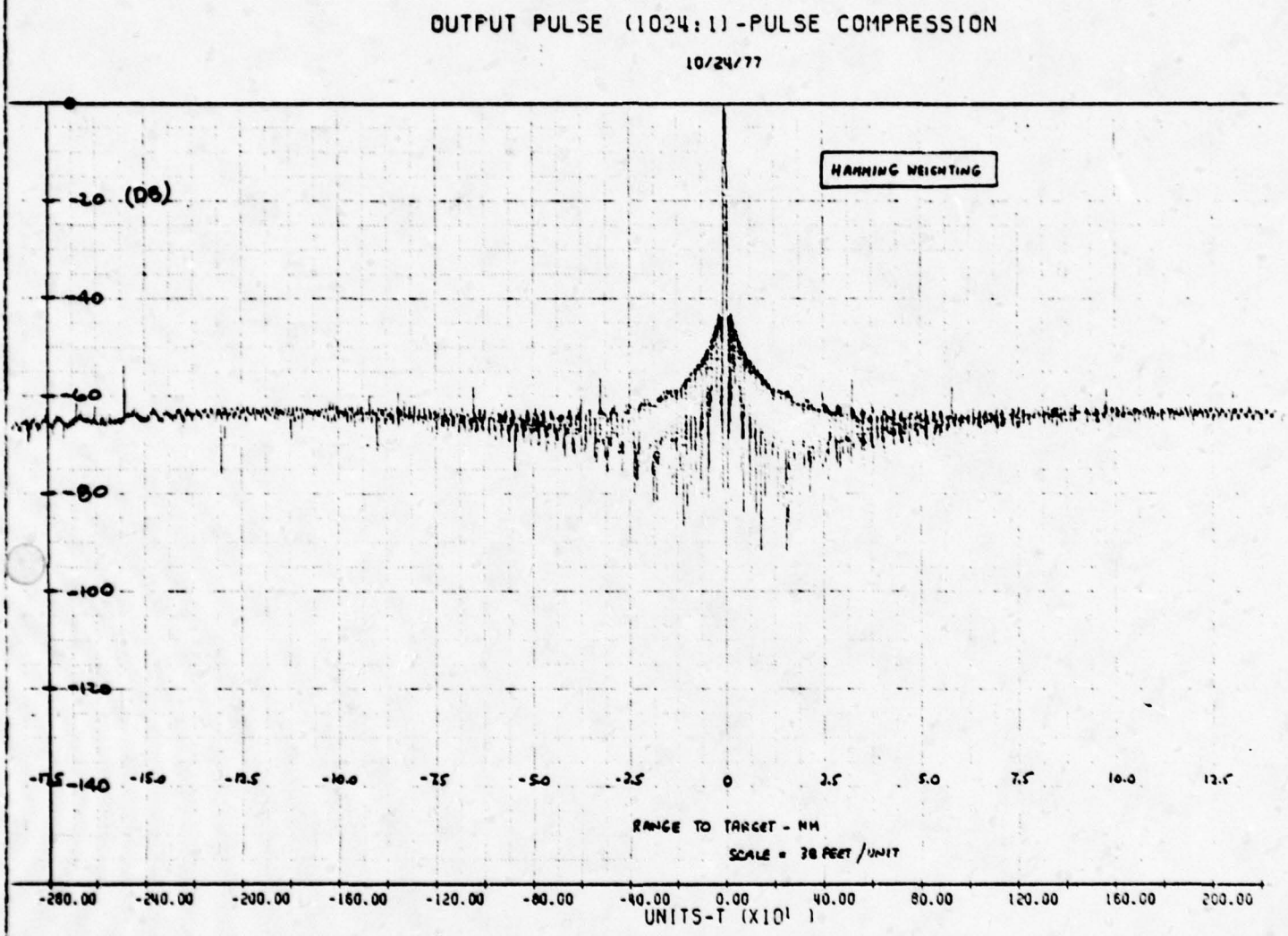


FIGURE 17 - HAMMING WEIGHTING

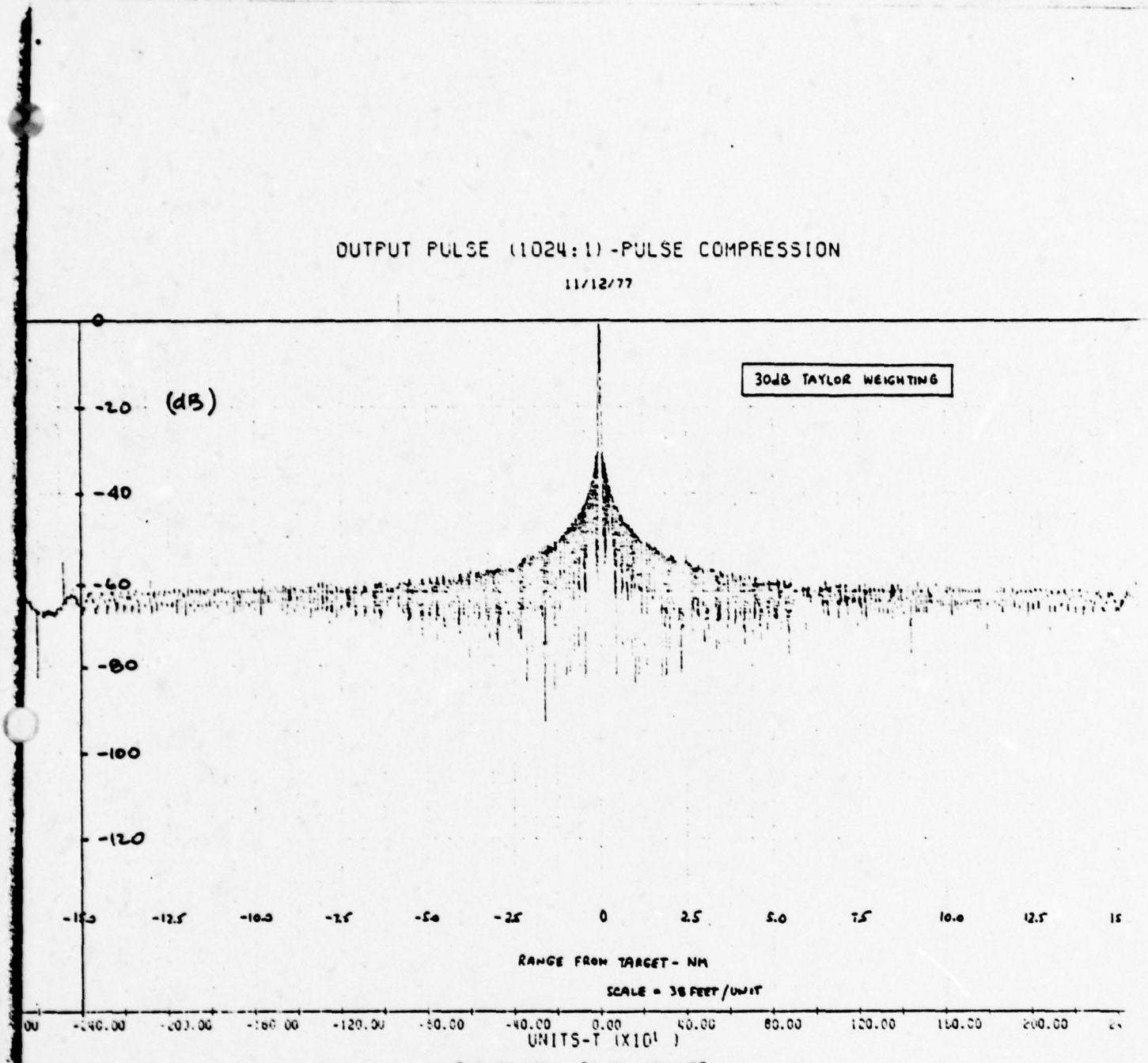


FIGURE 18 - 30dB WEIGHTS

SECTOR OF PULSE COMPRESSION

11/12/77

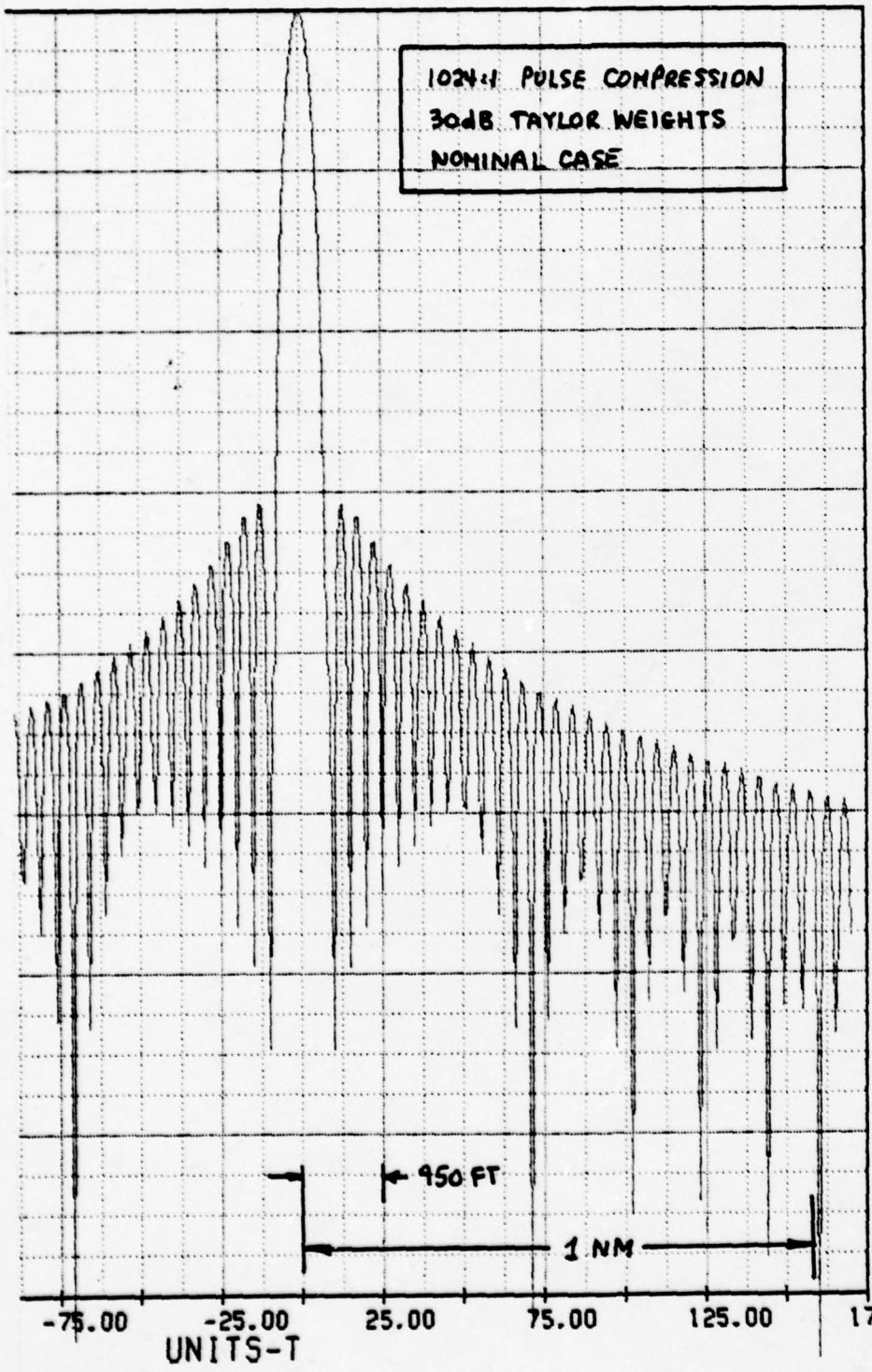


FIGURE 19 - (1024:1) 30dB NOMINAL

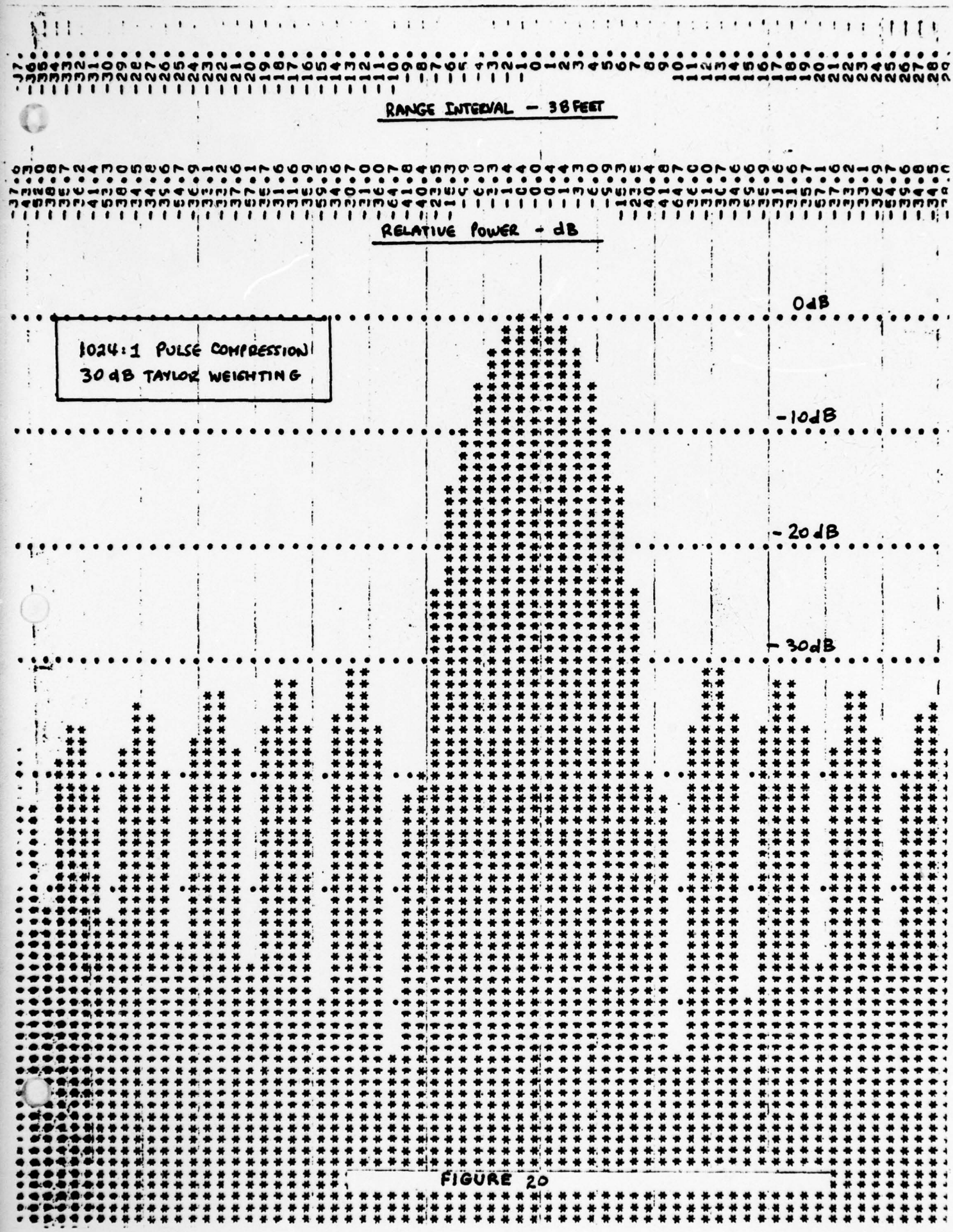

RANGE INTERVAL – 38 FEET
RELATIVE POWER – dB
0dB
-10dB
-20dB
-30dB
1024:1 PULSE COMPRESSION
30 dB TAYLOR WEIGHTING

FIGURE 20

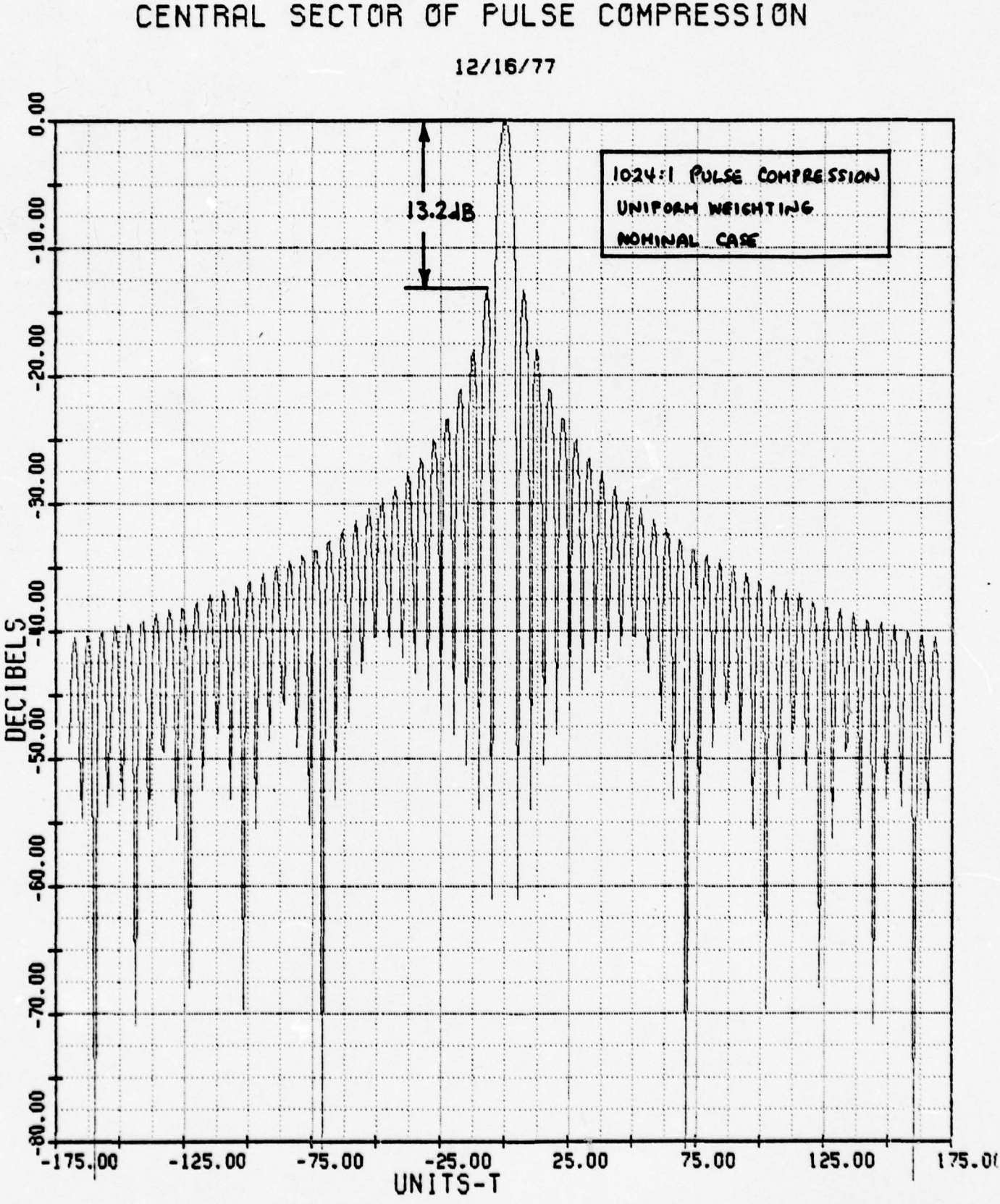


FIGURE 21 - UNIFORM WEIGHTING

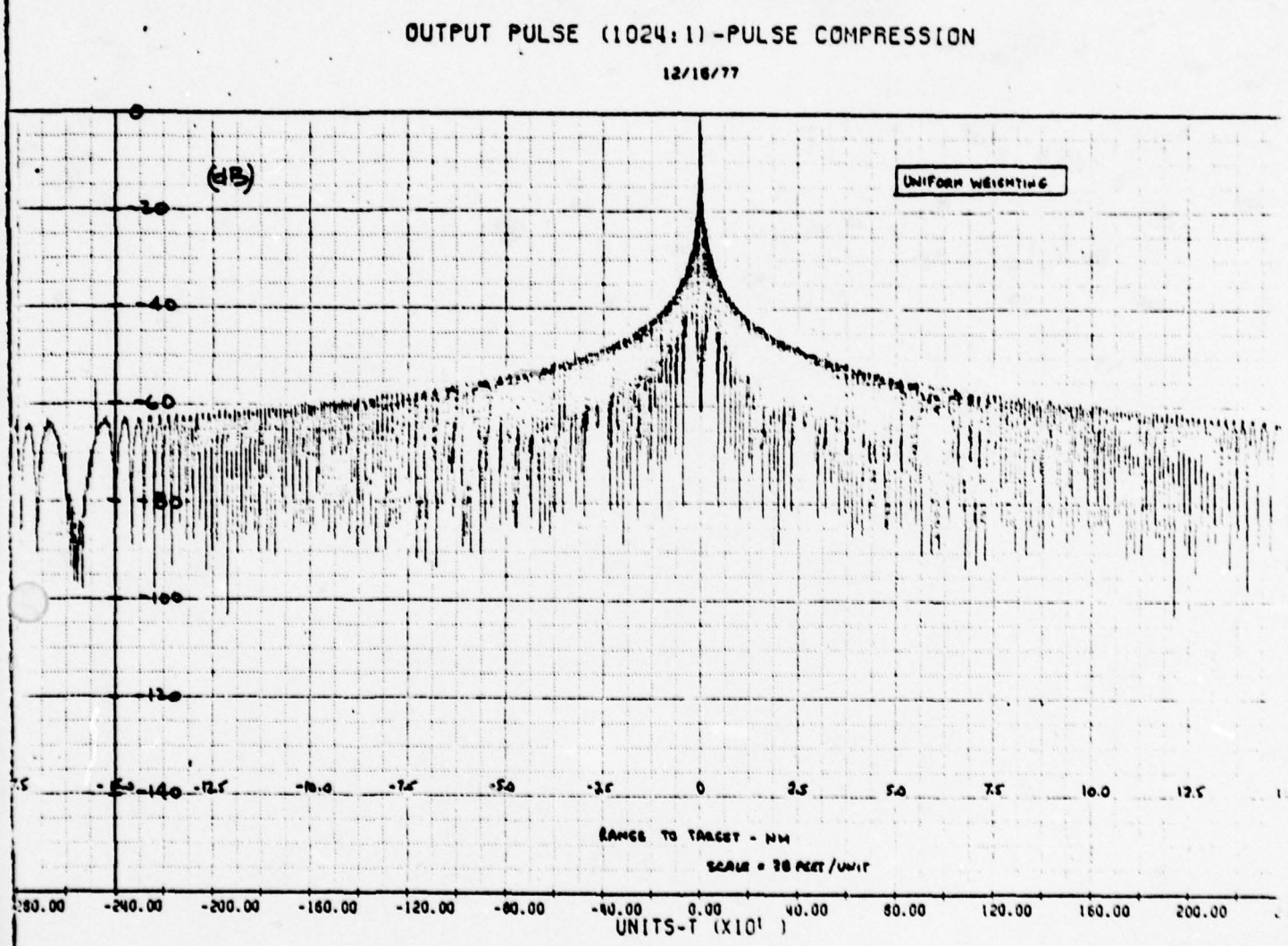
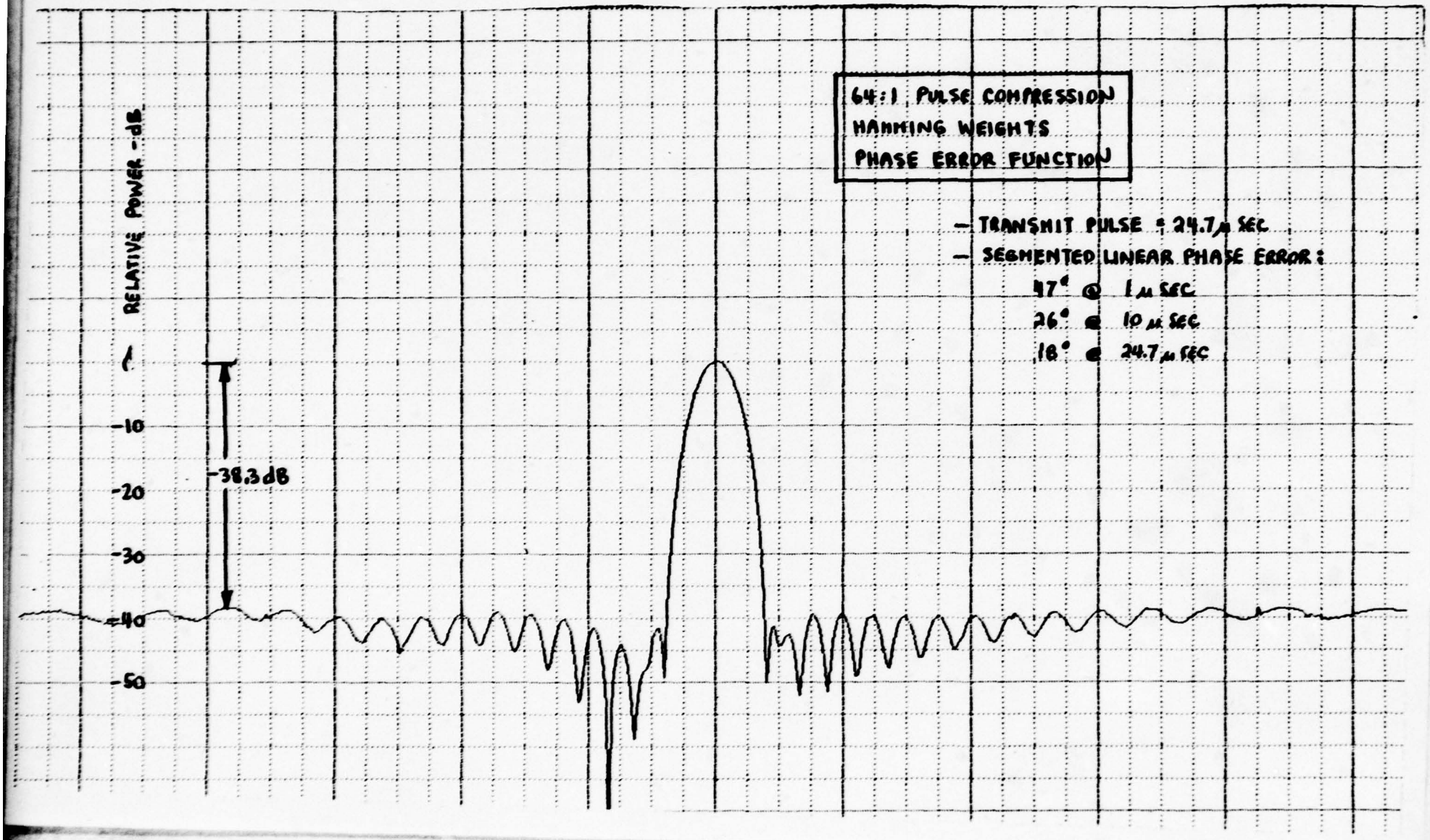


FIGURE 22- UNIFORM WEIGHTING

FIGURE 23


64:1 PULSE COMPRESSION
HAMMING WEIGHTS
PHASE ERROR FUNCTION
- TRANSMIT PULSE = 24.7 μ SEC
- SEGMENTED LINEAR PHASE ERROR:
47° @ 1 μ SEC
26° @ 10 μ SEC
18° @ 24.7 μ SEC
RELATIVE POWER - dB
0
-10
-20
-30
-40
-50
-38.3 dB

OUTPUT PULSE (1024:1)-PULSE COMPRESSION

11/12/77

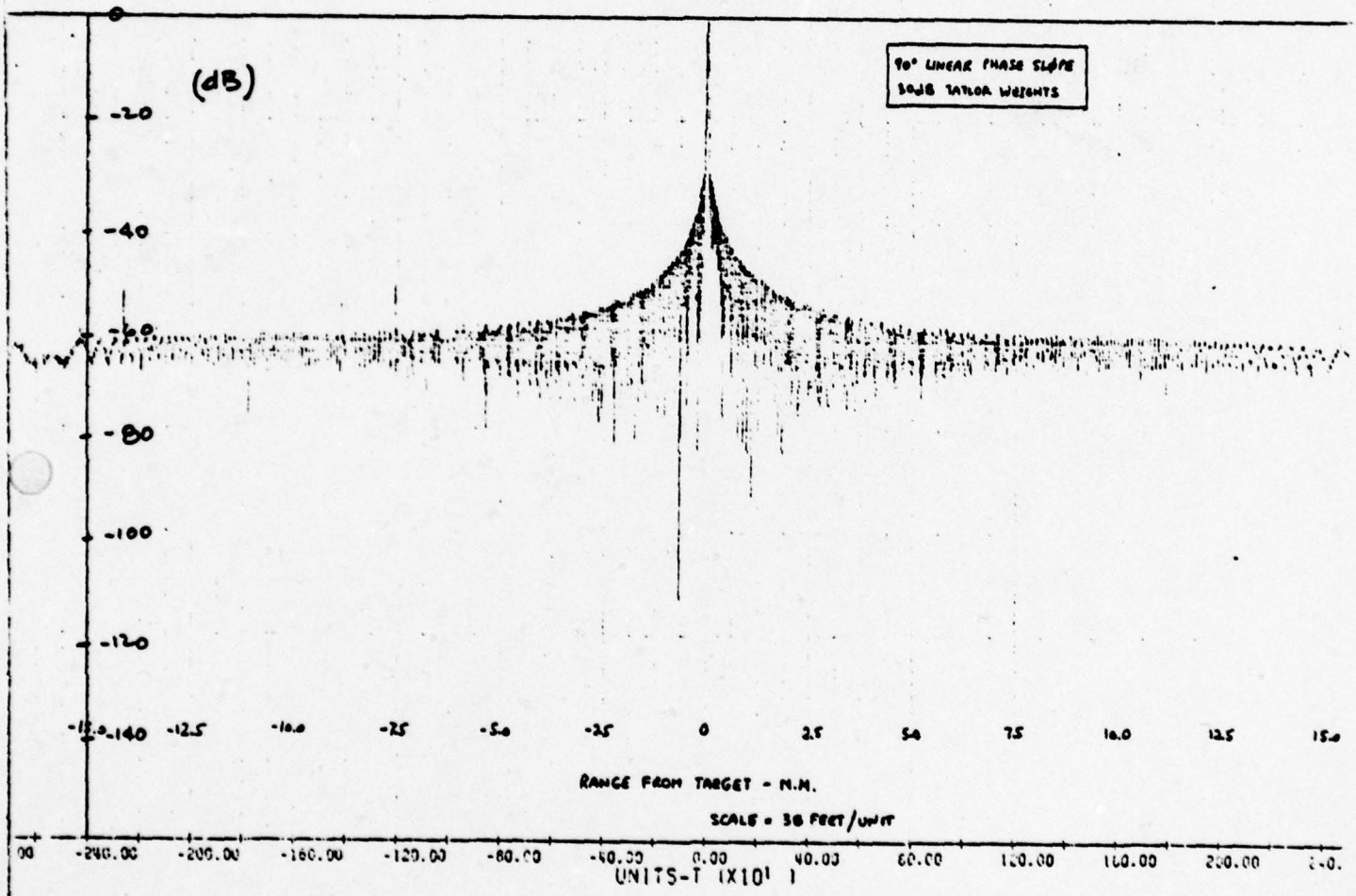


FIGURE 24 - PHASE ERROR FUNCTION

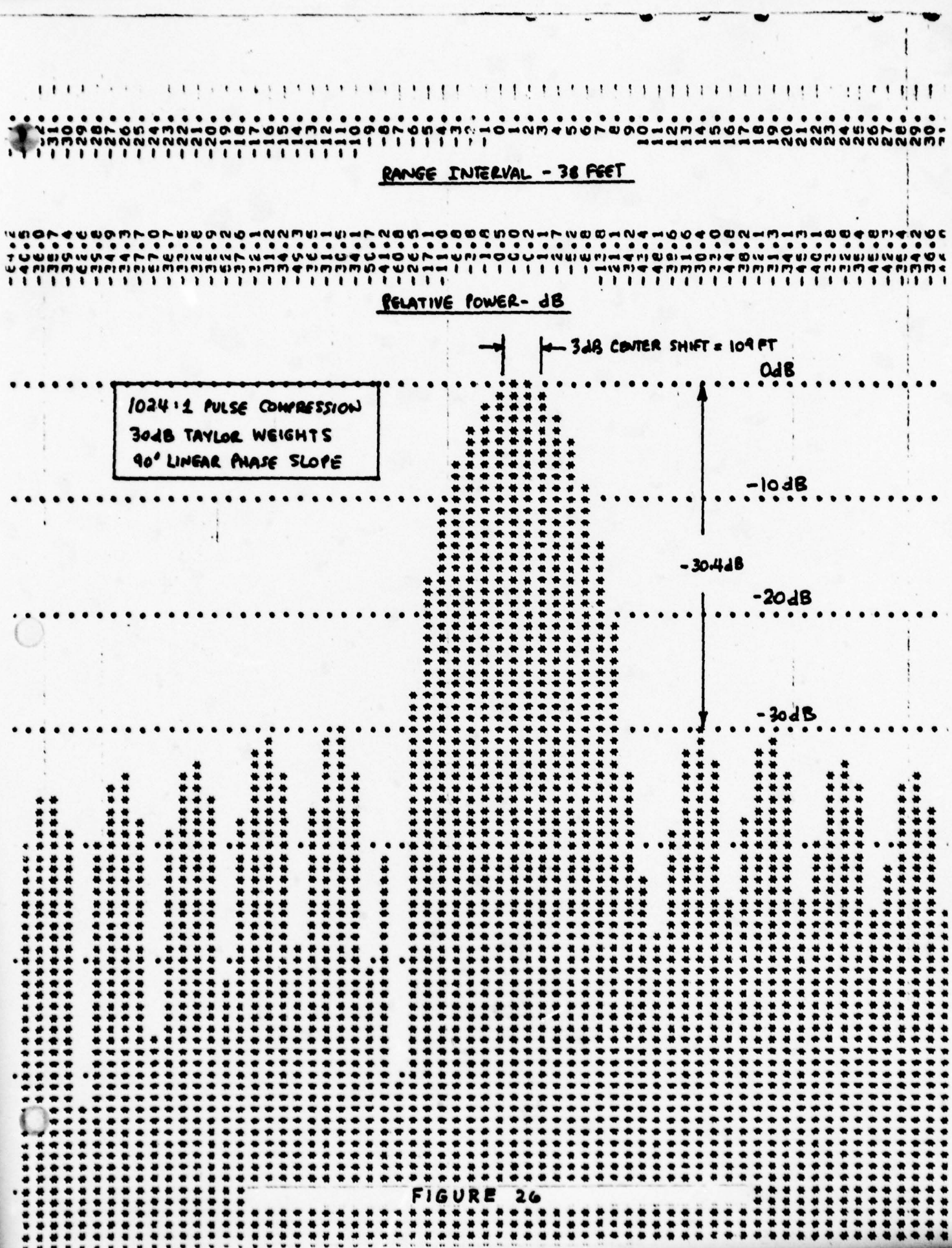

RANGE INTERVAL - 38 FEET
RELATIVE POWER - dB
3dB CENTER SHIFT = 109 FT
0dB
-10dB
-30.4dB
-20dB
-30dB
1024:1 PULSE COMPRESSION
30dB TAYLOR WEIGHTS
90° LINEAR PHASE SLOPE

FIGURE 26

CENTRAL SECTOR OF PULSE COMPRESSION

11/12/77

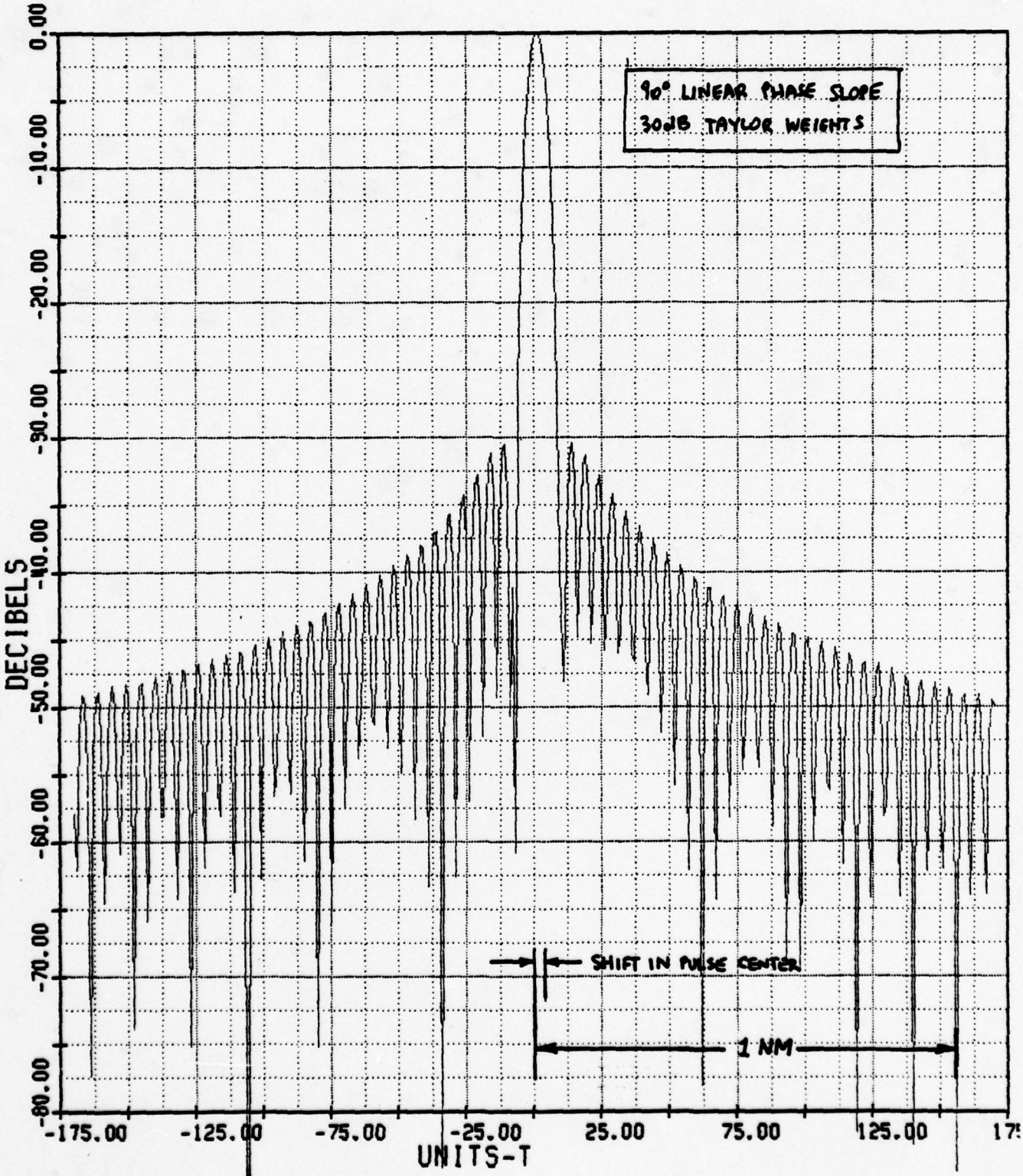


FIGURE 25

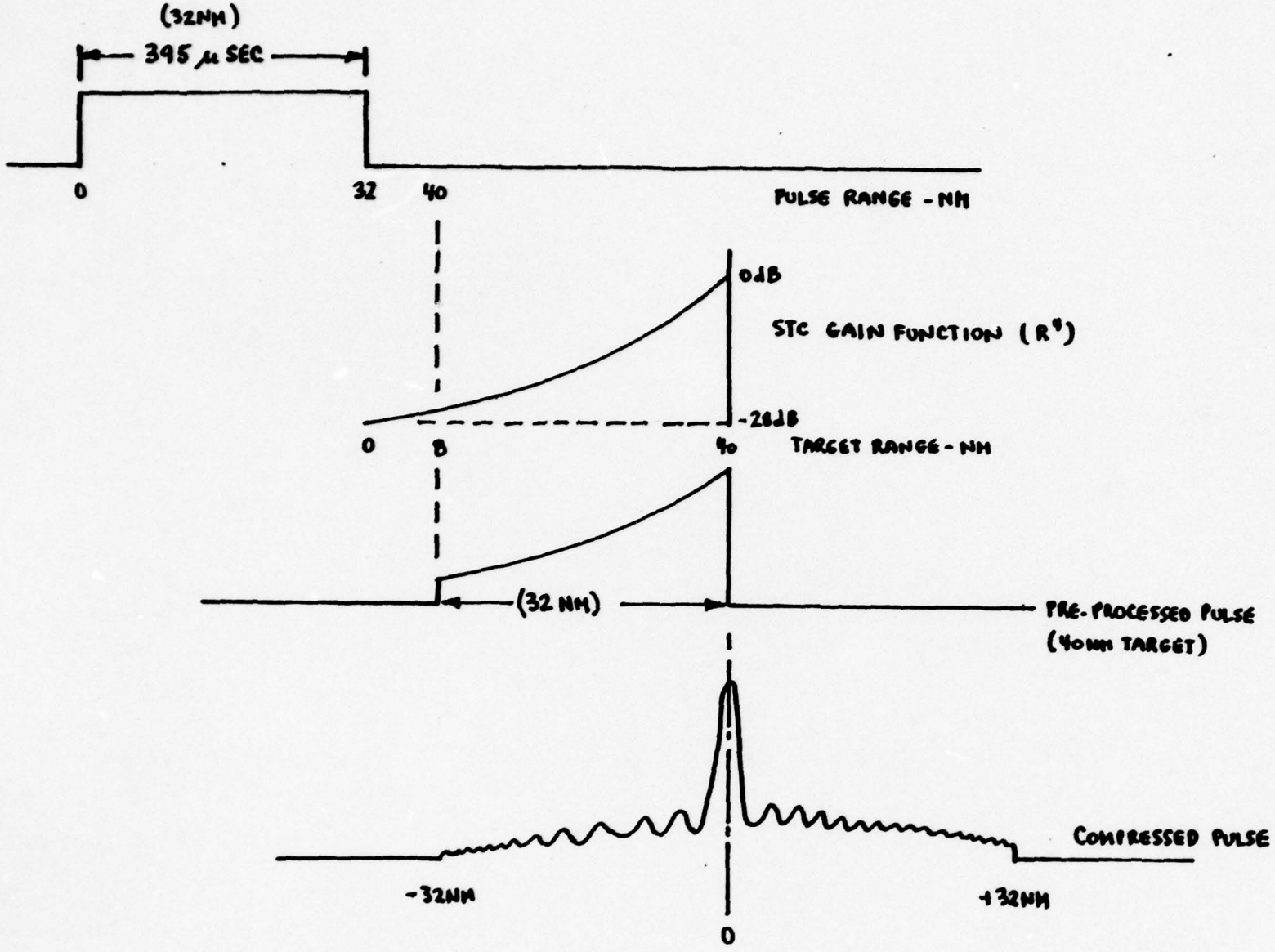


FIGURE 27 - SENSITIVITY TIME CONTROL (STC)

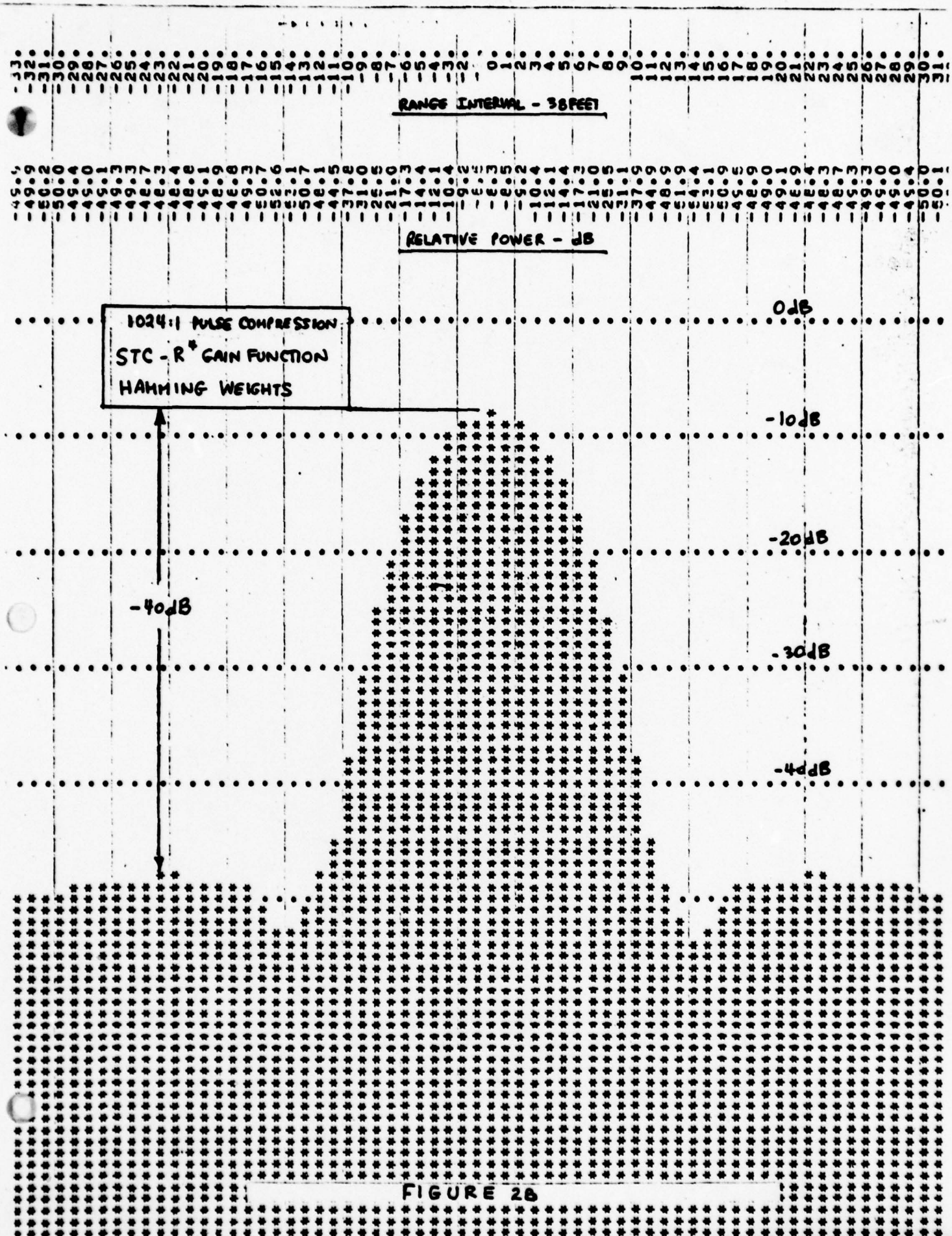

RANGE INTERVAL - 38 FEET
RELATIVE POWER - dB
1024:1 PULSE COMPRESSION
STC - R⁴ GAIN FUNCTION
HAMMING WEIGHTS
0dB
-10dB
-20dB
-30dB
-40dB
-40dB

FIGURE 28

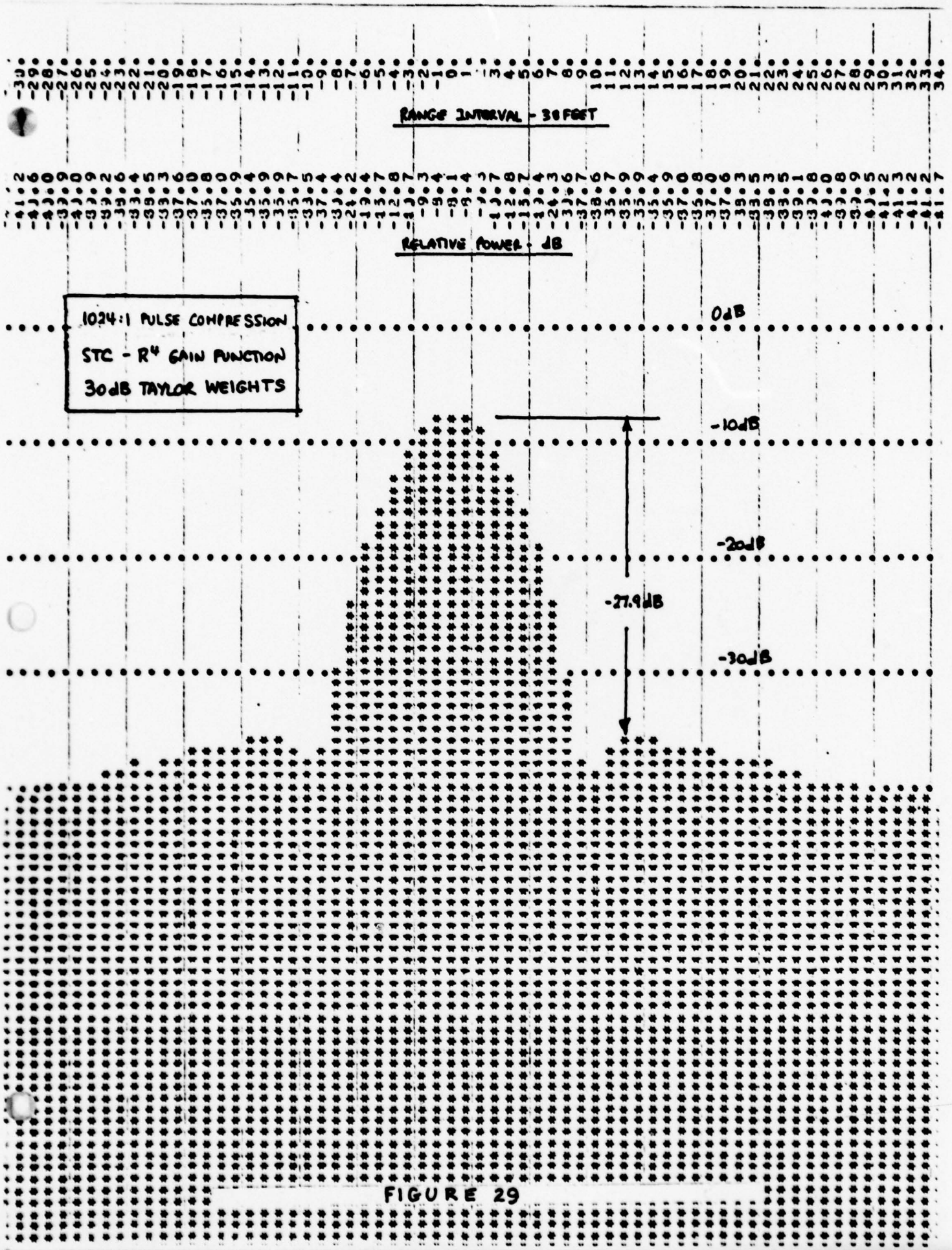

RANGE INTERVAL - 38 FEET
RELATIVE POWER - dB
1024:1 PULSE COMPRESSION
STC - R⁴ GAIN FUNCTION
30dB TAYLOR WEIGHTS
0dB
-10dB
-20dB
-27.9dB
-30dB

FIGURE 29

4.0 ANTENNA PATTERN PREDICTION

An antenna pattern simulation study was performed to quantitatively evaluate the effects of phase and amplitude variations on the overall array characteristics.

A 3 dB stepped amplitude taper (i.e. 0.5 KW, 0.5 KW, 1.0 KW, 1.0 KW, 2.0 KW, 2.0 KW, 2.0 KW, symmetrically) was used to achieve a transmit antenna pattern having its mean major sidelobes 21.5 dB below the main beam. A computer program utilizing a vectorial summation of the individual element response functions to obtain an array pattern was developed. The program allows for incorporation of a quantized error function at each element. The transmit pattern with no error sources, is shown in Figure 30.

This error analysis is directed to performance of the transmit pattern. The receive pattern will undergo additional processing in a real life application and is not addressed in this study.

4.1 Error Analysis

Amplitude and phase errors were introduced into the antenna elements of the baseline design to determine their effect on antenna pattern characteristics, specifically on the sidelobe levels of the pattern. The program was kept quite general with antenna parameters read from an input data file to provide a flexible analytic tool for obtaining the antenna pattern characteristics of any given error model and quiescent array configuration. The introduced errors are Gaussian distributed random phase and amplitude errors in the element channel of the transmit beam forming network.

The magnitude of the errors were defined in terms of their 1σ (RMS) amplitude and phase values for two distinct error models. Individual element errors were held to maximum $\pm 2\sigma$ limits. Transmit antenna array patterns were computed for fifty different random element error distributions and formed the basis for obtaining a mean value of the peak sidelobe levels.

Identical amplitude errors were postulated for both models (1σ value = $\pm$0.5dB for transmit) representing values considered to be realistic estimates for the contemplated hardware implementation. Expected phase errors are more difficult to predict; Model I representing realistic design goal values ($\pm 5^{\circ}$ transmit) and Model II representing worst case estimates ($\pm 8^{\circ}$ transmit) were considered. The peak sidelobe levels obtained for each of the error models for fifty error iterations are tabulated in Table 3, along with computations of the mean and the standard deviation. The introduction of error from Models I and II increase the mean peak sidelobe levels on transmit from a quiescent peak of -21.5 dB to -19.52 dB and -18.52 dB respectively. Antenna pattern plots (Figures 30 through 36) are included for each error model, the selected plots are of iterations representing the lowest, median and highest sidelobe level cases. As expected, the sidelobe levels are fairly uniform for the low sidelobe case, while the high sidelobe case generally represents a peak appearing at a single angular position.

The results of this portion of the study are summarized and indexed in Table 4.

TABLE 3

ANTENNA PATTERN PEAK SIDELOBE SUMMARY

ITERATION NO.	ERROR MODEL I 0.50 dB 5.00 deg	ERROR MODEL II 0.50 dB 8.00 deg
	SIDELOBE LEVEL	
1	-19.33	-17.78
2	-18.17	-16.89
3	-19.46	-18.43
4	-20.90	-20.22
5	-19.51	-18.57
6	-20.29	-19.94
7	-19.83	-18.77
8	-19.23	-18.72
9	-18.94	-18.39
10	-20.60	-20.43
11	-19.19	-17.92
12	-19.71	-19.04
13	-20.36	-19.07
14	-18.19	-17.33
15	-20.55	-19.42
16	-20.47	-18.92
17	-21.45	-21.01
18	-18.87	-17.74
19	-17.14	-15.70
20	-19.33	-18.14
21	-18.36	-16.91
22	-20.87	-20.30
23	-20.97	-20.51
24	-20.26	-19.38
25	-18.70	-17.57
26	-20.53	-19.34
27	-20.11	-19.15
28	-19.96	-18.36
29	-18.68	-17.48
30	-19.82	-18.53
31	-19.70	-17.87
32	-19.05	-18.40
33	-19.02	-17.99
34	-20.25	-19.25
35	-20.59	-20.00
36	-19.07	-17.96
37	-20.39	-19.87
38	-18.97	-17.74

TABLE 3

ANTENNA PATTERN PEAK SIDELOBE SUMMARY - (cont'd)

	ERROR MODEL	
	I	II
ITERATION NO.	0.50 dB 5.00 deg	0.50 dB 8.00 deg
39	-19.48	-18.77
40	-18.22	-17.17
41	-17.32	-15.93
42	-19.69	-18.28
43	-19.02	-17.60
44	-18.86	-17.95
45	-20.13	-19.52
46	-19.65	-18.93
47	-19.49	-17.98
48	-19.10	-18.15
49	-19.61	-18.71
50	-18.52	-17.99
MEAN	-19.52	-18.52
STANDARD DEVIATION	0.91	1.11

TABLE 4

DATA SUMMARY AND INDEX ANTENNA PATTERN ANALYSIS

FIGURE	MODE	ERROR MODEL		SIDELOBE LEVEL (dB)	BEAMWIDTH (DEG)
30	Transmit	Error Free		-21.5	8.34
31	Transmit	Model I	Minimum	-20.9	9.43
32	Transmit	Model I	Mean	-19.2	8.37
33	Transmit	Model I	Maximum	-17.1	8.41
34	Transmit	Model II	Minimum	-20.2	8.42
35	Transmit	Model II	Mean	-19.4	8.28
36	Transmit	Model II	Maximum	-15.7	6.35

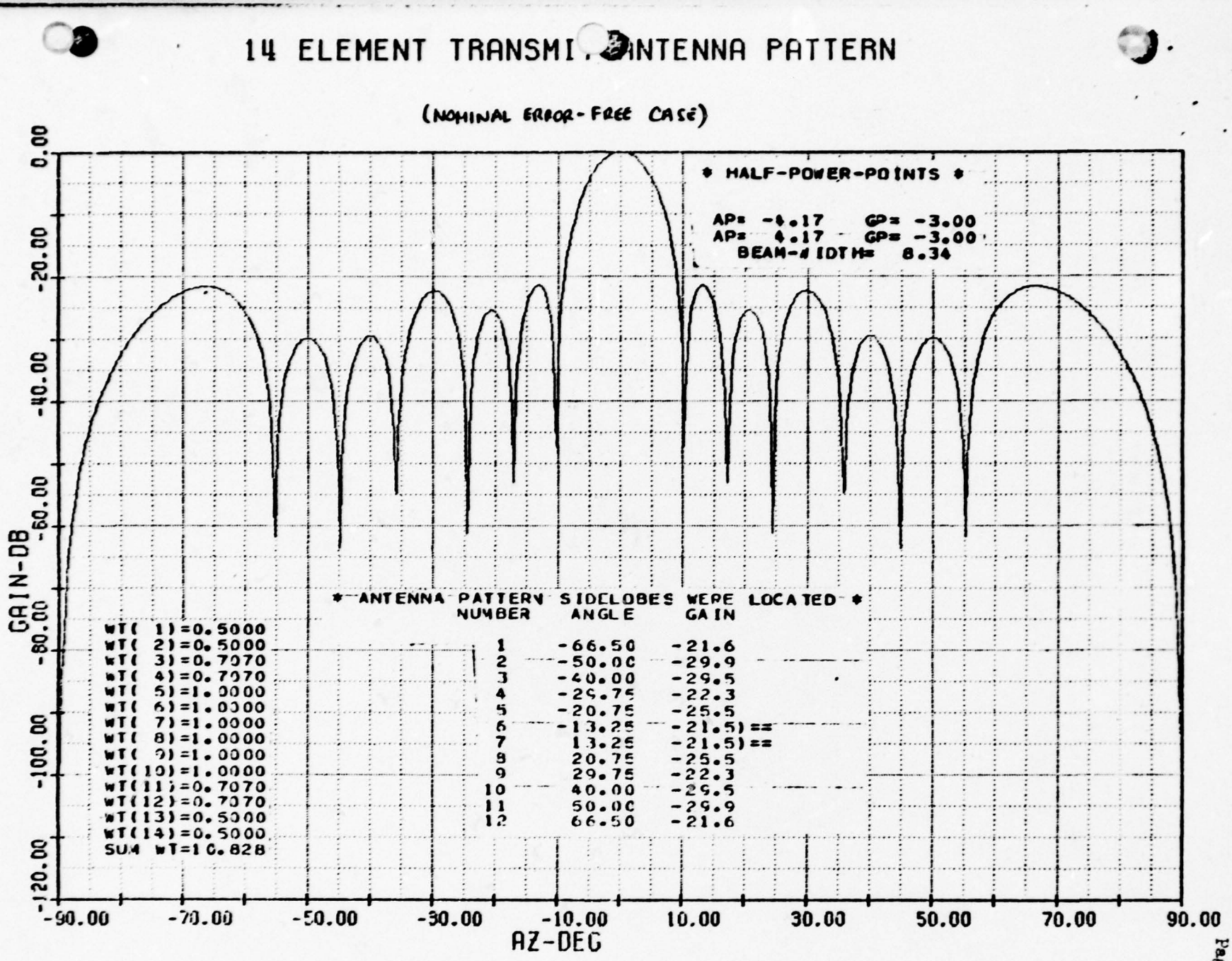


Figure 30 - Transmit Array Antenna Pattern (Nominal)

14 ELEMENT TRANSMIT ANTENNA PATTERN

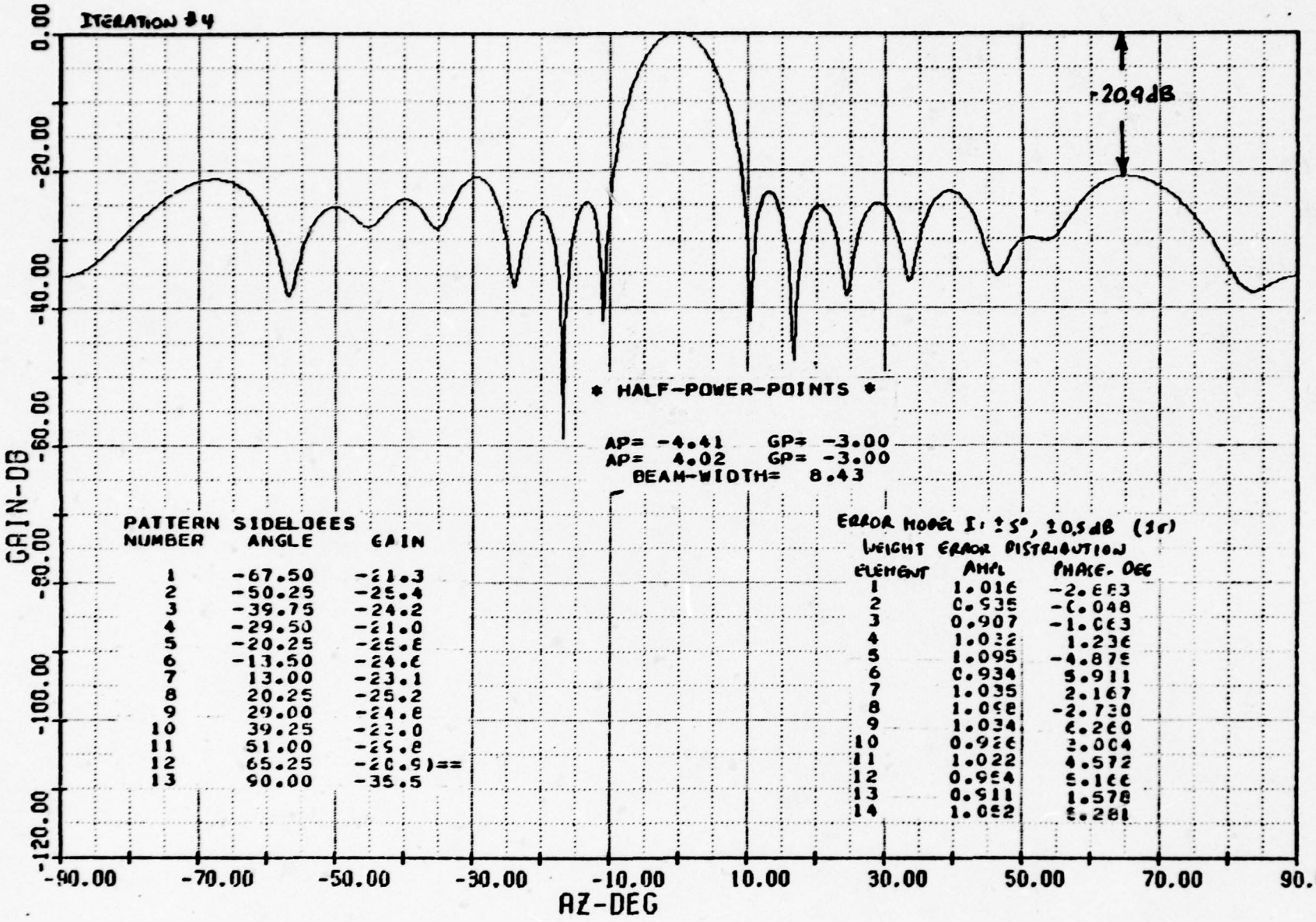


Figure 31 - Transmit Array Antenna Pattern (Error Model I - min. sidelobe level)

14 ELEMENT TRANSMIT ANTENNA PATTERN

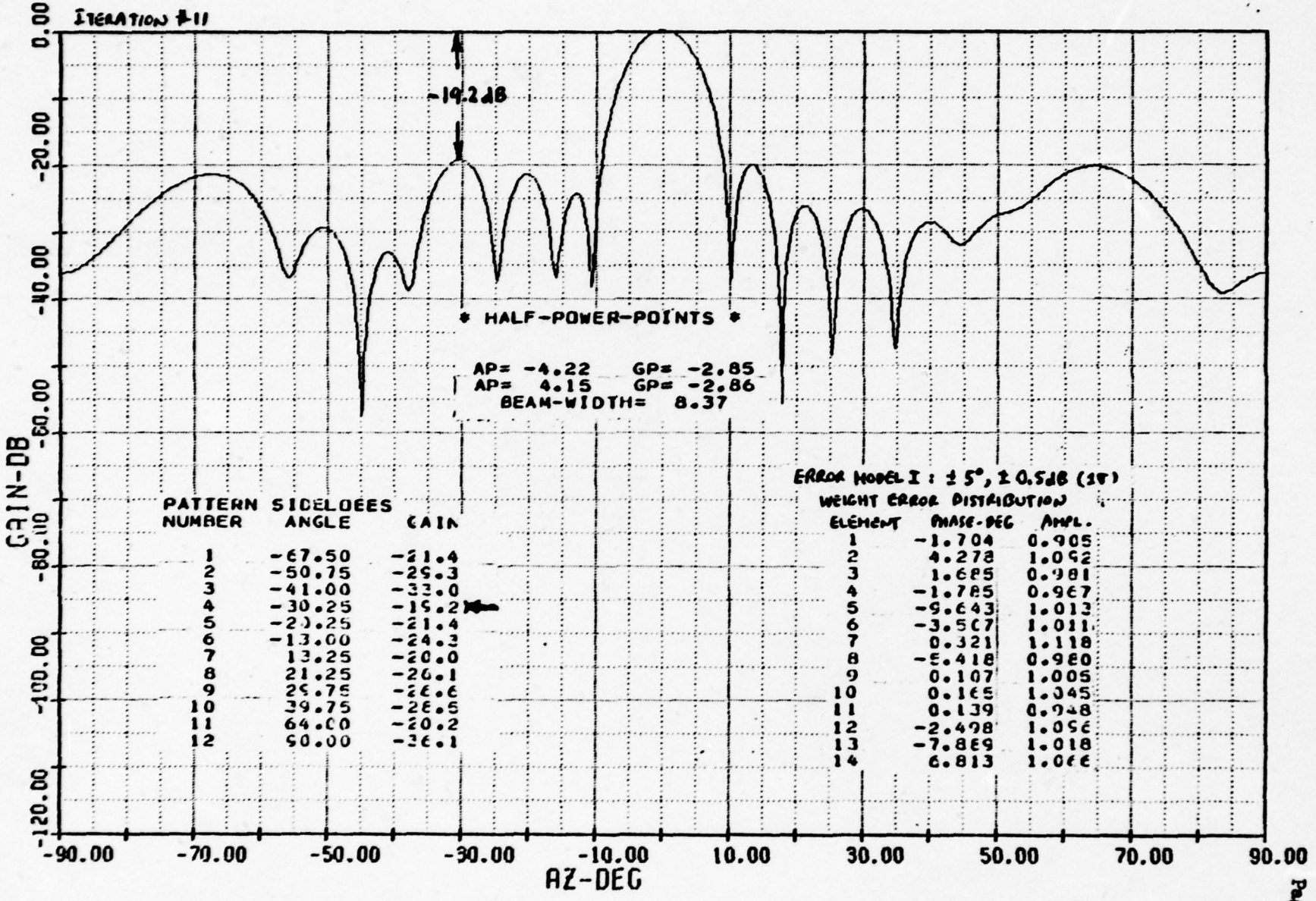


Figure 32 - Transmit Array Antenna Pattern (Error Model I - mean sidelobe level)

14 ELEMENT TRANSMIT ANTENNA PATTERN

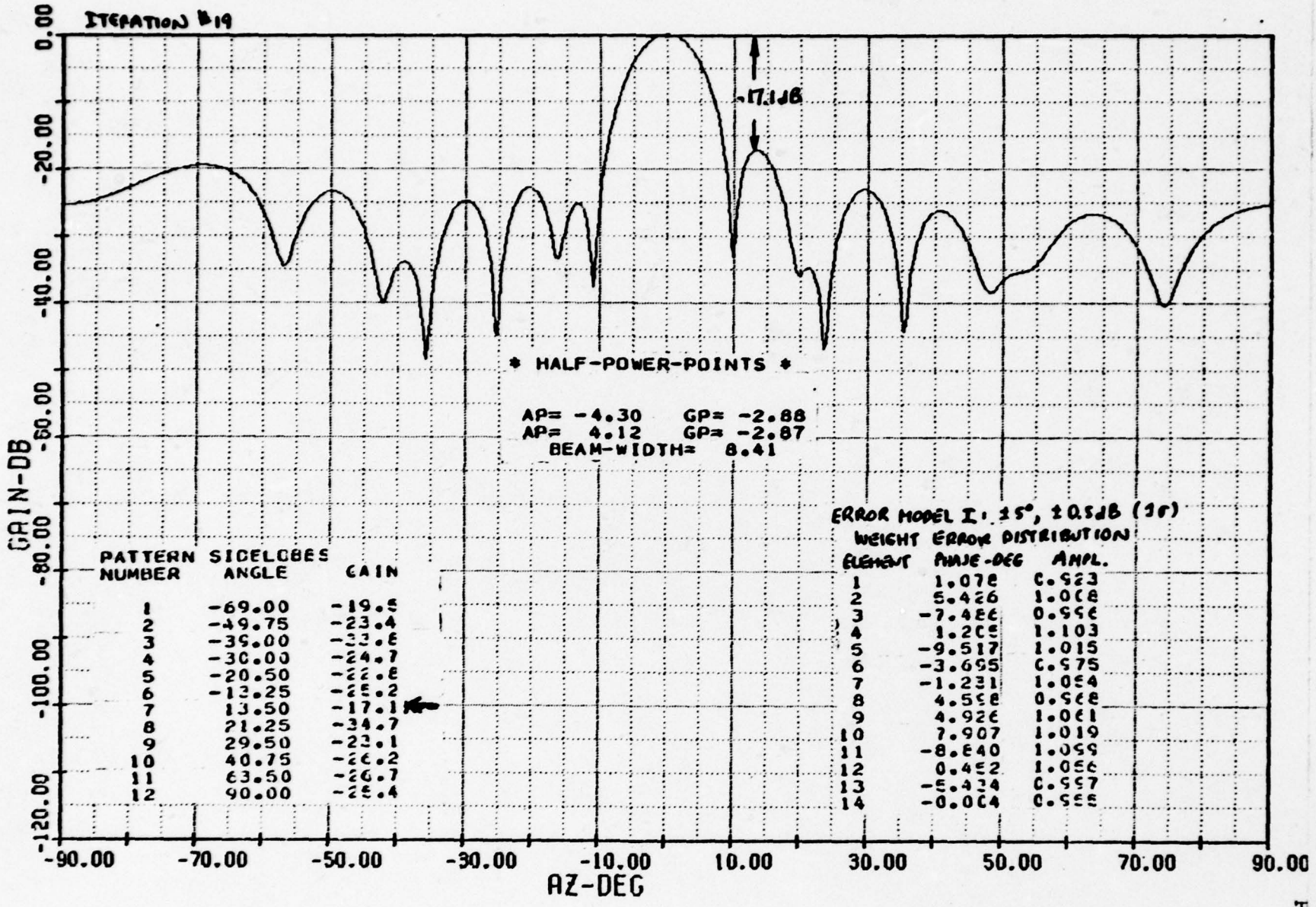


Figure 33 - Transmit Array Antenna Pattern (Error Model I - max. sidelobe level)

14 ELEMENT TRANSM. ANTENNA PATTERN

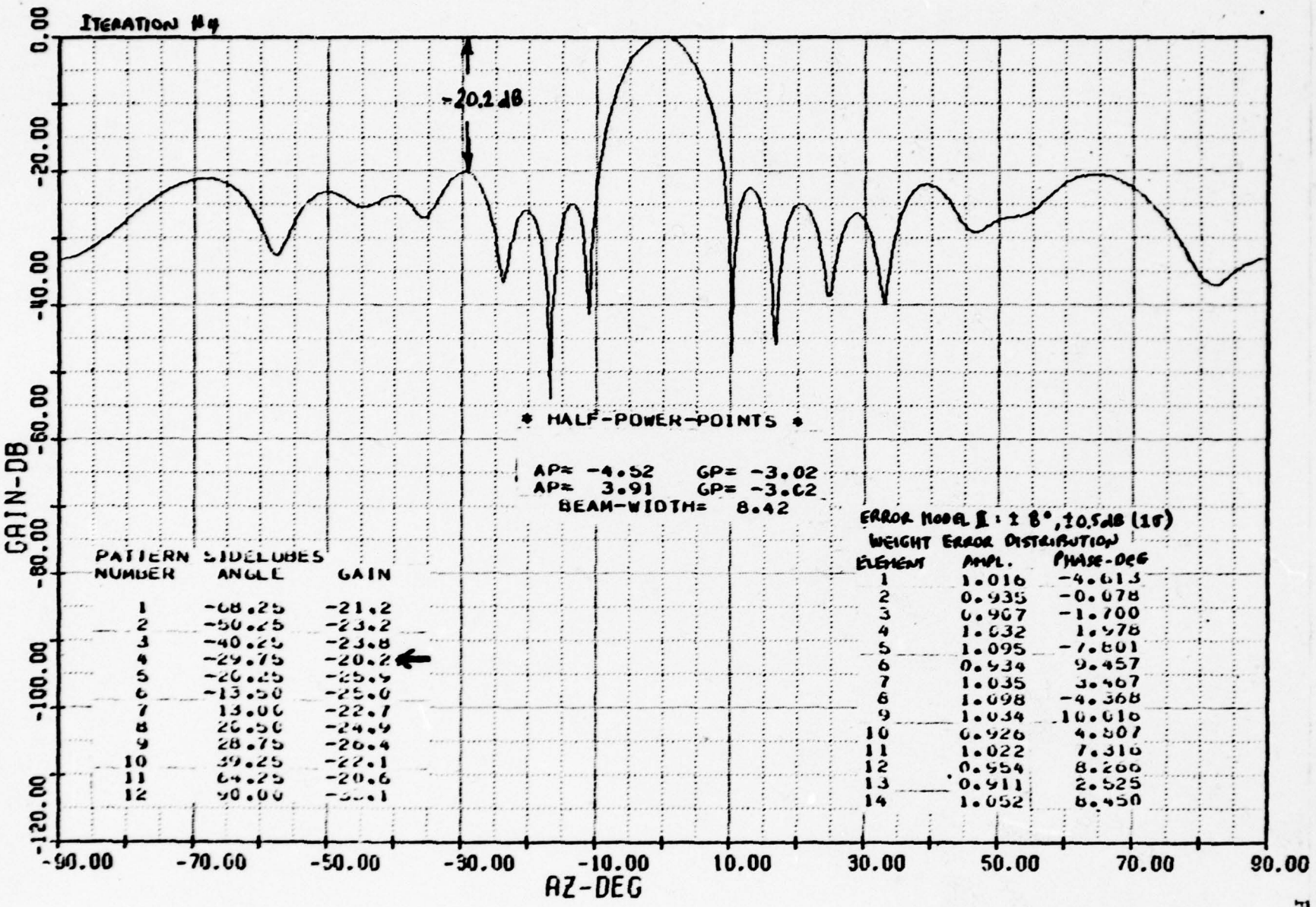


Figure 34 - Transmit Array Antenna Pattern (Error Model II - min. sidelobe level)

14 ELEMENT TRANSMIT ANTENNA PATTERN

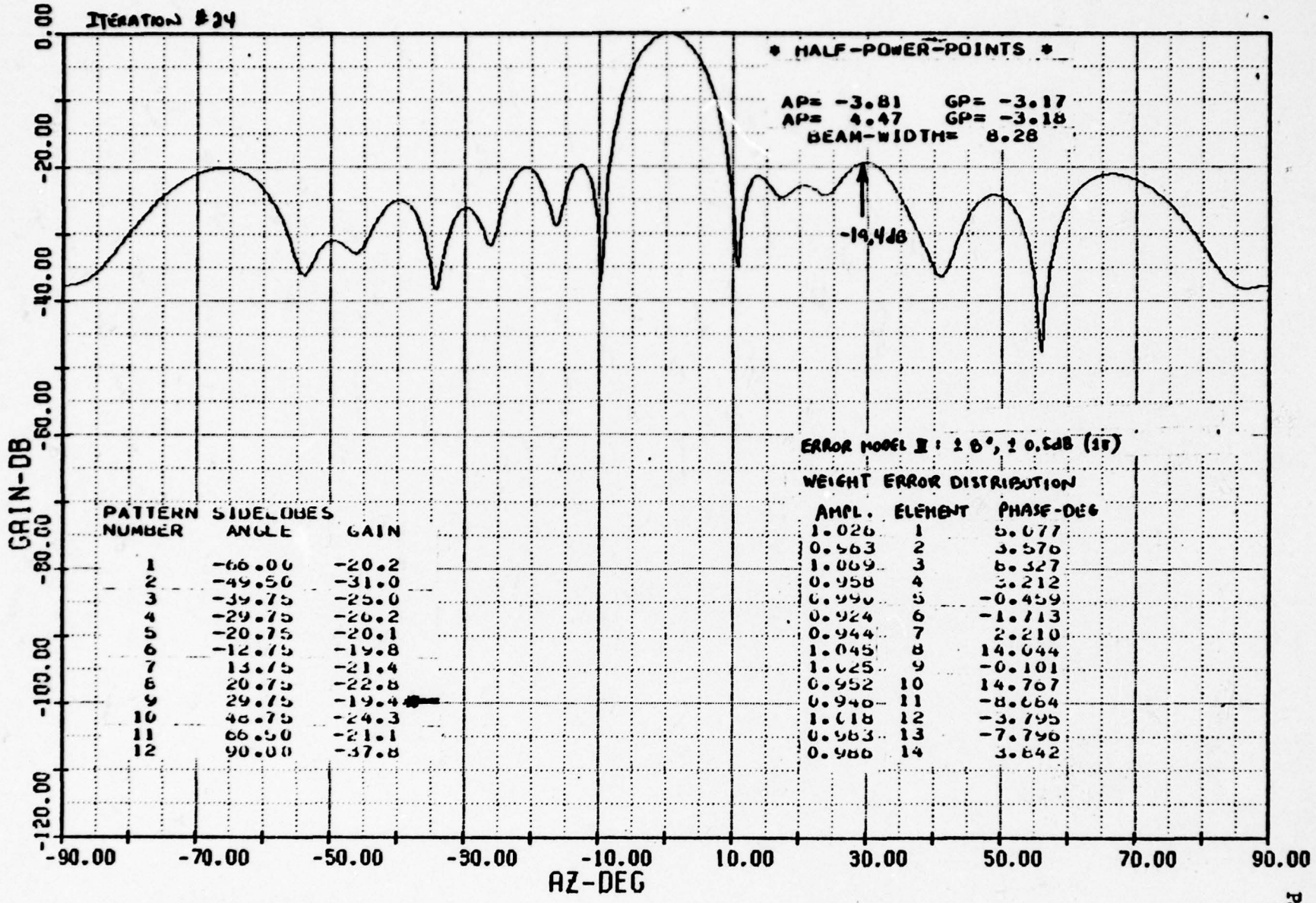


Figure 35- Transmit Array Antenna Pattern (Error Model II - mean sidelobe level)

14 ELEMENT TRANSMIT ANTENNA PATTERN

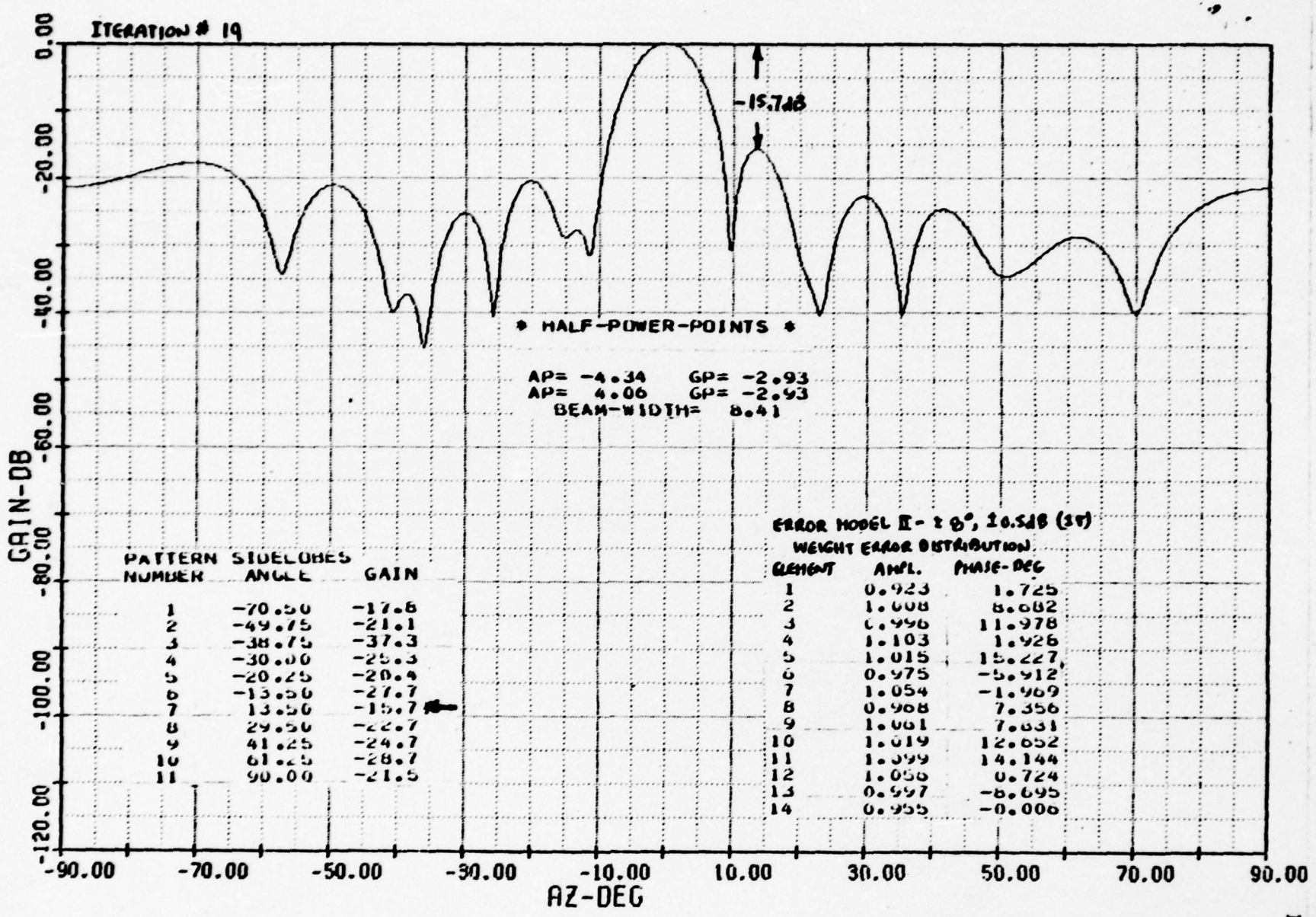


Figure 36 - TRANSMIT ARRAY ANTENNA PATTERN (Error Model II - max. sidelobe level)

5.0 RF DEPENDENCY OF STEADY STATE PULSE VOLTAGE

The essential quality of the RF transmit system is the minimization of antenna sidelobe levels. The major contributor to the increasing sidelobe levels are the inter-module phase deviations. These phase deviations are brought about by DC supply voltage droop at the input of the module. With a large capacitor, acting as an energy storage unit, control over the amount of pulse droop may be exercised. By utilizing the antenna pattern data of Section 4.0, the curve (Figure 37) relating mean peak sidelobe level to RMS phase error is generated. This curve may be now utilized to relate sidelobe performance to energy storage capacitance. This section will show that by judicious selection and matching of these capacitors, sidelobe levels approaching the quiescent or no error condition are achievable. Essentially there are four matching schemes available, these are discussed below.

5.1 Case I - No Capacitor Match

This situation assumes that the RF transmit modules have been phase matched by the manufacturer using a perfect or droop free power supply.

Using the GAC measured data relating phase shift, voltage droop and capacitance (Figures 12, 13 and 14), extrapolated intra-pulse phase error with time and the computer generated antenna patterns a relationship between power distribution system capacitance and mean peak antenna sidelobe level is established. For purposes of this analysis the phase error was selected at the 300 μsec point of a 500 μsec wide pulse. The 300 μsec point represents the mid point of the "reliable" data region, which is taken as being after the first 100 μsec turn-on region. This phase value is considered to be an RMS phase error which is related to sidelobe level via Figure 37, thus Figure 38 is generated.

5.2 Case II - No Capacitor Match - Frequency Dependent

The sidelobe dependency effects with frequency are also displayed in Figure 38. This curve was generated by computing the RMS phase variation with frequency (400 MHz - 450 MHz) for the 33.0 volt bias level as displayed in Figure 8. This constant value was then combined with the frequency independent values.

5.3 Case III - Phase Matched at Mid-Pulse for a Specific Capacitor Size

If each module is matched at mid-pulse with equal capacitances there is no net phase shift over the pulse. That is to say that the array will achieve a sidelobe level determined by the quiescent distribution and is independent of the capacitor value. Appendix II provides a mathematical proof of this case.

5.4 Case IV - Phase Matched at Mid-Pulse - Capacitor Tolerance and Frequency Effects

A more general and realistic situation than that described in Case III includes capacitor tolerance and frequency effects.

Typical large value electrolytic capacitors currently available have a rather broad tolerance ranging from -10% to +75% of the specified value. From this tolerance range, mean and RMS values were computed and related to RMS phase shift and sidelobe level. The results are plotted in Figure 39 indicating sidelobe level against nominal capacitor value. Also indicated on Figure 39 are the combined effects of frequency dependency (as described for Case II) and capacitor tolerance.

5.5 Conclusions

These matching schemes, provide a partial solution to controlling voltage droop. Further investigation of this approach was abandoned in view of the anticipated dynamic waveform and the multi-prf architecture of the next generation AEW radar. This approach, was considered to be beyond the scope of the study.

MEAN PEAK SIDELOBE VS PHASE ERROR

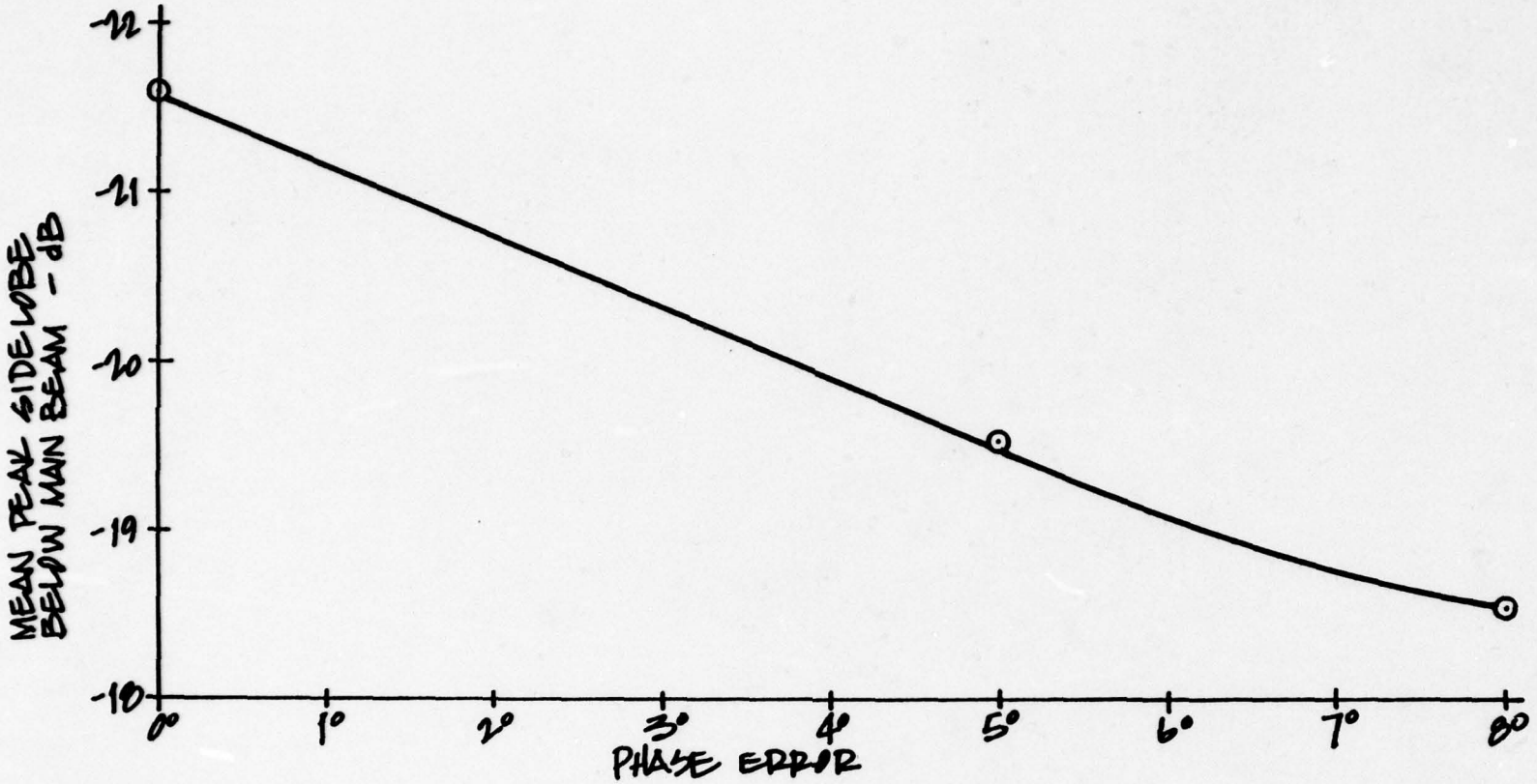


FIGURE 37

CASE I & II NO CAPACITOR MATCH

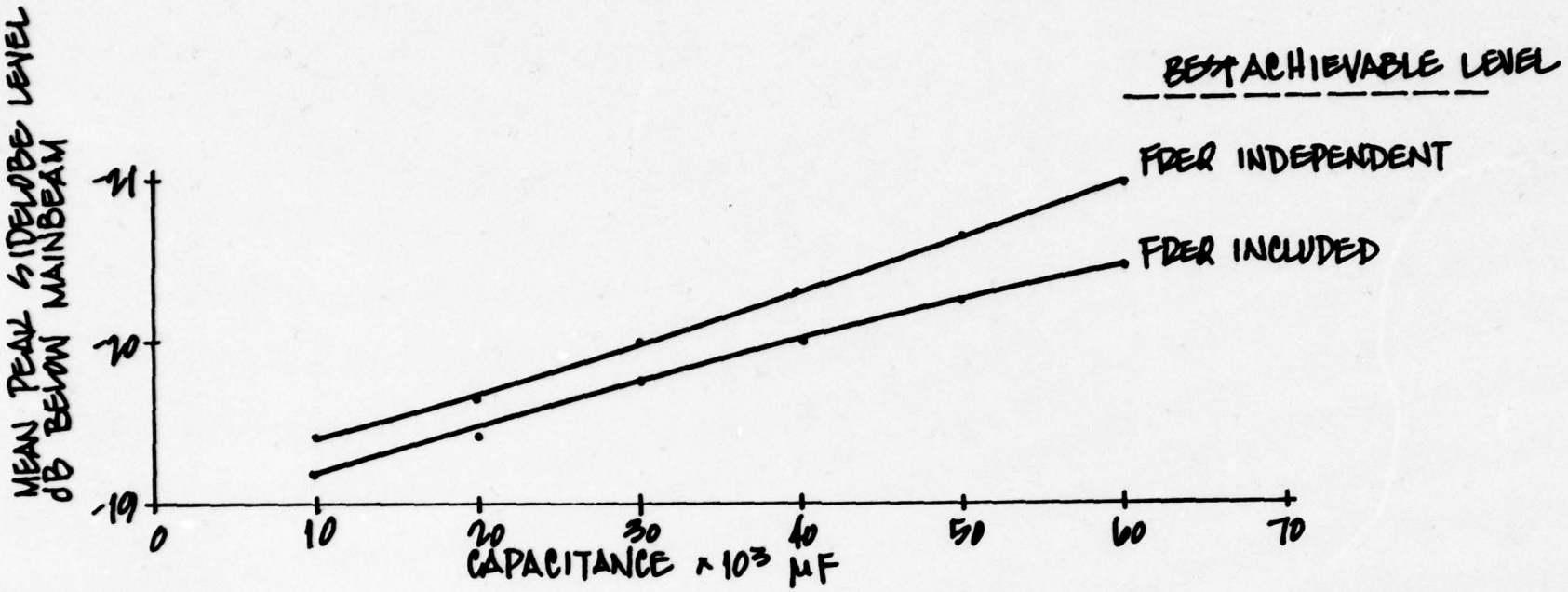


FIGURE 38

CASE IV PHASE MATCH AT MID-PULSE

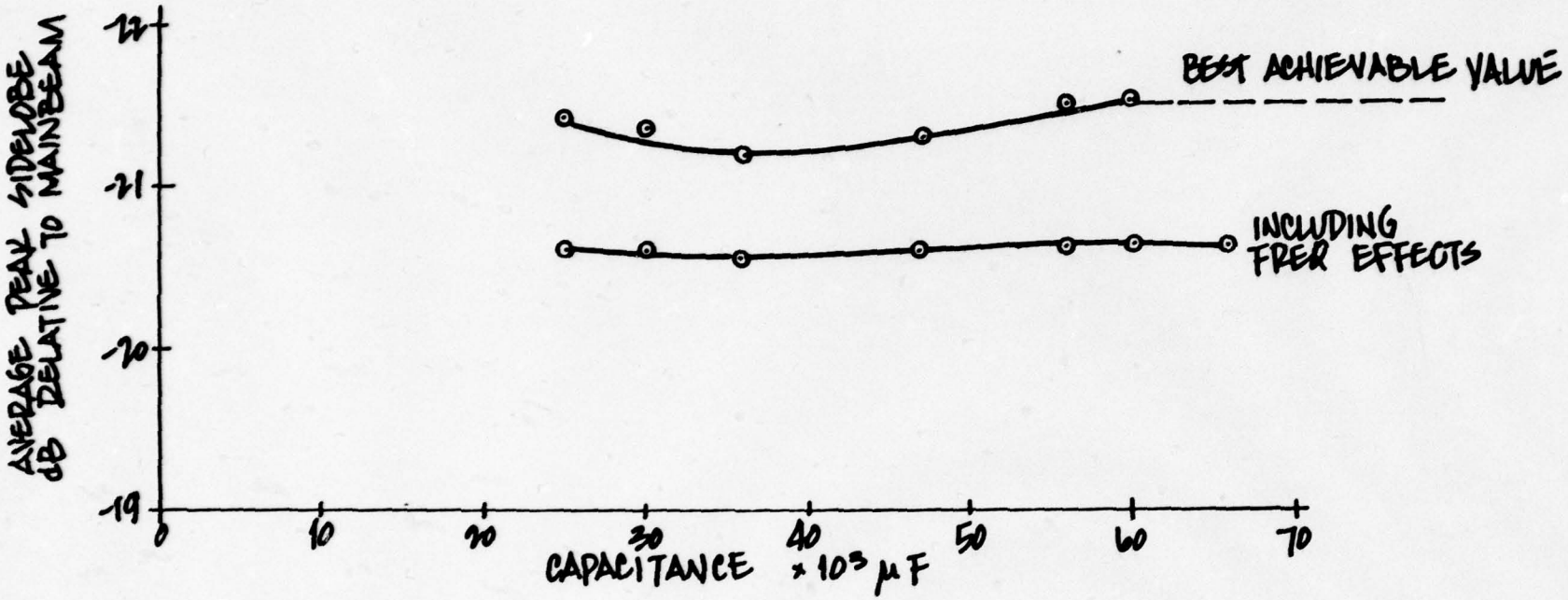


FIGURE 39

6.0 POWER DISTRIBUTION SYSTEM

Experiments performed with the solid state transmitter modules show that close regulation of the DC supply voltage is necessary to preserve radar system performance. The power supply parametric limits are established by utilizing the developed data from Sections 2.0 and 5.0.

The parameter variations developed that are to be considered in designing the power distribution system:

- Allowable overall DC supply voltage variation at the transmitter modules. Based on experimental data, a $\pm 3\%$ overall regulation is desired, yielding a 33 ± 1 VDC regulation requirement.
- Intermodule supply voltage tracking. Supply voltage variations between the 14 transmitter modules cause phase and amplitude errors and degrade system performance. The allowable supply voltage variation is ± 0.1 VDC.

Additionally, power supply noise and/or ripple should be kept below 50 mV_{rms} during the intrapulse, high current output period.

6.1 Design Concepts

Four alternate power distribution systems have been investigated, and are shown in Figures 40 through 43, and are summarized in Table 5. Each of these designs satisfies the following requirements:

- Only one array of 14 transmitters is energized at one time
- Individual transmitter module output is 2 KW with a 50% output/input efficiency. This implies a peak power input of 4 KW; V_{in} = 33V, I_{peak} = 121 A
- PRF = 300 pps; T_{pulse} = 500 µsec; Duty Cycle = 15%
- I_{av}/module = 18A
  I_{av}/array = 254A
- Main power supply ratings:
  - 12 KVA at 45 VDC unregulated at $254A_{av}$
  - 55 KVA at 33 VDC regulated at 1,700 A_{peak}
  - 8.5 KVA at 33 VDC regulated at 254 A_{av}
- Main power supply operating frequency: 18 KHz

TABLE 5

POWER DISTRIBUTION SYSTEMS ANALYSIS SUMMARY

CONFIGURATION	VOLTAGE REGULATION ±%	INTER MODULE TRACKING ±%	RIPPLE VAC rms	EFFICIENCY %	TOTAL WEIGHT LB	TOTAL VOLUME in^3	ELECTRO-MAGNETIC COMPATIBILITY
Central Regulated Supply	depends on wire size	can not be guaranteed	--	75	310 + cabling	5,000	unacceptable
Distributed System	3	0.5	100	75	1,500	45,000	good
Central Source with Local Energy Storage	10	5	432	75	560	15,000	good
Central Source with Local Regulation (Switching)	3	0.3	210	60	386	10,500	fair
Central Source with Local Regulation (Series Pass)	3	0.3	20	50	218	6,600	good

A power distribution system based on one centrally located power supply is shown in Figure 42. Three major disadvantages render this approach unacceptable. The peak current required by an array of 14 transmitters is 1,694 amps. Current pulses of this magnitude result in large weight penalties if protection against excessive radiation is provided. Large and heavy cabling is required to preserve the regulated source voltage. Additional resistances, will play an important part in determining the achievable module supply voltage regulation. For example, a 15 ft section of AWG-4 wire with a resistance of 3.7 milliohms has a 0.45 V drop with a 121 ampere current, and weighs approximately 2 lbs. Good regulation at the modules, therefore, can only be achieved through the use of heavy gauge cabling. This would add several hundred pounds to the system weight.

If no local energy storage unit is provided at the transmitter modules then the central power supply has to provide the full array peak current of 1,700 amperes instead of the 254 ampere average current. This requirement causes the central power supply size to increase sixfold over the other distribution system which utilize local energy storage. The centrally located power supply without local energy storage is thus judged to be unacceptable.

The second power distribution system, Figure 41, uses individual power supplies for each module. Each power supply weight is estimated to be 27 lbs. This yields the prohibitive weight of 1500 lbs for 56 individual module supplies. Weight and volume considerations, make this configuration unacceptable.

The third power distribution system, Figure 42, is comprised of a regulated central power supply and individual 50,000 μF energy storage capacitors located at each transmitter module. These large value capacitors result in high volume and weight for this configuration. In addition, local energy storage provides very poor voltage regulation. The supply voltage varies with transmitter duty cycle and various operating conditions. Therefore, this power distribution scheme is also judged unacceptable.

The fourth power distribution scheme utilizes a centrally located 45 VDC unregulated power supply and local 33 VDC voltage regulator modules. Since the regulators operate with a 12 V drop, the local storage requirements at the regulator input are less severe than in the previous system. A 10,000 μF capacitance has been determined to be adequate.

Two modes of regulation were considered for the local regulator modules. A switching regulator operating at 40 KHz would generate 210 mV rms ripple voltage during the intrapulse period. The overall system efficiency of operation is calculated to be 60%. A series pass regulator, on the other hand, would provide only 20 mV rms ripple and yield an overall efficiency of 50%. System weight would also be reduced significantly. Consequently, the series pass configuration is recommended for the local 33 VDC regulator modules.

6.2 Preferred Configuration

The preferred power distribution system configuration is shown in Figure 43. It has a centrally located 45 VDC unregulated power supply with 56 local series pass type regulators. Additionally, there are no stringent capacitor matching requirements. Total system volume and weight are 6,600 in^3 and 218 lb respectively. Table 6 summarizes the system operating parameters.

The central supply is powered from the aircraft 115 VAC 3 phase bus. It is a switching type converter operating at a nominal 18 KHz. The local regulators contain 10,000 μF of storage capacitance, so-that the central supply is required to provide only the 254 amperes average system current. Peak currents during output pulse transmission are drawn from the storage capacitors.

The preferred configuration places very few requirements on the cabling between the central supply and the local regulators. The current handling requirement is 18 amperes to each module or 254 amperes to each (of four) transmitter arrays. As much as 1 volt drop along the cabling can be tolerated by the system. Since the regulator modules will be placed next to, or integrated with the transmitting modules no further cabling requirements exist.

6.3 Power Supply Technology Projection

Significant improvements in power supply technology can be expected during the next few years. Major benefits of these advances to the power distribution system will be reduced size and weight, increased efficiency

TABLE 6

PREFERRED SYSTEM OPERATING PARAMETERS

ITEM	OUTPUT VOLTAGE (V)	OUTPUT CURRENT PEAK (A)	OUTPUT CURRENT AVERAGE	EFFICIENCY (%)	NUMBER REQUIRED TOTAL PER AIRCRAFT	VOLUME in^3	WEIGHT (LB)
Central Unregulated Supply (12 KVA output)	45VDC unreg.	--	254	88	1	1000	50
Local Regulator Series Pass Type	33VDC reg.	121	18	60	56	100	3
TOTAL	--	--	--	50	--	6,600	218

and more reliable operation. Technological advances are expected in the following areas:

- o Transformer core materials
- o Semiconductor rectifiers
- o Large filter capacitors
- o Semiconductor technology
- o Energy storage/filter capacitor.

Research in ferrite technology is expected to reduce the required core size and weight by as much as 50% by 1985.

Advances in tantalum capacitor packaging are expected to reduce large filter capacitor size and weight by at least 50%. The major requirement here is to increase capacities in solid or wet-slug tantalum capacitors from the presently available small 100 μF units to larger 10,000 μF units in single packages.

Fastest advancement is in semiconductor technology. Low voltage Schottky as well as ion-implanted rectifier diodes of sufficient power handling capability for the main power supply should be available shortly. This will increase operating efficiency at a reduced weight. For the distributed regulators a single, monolithic voltage regulator unit with 100-150 A output current at the required 33 VDC output voltage can be expected within the next 5 to 7 years. The weight of such a regulator unit should be under 4 ounces. Figure 44 show the expected impact of technological advances during the next ten years on the preferred power distribution system.

CENTRAL POWER SOURCE

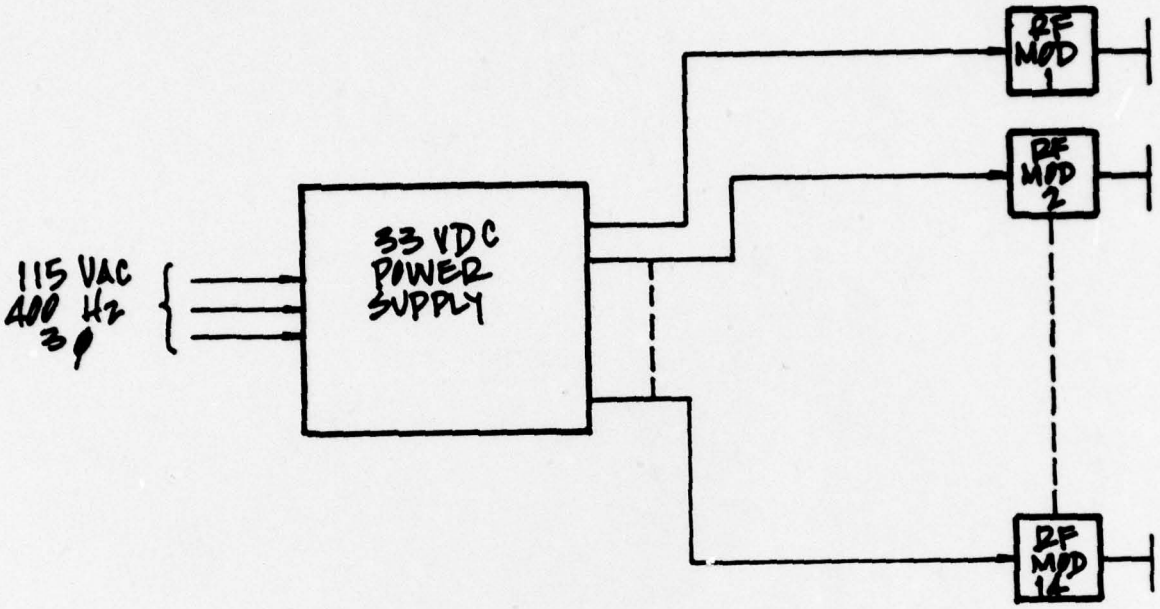


FIGURE 40

DISTRIBUTED POWER SUPPLY SYSTEM

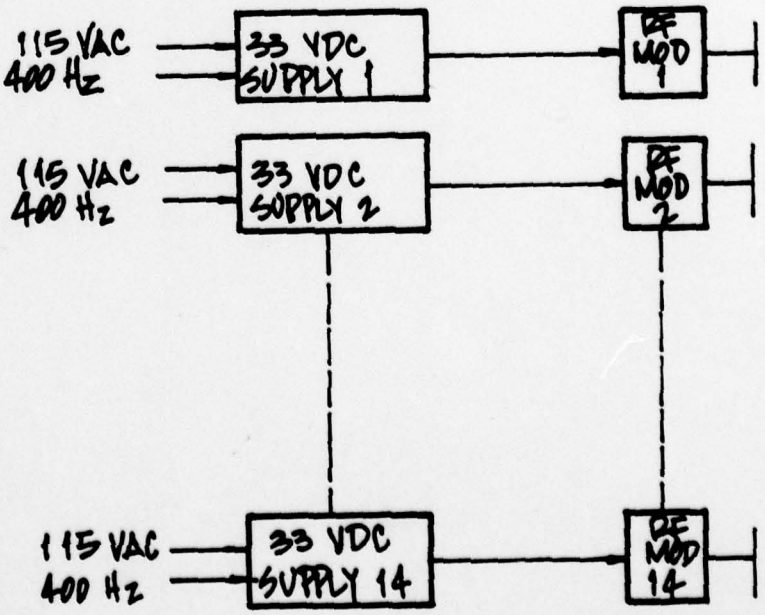


FIGURE 41

CENTRAL POWER SOURCE WITH LOCAL ENERGY STORAGE

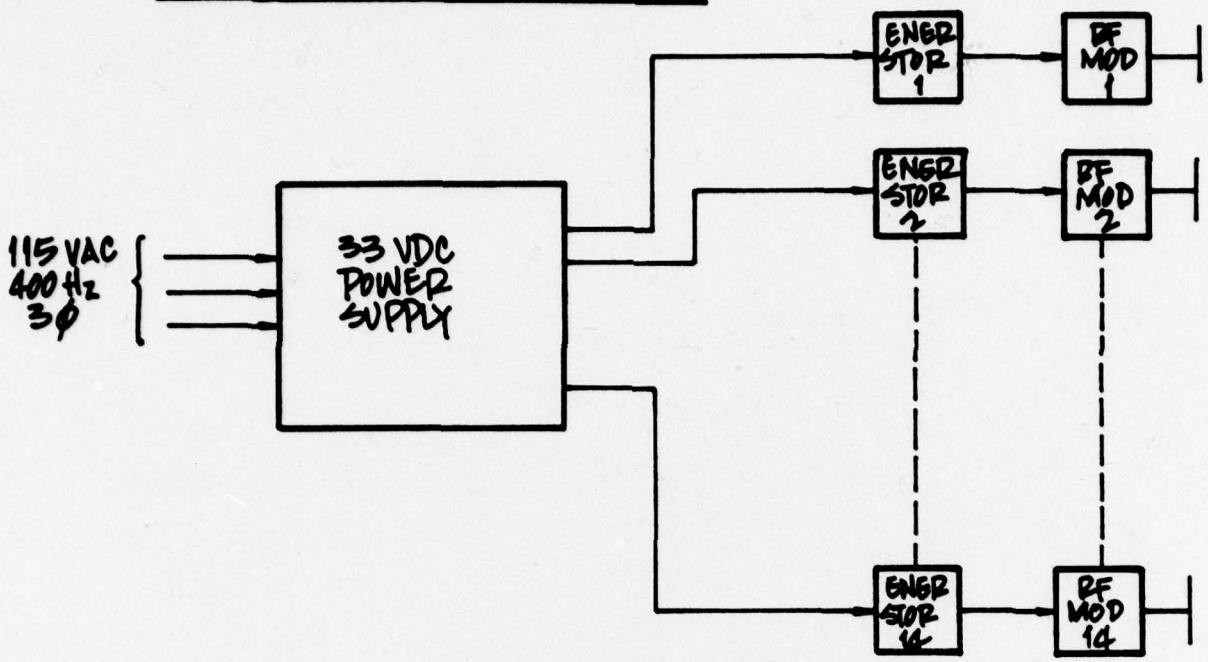


FIGURE 42

CENTRAL POWER SOURCE WITH LOCAL REGULATION

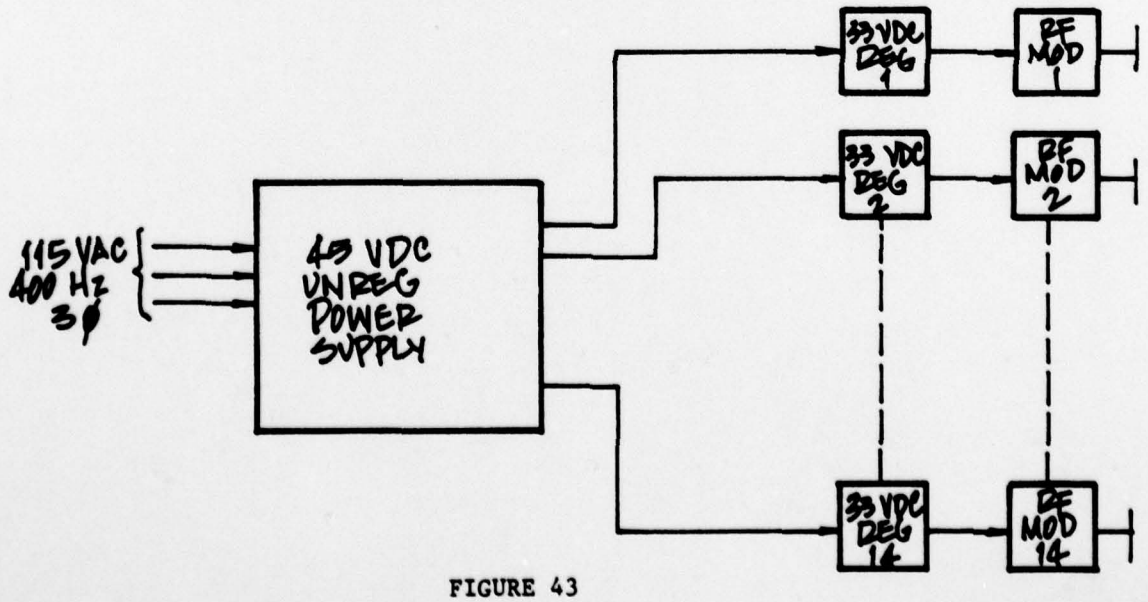
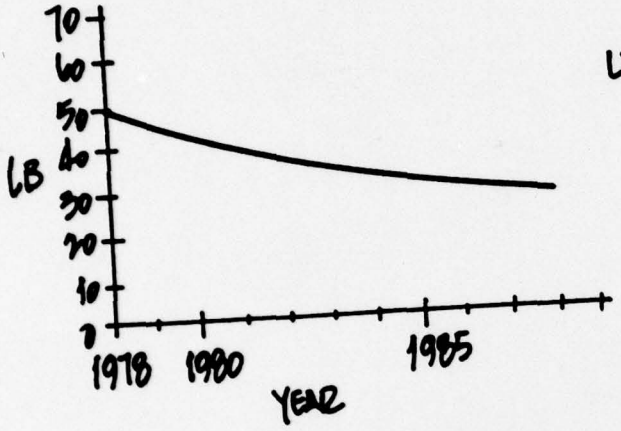
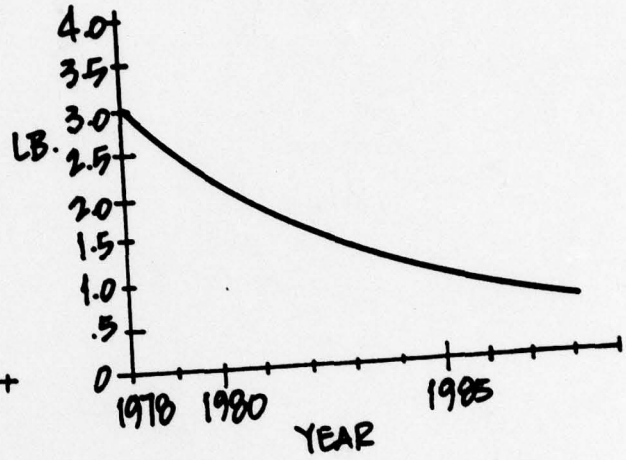


FIGURE 43

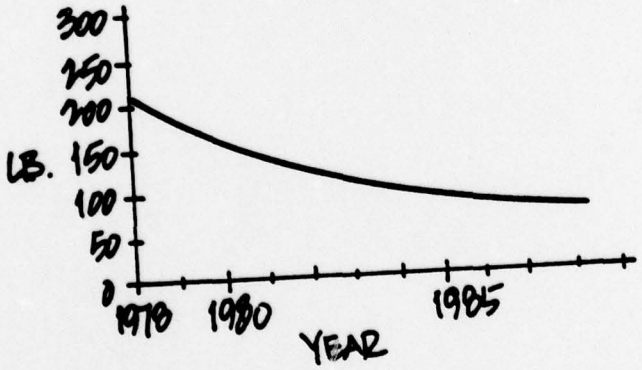
EXPECTED IMPACT OF TECHNOLOGICAL ADVANCES ON POWER DISTRIBUTION SYSTEM WEIGHT



A. CENTRAL UNREGULATED SUPPLY



B. DISTRIBUTED REGULATORS



C. CENTRAL SUPPLY & DISTRIBUTED REGULATORS

FIGURE 44

7.0 Environmental Control System (ECS)

To maintain the transmit/receive modules at their most efficient operating temperature and to assure maximum reliability, cooling air is provided via a manifold to a plenum duct which is an integral part of each module. Each module is mounted to a single spanwise manifold which has outlet provisions to force cooling air into each module plenum via force-fit nipples. High heat-dissipating components within the module are mounted to a cold plate wall in contact with the plenum wall. Heat is dissipated through the cold plate by coming in contact with cooler air in the manifold and is exhausted through a series of openings along the horizontal surface of the plenum. The heated air is discharged into the module bay between the aft beam and the array mounting support, and then is leaked overboard through louvers in the bottom surface of the bay.

The manifold has been presently sized to provide sufficient cooling air based on the maximum heat load of each module of approximately 390 w, for a total of 5000 w. Preliminary investigations into cooling air requirements indicate a flow rate of 6 to 8 lb/min at $60^{o}F$.

Detailed size and weight estimates are shown in Table 7.

TABLE 7

CONFORMAL RADAR COOLING PROVISIONS

WEIGHT ESTIMATE

		FIBER GLASS* LBS	ALUMINUM** LBS
Fuselage $4.5"^2$ Duct			
Length 196.0"		3.5	6.0
Fuselage coupling		1.0	1.0
Orifice Plate		2.0	2.0
Hardware		1.0	1.0
Local Support Brackets		2.0	2.0
	SUB TOTAL	8.5	12.0
Wing $4.5"^2$ Duct			
Length 200.0"		3.6	6.2
Orifice Plate		2.2	2.2
Hardware		2.0	2.0
Wing Fold Coupling		3.0	3.0
Wing to Fus. Connect		4.4	7.4
Local Support Brackets		3.0	3.0
	SUB TOTAL	18.2	23.8
	TOTAL/SIDE	26.7	35.8
	TOTAL/AC	53.4	71.6

*Preferred
**Alternate

8.0 PROJECTED POWER TO WEIGHT ESTIMATES

Estimates of achievable RF power output to weight ratios are derived and shown in Table 8 for currently achievable hardware and also for projected 1985 hardware. The power output levels included are for a uniformally excited array of fourteen 2 KW transmit/receive modules which yields the maximum power to weight ratio; it is for this configuration that the power supply has been sized.

TABLE 8

WEIGHT AND POWER/WEIGHT TABULATION

ITEM		1978 TECHNOLOGY	1985 TECHNOLOGY
Central Supply		50 lbs	30 lbs
Local Regulators and Engergy Storage 14 Required		3 lbs each 42 lbs total	1 lb each 14 lbs total
Transmit/Receive Modules 14 Required		3.5 lbs each 49 lbs total	
Ducting Fiber-Glass		Wing Arrays 18.2 lbs (per wing) Fuselage arrays 8.5 lbs (2 per aircraft)	
UHF Exciter		4 lbs	4 lbs
UHF Corporate Feed & Associated Cabling		10 lbs	10 lbs
TOTALS	WING	173.2	125.2
	FUSELAGE	163.5	115.5

Power (RF Output)

14 elements

2 KW Uniform Distribution = 28 KW Peak

4.2 KW Average

Power/Weight Ratio

Uniform Distribution

Wing	24.2 w/lb	33.5 w/lb
Fuselage	25.7 w/lb	36.4 w/lb
Mean	25.0 w/lb	35.0 w/lb

APPENDIX 1
ACCEPTANCE TEST DATA

MICROWAVE POWER DEVICES, INC.
Adams Court, Plainview, L.I., New York 11803 • Tel. 516-433-1400 • TWX 510-221-1862

TEST DATA SHEET

CUSTOMER: Grumman Aerospace Corp. P.O. No.
MPD MODEL No. PCA 435-13/3493 JOB No. S/N 2

TEST CONDITIONS: Room Ambient
B+ = 33.5 VDC I_{idle} = 400 mA

DATA

FREQUENCY RESPONSE: 50 Ohm Load: Pin = +10 dBm, + 0.5dB, - 0.5 dB
Duty Cycle: 15%

Freq. MHz	Pout Peak (≥ 1000 W)	It Amps	Jitter (≤± 5 n.sec.)	Pulse Width μ sec.	Rise Time nano sec.	Fall Time nano sec.
400	1170	15	0	0.5	< 100	10
415	1285	13.8	0	0.5	< 100	10
425	1200	13.1	0	0.5	< 100	10
435	1150	12.8	0	0.5	< 100	10
450	1080	12.4	0	0.5	< 100	10

RF INPUT OVERDRIVE OF 10 dB: ✓ (Checked)
INPUT VSWR: ≤ 1.1:1 (≤ 1.3:1) OUTPUT VSWR: ≤ 1.2:1 (≤ 1.3:1)
GAIN & OUTPUT POWER VARIATION, 6 MHz: ✓ dB (≤ ± 0.2 dB)
PHASE DEVIATION OVER ENTIRE BAND: ±8° degrees (≤ ± 6 degrees)
PHASE DEVIATION OVER ANY 6 MHz: ✓ degrees (≤ ± 3 degrees)

INTRAPULSE PHASE DEVIATION:

Freq. MHz	Pulse Width 0.5 to 10 μ sec. (≤ ∓ 6 degrees)	Pulse Width 10 to 500 μ sec. (≤ ∓ 3 degrees)
400	±2.0° above midpulse	< ±3.5° above midpulse
415	< ±1.5° "	±3.0° "
425	< ±2.0° "	< ±3.0° "
435	< ±2.0° "	±3.0° "
450	< ±2.0° "	±2.5° "

MIDPULSE
+1°
-1°
-1°
-3°
+1°

INTER MODULE PHASE DEVIATION:

Freq. MHz	Midpulse (≤ ∓ 3 degrees)	Other Positions (≤ ∓ 6 degrees)
400	+8.4°	< ±2° over midpulse
415	+0.4°	< ±2° "
425	+1.7°	< ±2° "
435	-2.6°	< ±2° "
450	-4.5°	< ±2° "

NOTES: ( ) Indicates Specification Limits

Weight: 3-1/2 lbs.

Data Taken By J.S. Date 6/n/77 Appr. Date

TD 2161B REV. - APPR. Date 4/--/--

THIS PAGE IS BEST QUALITY PRACTICABLE
FROM COPY FURNISHED TO DDC

APPENDIX II

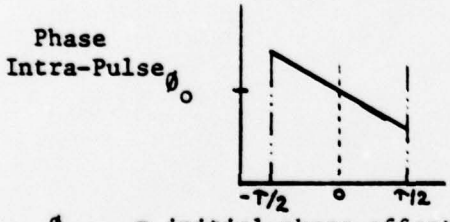
MATHEMATICAL VERIFICATION OF MID-PULSE MATCHING

If the phase response of each module is matched to zero at mid-pulse there is no net or time average effect on sidelobe level.

For a linear array of equally spaced elements, the relative amplitude of the radiated field intensity is given by:

$$(1) \qquad E(\theta) = \sum_{k=o}^{N-1} a_k e^{j(\beta\, dk \sin\theta + \alpha + \phi_k)}$$

where:
- $E(\theta)$ = Electric field intensity with observation angle θ
- θ = Angle measured from array normal
- β = $2\pi/\lambda$ $\quad\lambda$ = wavelength
- a_k = amplitude weighting of kth element
- N = number of elements
- α = phase angle for beam steering, set to zero
- d = inter-element spacing (uniform)
- ϕ_k = phase variation of kth element



$$\phi_k = \phi_o + \delta t$$

- ϕ_o = initial phase offset (constant value, set to zero)
- δ = slope of phase variation with time t

The desired function is the time average Electric Field intensity $\hat{E}(\theta)$ over the period of the pulse:

$$(2) \qquad \hat{E}(\theta) = \frac{1}{T}\int_{-T/2}^{T/2} E(\theta, t)\, dt$$

T = pulse width

Substituting we have:

$$(3)\quad \hat{E}(\theta) = \frac{1}{T}\int_{-T/2}^{T/2} \sum_{k=o}^{N-1} a_k e^{j(\beta\, dk \sin\theta + \delta t)}$$

$$= \frac{1}{T} \sum_{k=o}^{N-1} \left\{ a_k e^{j(\beta dk \sin\theta)} \int_{-T/2}^{T/2} e^{j\delta t}\, dt \right\}$$

Integrating and using the Euler identity,

$$(4)\quad \hat{E}(\theta) = \sum_{k=o}^{N-1} a_k e^{j\beta dk \sin\theta} \frac{1}{\delta T} \left\{ 2 \operatorname{Sin} \left(\frac{\delta T}{2}\right) \right\}$$

$\delta T/2$ is a small value, so that $\operatorname{Sin} \frac{\delta T}{2} \simeq \frac{\delta T}{2}$

$$\frac{1}{\delta T} \cdot 2 \cdot \frac{\delta T}{2} = 1$$

Therefore: $\hat{E}(\theta) = \sum_{k=o}^{N-1} a_k e^{j\beta dk \sin\theta}$

which is independent of symmetrical intra-pulse phase variations.

APPENDIX III

SERIES-PASS REGULATOR DESIGN

A representative series-pass regulator is shown in Figure 45. The design takes advantage of recent advances in high power semiconductor technology and is able to meet the power output requirement of 121 amps and 33 VDC with two solid state circuit packages in addition to the input and output capacitors.

Q1 is a hybrid, positive regulator in a TO-3 package. A simplified schematic of this regulator is shown in Figure 45. The unit is capable of supplying 5 amperes of drive current to the series pass output Darlington transistor in Q2. This drive current is provided by an internal drive circuit represented schematically by a pullup resistor. The output current from Q1 is amplified by Q2 which is rated at 250 amps and resides in a 5 in^3 package. Q2 requires a base current of 0.25 amperes to supply the required 121 amperes to the RF transmitter module. As the output voltage reaches 33 VDC, R1 and R2 feedsback a fraction of this voltage. When the feedback voltage reaches 7 volts, the current bypass transistor is turned on in Q1 and the output drive current is shorted to ground. The regulator will continue to operate at this equilibrium point.

For input/output filtering high density tantalum capacitors are used. All components are mounted in a light weight housing with good thermal conductivity to the cold rail.

The regulator described should be constructed and tested to insure its compliance with all performance requirements and to determine its dynamic behavior under load.

REPRESENTATIVE SERIES-PASS REGULATOR

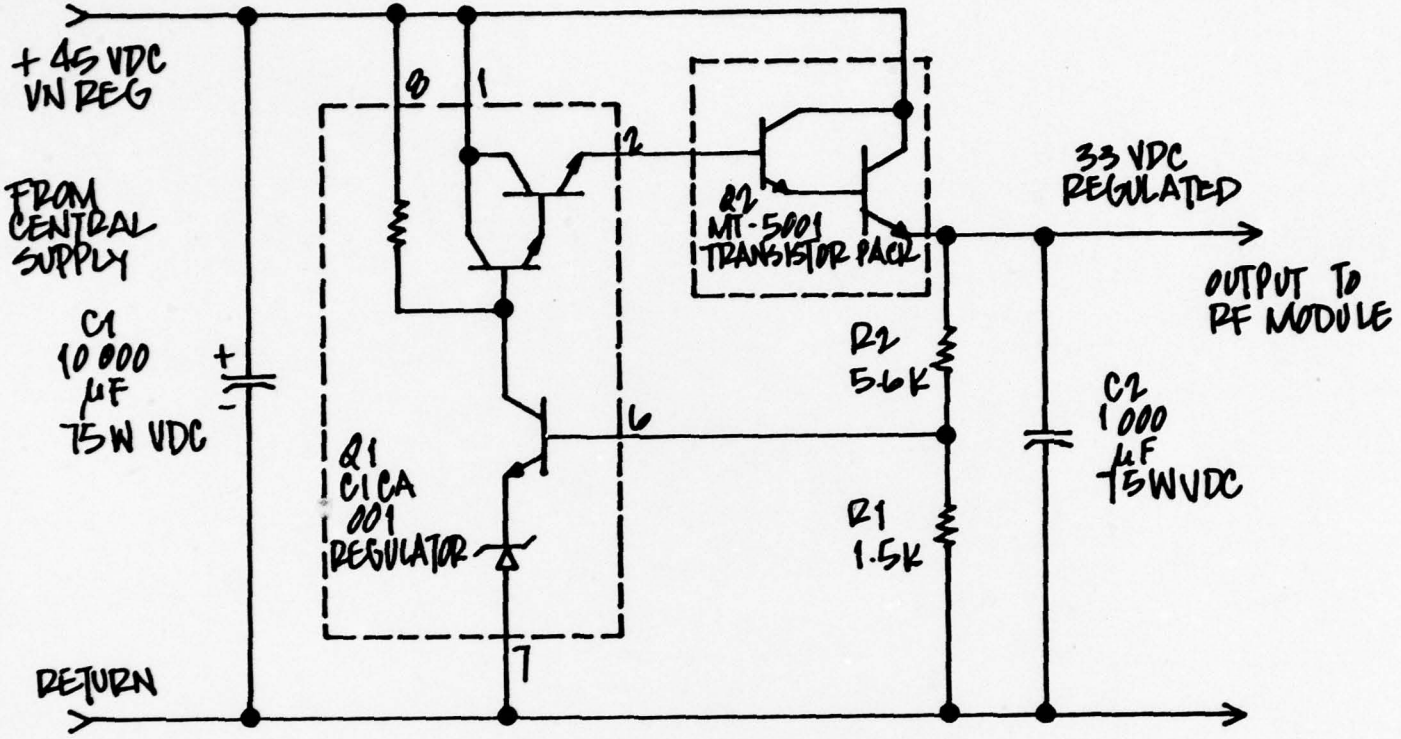


FIGURE 45